The Convergence of Heat, Groundwater & Fracture Permeability:

Innovative Play Fairway Modelling Applied to the Tularosa Basin

DOE Contract #DE-EE0006730

■ PHASE 1 PROJECT REPORT ■

October 16, 2015

Submitted By:

Ruby Mountain Inc.

Salt Lake City ■ El Paso ■ Seattle ■ Newport Beach

and

EGI Energy & Geoscience Institute AT THE UNIVERSITY OF UTAH

The Convergence of Heat, Groundwater & Fracture Permeability: **Innovative Play Fairway Modelling Applied to the Tularosa Basin**

PHASE 1 PROJECT REPORT

This report is submitted to the U.S. Department of Energy (DOE) in fulfillment of requirements of Contract #DE-EE0006730 which was awarded to develop a methodology for, and conduct, a Geothermal Play Fairway Analysis in the Tularosa Basin located in South-Central New Mexico and Far West Texas. Ruby Mountain Inc. (RMI) is the prime contractor to DOE under the grant award. The Energy and Geoscience Institute (EGI) at the University of Utah is the prime subcontractor to RMI.

This report summarizes the activities and key findings of the project team occurring during Phase 1 (August 2014 – October 2015) of the Tularosa Basin Geothermal Play Fairway Analysis Project. Questions regarding the contents of this document should be directed to:
RMI Senior Project Manager Carlon R. Bennett at carlonbennett@gmail.com

Submitted By:

Ruby Mountain Inc.

Carlon R. Bennett, Project Manager
2373 East 1300 South, Salt Lake City, UT 84108
801-538-5003 ● rubymountaininc.com

and the

EGI Energy & Geoscience Institute
AT THE UNIVERSITY OF UTAH

Gregory D. Nash, Ph.D. Principal Investigator
423 Wakara Way #300, Salt Lake City, UT 84108
801-581-5126 ● egi.utah.edu

TABLE OF CONTENTS

■ ACKNOWLEDGEMENTS

Ruby Mountain Inc. and EGI wish to thank the following individuals and organizations for their cooperation, support and assistance throughout the implementation of Phase 1 of this project:

- U.S. Department of Energy (DOE) for its financial support, oversight, and guidance through Contract # DE-EE0006730;
- U.S. DOE Geothermal Technologies Office (GTO) & Staff - Eric Haas, Director;
- Fort Bliss Directorate of Public Works (DPW) & Staff - Alfredo Riera, Director;
- Fort Bliss Directorate of Public Works (DPW) - B. J. Tomlinson, Chief, Sustainability & Energy Division;
- Fort Bliss Directorate of Public Works - Environmental Division (DPW-E) Staff;
- Fort Bliss Office of the Staff Judge Advocate;
- White Sands Missile Range – Samuel O. Sanchez, April E. Banks & Craig Collins;
- El Paso Water Utilities - Alfredo Ruiz, Associate Hydrogeologist;
- University of Texas at El Paso - Diane Doser, UTEP Department of Geologic Sciences;
- New Mexico Environment Department - Water Quality Bureau;
- Fort Bliss Water;
- City of Alamogordo Water Utilities;
- New Mexico Office of the State Engineer – District IV;
- Alamogordo Public Schools;
- Michael Hillesheim, Sr. Systems Engineer - National Renewable Energy Laboratory; and,
- Mr. Dennis Wike, in his capacity as a civilian contractor to Fort Bliss DPW.

■ PROJECT TEAM

Mike Weathers, DOE Golden Field Office Contract Manager

Ruby Mountain Inc.

- Carlon R. Bennett, Project Manager
- Jon Lear, RMI Principal
- Phil L. Jones, Project Administrative & Research Assistant
- Dan Lear, Staff Attorney
- Brigitte Swanson, Consultant

Energy & Geoscience Institute at the University of Utah

- Gregory Nash, Ph.D., Project Principal Investigator
- Joseph Moore, Ph.D., Research Professor
- Stuart Simmons, Ph.D. Research Professor
- Rasoul B. Sorkhabi , Ph.D., Research Professor
- Adam Brandt, Student Research Assistant
- Nancy Taylor, Assistant Business Manager
- Benjamin Barker, Ph.D., Consultant

EXECUTIVE SUMMARY

The Convergence of Heat, Groundwater & Fracture Permeability: Innovative Play Fairway Modelling Applied to the Tularosa Basin

The Tularosa Basin Play Fairway Analysis (PFA) project tested two distinct geothermal exploration methodologies covering the entire basin within South Central New Mexico and Far West Texas. Throughout the initial phase of the project, the underexplored basin proved to be a challenging, yet ideal test bed to evaluate effectiveness of the team's data collection techniques as well as the effectiveness of our innovative PFA.

Phase 1 of the effort employed a low-cost, pragmatic approach using two methods to identify potential geothermal plays within the study area and then compared and contrasted the results of each method to rank and evaluate potential plays. Both methods appear to be very effective and highly transferable to other areas.

The first method was a deterministic approach developed by the petroleum industry and the second a stochastic method (weights of evidence) that has been used for mineral exploration and which has seen some use in geothermal exploration. To support PFA, an exhaustive data collection was undertaken to stock a geographic information system (GIS) with geospatial data to support the development of evidential layers representing heat of the earth, fracture permeability, and ground water for the transfer of heat. Data was also added to support future marketing.

Data for PFA would ideally be evenly spaced and contiguous throughout the study area. However, a significant and technically sufficient dataset was created covering large parts of the study area.

The deterministic petroleum industry PFA was modified for geothermal use and it identified eight plays, including a known geothermal resource at McGregor Range. Certainty was also assessed deterministically based upon the spatial distribution and correlation of input data representing heat.

The weights of evidence (WoE) PFA required training data representing known geothermal systems and hot springs. A paucity of sites within the study area led to the use of training sites elsewhere in New Mexico, Utah, and Nevada. WoE statistically evaluates the relationships of the input data with the training sites, calculates weights for each dataset, and produces a posterior probability raster surface (PFA model) and supporting statistics. This PFA identified ten plays, six of which were also identified using the aforementioned deterministic method, including the known resource at McGregor Range. WoE analysis also produces a confidence map which showed the plays area being relatively high confidence. However, data constrained within the study area was examined using probability kriging to create an additional certainty layer which was more conservative.

Considering the proximity to control data and certainty analyses, four of the twelve identified plays were considered to be from medium to high priority. The remaining plays lack certainty primarily due to a lack of certain evidential data at these locations.

Support work was also done to help better understand the geology of the region and to aid in marketing. This included:

- Economic analysis of the higher priority plays;

- Basement structure analysis;
- Strain surrogate (Z/R ratio) calculations;
- Geochemistry;
- Surface thermal anomaly mapping;
- Hydrothermal alteration mapping; and,
- Mineralogy mapping to map brittle v non-brittle rock (future EGS support).

Phase 1 of this study has not only exponentially increased the level of understanding of the basin from a geothermal resource perspective, but could very well lay the groundwork for a clean energy future in the region. Several distinct potential markets for geothermal energy exist within the Tularosa Basin, including three of our nation's premier military installations (Fort Bliss, White Sands Missile Range and Holloman Air Force Base) as well as the El Paso, Texas metropolitan area (home to over two million people).

In large part, the PFA team developed the project due to the potential marketability of geothermal power to these distinct areas. As an example, due to the vastness of both Fort Bliss and White Sands, both installations require power in numerous remote training locations and currently purchase power from major utilities in Texas and New Mexico, and also from several different small electric cooperatives. The power purchased in these remote areas can sometimes be costly (up to 17-21 cents per kWh in some instances) and on occasion is subject to frequent interruption.

DOE funding for this project facilitated the identification of geothermal resources for the first time on a Tularosa Basin-wide scale bringing a substantial amount of disparate data into a common database for analysis. The project team believes that this study could have a significant impact toward reducing geothermal exploration costs, and by doing so, lead to the development of new geothermal resources.

The project team, led by Ruby Mountain Inc. and The Energy and Geoscience Institute at the University of Utah, had no significant departure from stated goals or methods and brought Phase 1 to a successful conclusion on budget and on time while substantially exceeding cost sharing targets.

SECTION 1: INTRODUCTION

1.1 Geothermal Play Fairway Analysis (PFA) For Risk Reduction

Play fairway analysis (PFA) was developed by the petroleum industry to reduce risk over basin-wide areas by identifying small areas that meet play criteria (Fraser, 2001). PFA has already crossed-over into the geothermal arena, although prior to this DOE GTO initiative it had not been widely applied.

There are two basic model types of geothermal PFA: (1) knowledge-based (deterministic), where genetic geothermal data are considered through direct spatial correlation and (2) data driven, often stochastic, statistical models where data from training sites provide evidence to support probability calculations.
Nash et al. (1996) reported results of an early DOE supported effort, covering part of Nevada, where limited data was used in a knowledge-based model based upon genetic relationships of the input data to known geothermal occurrences within the study area. Coolbaugh (2003) used a greatly expanded GIS database, including numerous training sites, for weights of evidence (WoE) and density function calculations coupled with weighted fuzzy modelling, for models covering the Great Basin. Sabin et al. (2004) discuss the merits of geothermal Occurrence Models based on co-occurrence of geothermal associated phenomena and using these to identify other localities with similar co-occurrences. Younes et al. (2007, 2007) discuss the use of feature distances from producing geothermal wells as evidence and integrate these into a knowledge-based weighted-sum model, which yielded 97% accuracy based upon the prediction of known occurrences in kita and Iwate prefectures, Japan.

Fry analysis, spatial association analysis, and evidential belief functions were applied for geothermal modeling in West Java, Indonesia by Carranza et al, 2008. In this study 127 training sites were used. A similar study was carried out by Moghaddam et al. (2013) for Akita and Iwate, where numerous training sites were required. Hossein et al (2007, 2010), applied a knowledge-based method, using Boolean logic on vector evidence layers, to create a geothermal model for Iran, where layers were combined using Intersect and Union techniques in ArcGIS.

All models rely on the spatial correlation of data known to be directly associated with geothermal systems. The chief strength of statistical models is that they are not biased by the user and that probabilities may be derived. However, the results are sometimes not trusted by explorationists, decision makers, and investors. Additionally, statistical models require significant amounts of training data from known geothermal systems or hot springs, which can be limited. The chief strength of knowledge-based modelling is that training sites/data are not required because they rely on the knowledge of experienced explorationists. In frontier areas, with few if any training sites, this type of model would be the practical choice. Additionally, this type of model is more easily understood by decision makers and investors and the contribution of each factor is easily extracted. Finally, there is currently no evidence that knowledge-based or statistical models are superior.

PFA can lead to the discovery of new geothermal resources by reducing large formidable regions to smaller more focused areas for exploration. This reduces risk and up-front expenses. Both of the PFA methods used in the project have excellent potential for application, not only in the Tularosa Basin but in other areas as well – a very important consideration for the cost effective identification and development of geothermal resources across the entire United States.

1.2 Tularosa Basin Project Objectives

The overriding objectives of this project are to: (1) develop a knowledge-based PFA applying petroleum industry logic; (2) develop a stochastic WoE model; and, (3) compare and contrast the results. Additional objectives include economic modeling for the highest priority identified plays and development of a GIS database to support the project and marketing with the final future objective of power production.

1.3 Overview of Study Area

The Tularosa Basin is a graben located in the southern Rio Grande Rift (Fig. 1). The study area covers approximately 6500 km^2, much of which is underexplored. Several factors went into the selection of the Tularosa Basin. It was primarily chosen because it is a challenging, yet ideal test bed to evaluate effectiveness of PFA.

Additionally, Tularosa Basin is home to several military installations including White Sands Missile Range and Fort Bliss, which are the first and second largest U.S. Army bases in the United States, together covering more than 10,000 km^2 of southeastern New Mexico. The much smaller Holloman Air Force Base also lies within the study area. Geothermal development in this area could help the military achieve its Net Zero Energy goals.

1.4 Study Area Characteristics

The Tularosa Basin study area has a complex tectonic history beginning with Paleozoic siliciclastic sedimentation on a once low-lying shelf of the North American Craton. This was followed by periods of crustal shortening, including Late Paleozoic deformation related to Ancestral Rocky Mountains uplift and the Late Cretaceous Laramide Orogeny. The current landscape has been shaped by extensional tectonics, with the resultant development of the Rio Grande Rift. Extension began in the Late Paleogene and is accompanied by high heat flow. However, seismic activity is infrequent, relative to that in the Great Basin to the northwest, indicating that extension may be slowing in this area.

Figure 1. Tularosa Basin study area, about half of which is military lands.

Historical earthquakes in the area are, in general, clustered in the northern part of the basin, suggesting that the basin opened on the southern end and active rifting is now focused in the northern reaches (Fig. 2).

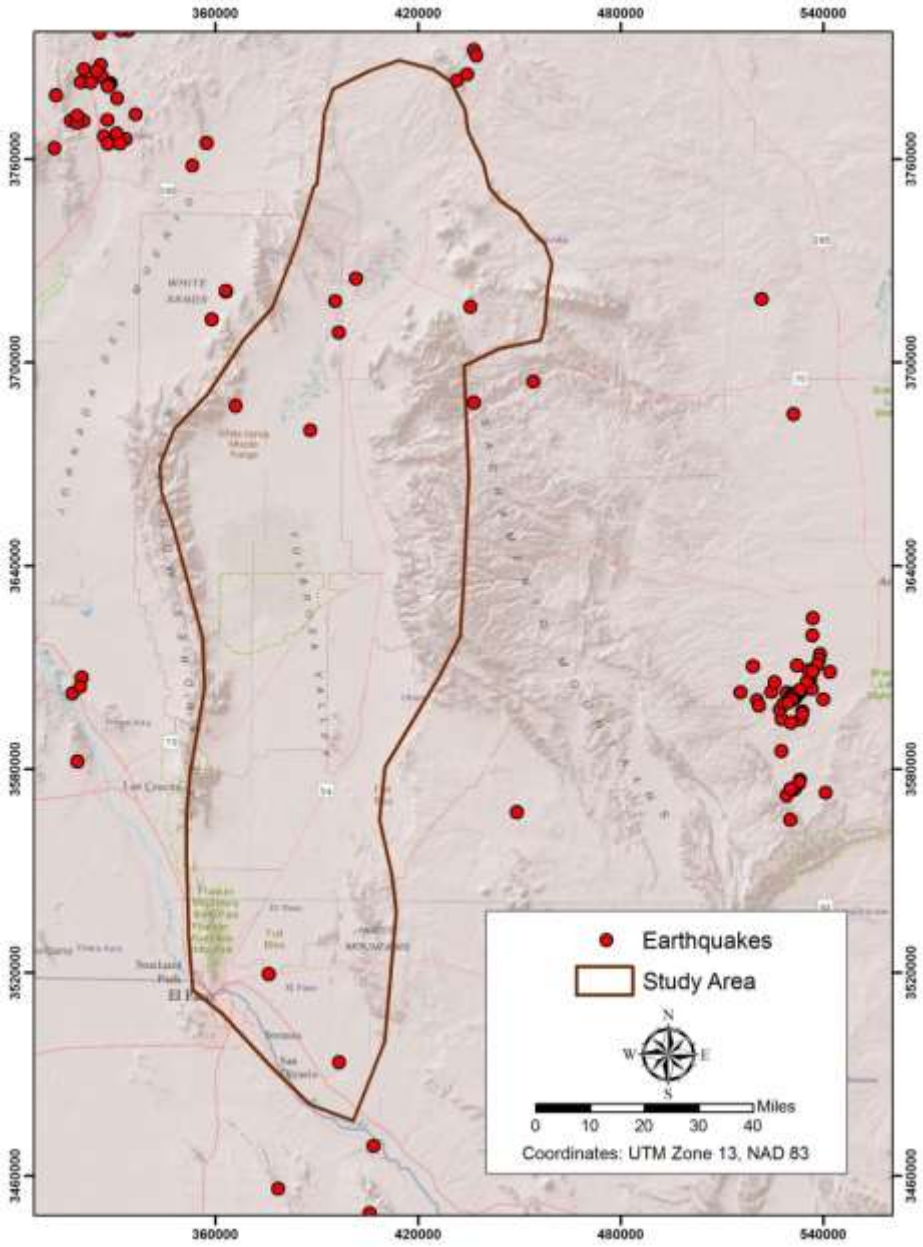

Figure 2. Tularosa Basin earthquakes, which tend to cluster at the north end of the valley, suggesting that active extension is migrating northwardly.

Four slim holes drilled in a 1997 SANDIA sponsored program near Davis Dome, in the southeastern part of the basin (Fig. 3), recorded high temperatures between 170°F and ~190°F (Finger and Jacobson, 1997) suggesting the presence of a promising geothermal system. More recently a study of McGregor Range, Fort Bliss, sponsored by the U.S. Department of Energy Geothermal Technologies

Office and implemented by Ruby Mountain Inc., resulted in the drilling of a new test well, RMI 56-5, again near Davis Dome, that reached a depth of 3,030 feet and encountered a high temperature near 200°F. Initial tests suggest a production rate of 300 gpm (Barker et al, 2015) and water chemistry suggests a reservoir temperature of 235°F (Barker et al., 2014).

The presence of a known geothermal system, Quaternary faults, and relatively high heat flow, suggest that additional geothermal systems may be present in the study area. This, along with military needs for green energy, gave rise to the need of basin-wide PFA to determine if additional promising plays exist.

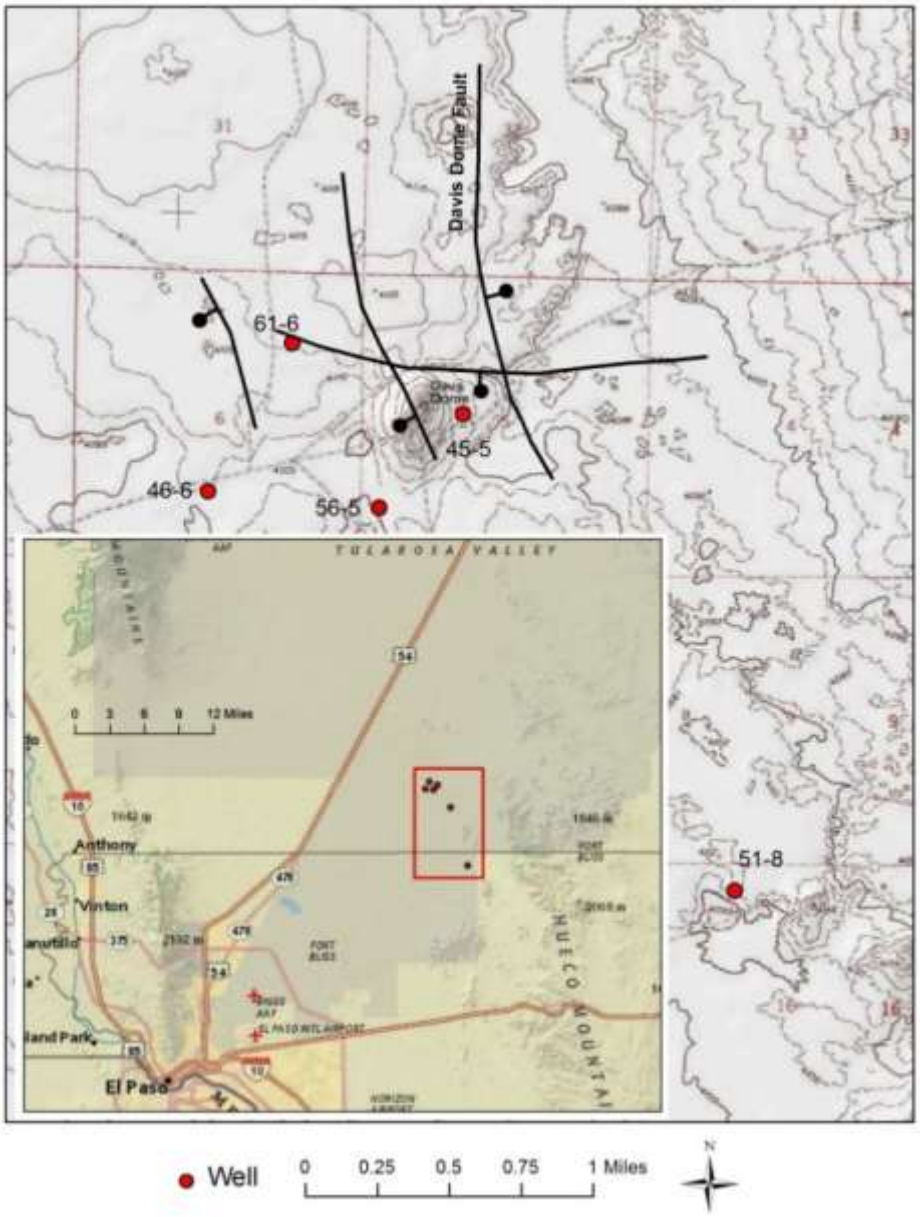

Figure 3. SANDIA slimholes 51-8, 46-6, 61-6, and 45-5 and RMI 56-5.

SECTION 2: DATA ACQUISITION & PROJECT DATABASE

2.1 Data Collection

From the onset of the Tularosa Basin PFA effort, the most daunting challenge was the accumulation of adequate data in the underexplored Tularosa Basin. Lack of credible data in adequate quantity would have posed a barrier to PFA model development. Through a variety of means, the project team was able to collect more data than thought possible at commencement of the effort.

As per DOE guidelines, all datasets used in Phase 1 of this study were derived from existing databases/repositories, previously published literature and existing unpublished data collected from local/regional sources. An exhaustive data collection effort was undertaken to support the development of layers of evidence for heat of the Earth, the presence of ground water for heat transfer, and the presence of faults for fracture permeability.

Operating on the assumption that increased outreach to, and cooperation from, potential stakeholders would lead to greater data collection success, the project team worked with key organizations and military reservations within the project study area to collect data and help facilitate information exchange about the Play Fairway Analysis effort.

Rather than having a single project kickoff meeting with all potential stakeholders invited, the team opted to meet with key stakeholder groups individually to brief them on the PFA concept in general, our project specifically, and to assess their level of interest in geothermal energy development in the area, and obviously to submit formal data requests. Specifically the following actions were undertaken as part of the data collection effort:

1. Internet literature review
   RMI initiated the data gathering process in mid-August of 2014, scouring the internet and online databases for data relevant to the effort as requested by EGI's Dr. Greg Nash. Almost 500 papers and websites were reviewed which resulted in collection of almost 60 relevant documents, 45 web links to online research, heat flow maps and several water well maps - the most expansive of which was from the NM State Engineer's Office.

2. Review of pertinent data on existing databases
   RMI also located 15 searchable online databases and sent links to those websites to Dr. Nash at EGI. In addition, Dr. Nash accessed and collected information from several additional online databases including the NGDS, USGS, the State of New Mexico Geothermal Resources Database among others.

3. Collection of local/regional data
   Early on in the effort, RMI began to reach out to an initial set of stakeholders in the region for purposes of data collection. Initial contacts made included: Fort Bliss, El Paso Water Utilities, the University of Texas at El Paso, New Mexico State University and Mike Hillesheim with the National Renewable Energy Laboratory, White Sands Missile Range, the City of Alamogordo Water Utilities, Alamogordo Public Schools, the New Mexico State Engineer's Office – District IV, the New Mexico Environment Department's Water Quality Bureau in Las Cruces, Fort Bliss Water and the U.S. Army Corps of Engineers.

RMI collected a substantial amount of useful data from El Paso Water Utilities which included well locations, temperatures, well logs and water chemistry data for dozens of locations throughout El Paso County in the southern part of the study area, including several locations where warm water is known to exist. Although data was received from many sources, the cooperation from El Paso Water Utilities was by far the most successful during Phase 1.

Lastly, the project team realized that despite the extensive desktop reconnaissance and outreach efforts to key local agencies, there would likely be gaps in the data collection. To address this issue, RMI created an extensive list of additional contacts for agencies in New Mexico and for communities/utilities and water districts throughout the Tularosa Basin. This was done so that RMI could reach out to those agencies to infill data throughout the study area. RMI contacted many agencies on the list to help address data gaps, however not all agencies were responsive and additional follow up is planned for Phase 2.

2.2 Liaison with Military

While Fort Bliss was made aware of the PFA project upon initial implementation of the effort, a formal presentation to relevant staff was delivered on Wednesday, January 7, 2015. A copy of that presentation was previously submitted to DOE. Representatives from various directorates (departments) on the Post attended the meeting and it was determined that a Memorandum of Agreement (MOA) was needed for purposes of collaboration and information exchange. RMI drafted an MOA for submittal to the Office of the Staff Judge Advocate at Fort Bliss and it was executed by both parties.

Subsequent to execution of the MOA, RMI continued to brief our Fort Bliss staff contacts on project progress, and in fact, our project point of contact even accompanied Project Manager Carlon Bennett to White Sands Missile Range in order to help facilitate information exchange. Fort Bliss was very helpful during Phase 1 of the effort in setting up project briefings/data collection meetings with Fort Bliss Water and El Paso Water Utilities as well as arranging contact with the Army Corps of Engineers.

Concurrently with the efforts at Fort Bliss, a dialogue was opened up with White Sands Missile Range staff to both assess their interest in geothermal development and to gather any pertinent information which might be helpful in PFA development. Several meetings were held with WSMR staff and the Post has agreed to share results of some upcoming data collection with our project team.

Facilitating ongoing information exchange and maintaining positive working relationships with the Army is significant to the project. This is true not only because most of the identified geothermal plays up to this point are located on military lands, but also because the military is likely the largest beneficiary of geothermal development within the basin.

Any effective PFA methodology developed through this project will be a valuable tool for the geothermal industry interested in developing geothermal resources, but this is particularly true for DoD energy managers/decision makers who are charged with making significant, long-term energy investments with limited access to reliable, understandable geothermal data.

At present RMI and EGI estimate that over two dozen military installations – most located in the Western U.S. - are projected to have some level of geothermal power production potential.

2.3 Project Database Development

As stated previously, an exhaustive desktop reconnaissance effort was undertaken to gather and review data on the region. The principal goals of this effort were to:

- find data that are a direct indication of heat including temperature gradients, heat flow, and water chemistry to facilitate the calculation of geothermometers;
- find geologic data that may indicate fracture permeability; and,
- locate data indicating the presence of ground water.

The SMU Geothermal Laboratory 2011 heat flow map was also added (Blackwell et al., 2011). These data were collected in a digital format from multiple websites and in analog form from publications. The majority of data collected was evaluated and integrated into the project GIS, which was developed and maintained by EGI.

From our Phase 1 effort, 99 temperature gradient points, 414 water chemistry analyses with good charge balance, Quaternary faults, Pleistocene Lake Otero, and 6,192 water wells which penetrated ground water were added to the GIS. References to the data sources are listed in the GIS shapefile tables and/or metadata which are to be uploaded to the U.S. Department of Energy Geothermal Data Repository (GDR).

Supporting data were also added to the GIS for project support and to aid in future marketing efforts. These included land ownership, geology, shaded relief, regional Bouguer gravity, regional total magnetics, earthquakes, average temperature, depth to ground water, and volcanic age maps. Digital elevations models were also incorporated.

Additionally, both day and night acquisition ASTER (Advanced Spaceborne Thermal Emission and Reflection Radiometer) data were added and used to (1) map possible surface temperature anomalies, (2) relative outcrop clay, calcite, silica, and gypsum concentrations (mineralogic EGS implications), and (3) hydrothermal alteration.

Data collected during Phase 1 has been added directly into a GIS database or reformatted as necessary to allow its incorporation. All data will be carefully georeferenced to a common coordinate system, projection, and datum to facilitate model integration. Potential error and uncertainty related to the sources will be noted in the metadata and attribute tables.

SECTION 3: APPROACH TO PHASE 1 PFA DEVELOPMENT

3.1 Deterministic Play Fairway Analysis: Petroleum Logic Approach

The first PFA completed in the project was based upon petroleum industry logic. For petroleum PFA development, data representing charge, reservoir, and seal are integrated into representative composite risk segment (CRS) maps, which are then in turn integrated into the final PFA. In our geothermal PFA effort, we substitute heat of the Earth, ground water for heat transfer, and fracture permeability for the three CRS layers. Seal is not of great consequence because our PFA is designed to locate areas with high potential for fault related fracture permeability rather than permeable rock reservoirs upon which petroleum systems rely.

Classification rules for petroleum industry logic PFA are relatively simple and easy to understand. If all three CRS layers have the same risk class, then the final PFA class is the same. If a single CRS risk class is of higher risk, then the final PFA class is of the higher risk class. Examples can be seen in (Table 1).

Table 1. Petroleum PFA classification rule examples.

Charge CRS Class	Reservoir CRS Class	Seal CRS Class	Final PFA Class
Low Risk	Low Risk	Low Risk	Low Risk
Low Risk	Low Risk	Medium Risk	Medium Risk
Low Risk	High Risk	Low Risk	High Risk
Medium Risk	Medium Risk	Medium Risk	Medium Risk
Medium Risk	Medium Risk	High Risk	High Risk
High Risk	High Risk	Low Risk	High Risk

This simple classification scheme works well where a relatively even spatial distribution of all input data sets is present. However, modifications were necessitated because this was not the case for our study area. The modifications will be elucidated throughout the following descriptions of CRS and PFA development.

Heat of the Earth CRS

To develop this CRS, temperature data points representing temperature gradients and quartz Geothermometers were interpolated into statistical surfaces using the deterministic IDW (inverse distance weighted) technique found in the ArcGIS software package. The statistical surfaces were then classified in the ArcGIS map document using Layer Properties>Symbology as follows:

Temperature gradients (Fig. 4):
0 ^{o}C/km – 60 ^{o}C/km = High Risk
60 ^{o}C/km – 80 ^{o}C/km = Medium Risk
>80 ^{o}C/km = Low Risk

Quartz Geothermometer (Fig. 5):
0 ^{o}C – 60 ^{o}C = High Risk
60 ^{o}C – 80 ^{o}C = Medium Risk

>80 ^{o}C = Low Risk

The ArcGIS Reclassify tool was then used to permanently apply these classes to new output files (ArcToolbox>Spatial Analyst Tools>Reclass). The output raster files were then vectorized (ArcToolbox>Converation Tools>From Raster>Raster to Polygon) for CRS integration.

Heat flow (Fig 6) was digitized as vector data directly from the SMU 2011 heat flow map (Blackwell et al., 2011). It was classified as follows (mW/m^2):
55 – 70 = High Risk
70 – 85 = Medium Risk
>85 = Low Risk

New fields were then added to each of the three CRS input file tables, with field heading names unique to the given dataset (e.g. TempGrad_Class), and populated with risk classes. These will be carried over in the following Union process, which is the next step.

The ArcGIS Union overlay method (Geoprocessing>Union) was then applied to the three heat CRS input vector layers. This produces a “spaghetti map” (Fig 7). A new Final_Class field was then added to the table of the output “spaghetti” vector file. Data queries were then be run to select sets of data for classification, e.g. "Qtz_Risk" = 'Low' AND "TG_Risk" = 'Low' AND "HF_Risk" = 'Low', and, for the records selected, the new Final_Class field was populated as Low Risk in this example.

This initially followed the petroleum PFA classification rules. However, since there is an uneven spatial distribution of data, the heat CRS was overlain with input temperature gradient and quartz geothermometer data points and the vectorized heat flow map to help classify problematic areas. For instance a polygon may have input classes of (1) temperature gradient = High Risk, (2) heat flow = Low Risk, and 3) quartz geothermometer = Low Risk. This, according to petroleum industry logic, would make the polygon High Risk. However, upon inspection of the input data, if no temperature gradient control points were found within or nearby the polygon, this dataset would have been considered low priority. Conversely, if geothermometer control points, in the Low Risk class, were found within the polygon this data would be assumed high priority. This would give the quartz geothermometer dataset precedence and the polygon would have been classified as Low Risk. This requires additional work and data observation, but we believe that is it appropriate and so this method was used to classified questionable polygons. It takes more time, but it also helps the explorationist become better acquainted with the data.

The ArcGIS Dissolve method (ArcToolbox>Data Management Tools>Generalization> Dissolve) is then applied, based on the final risk field, to simplify the polygons for the final Heat CRS (Fig. 8).

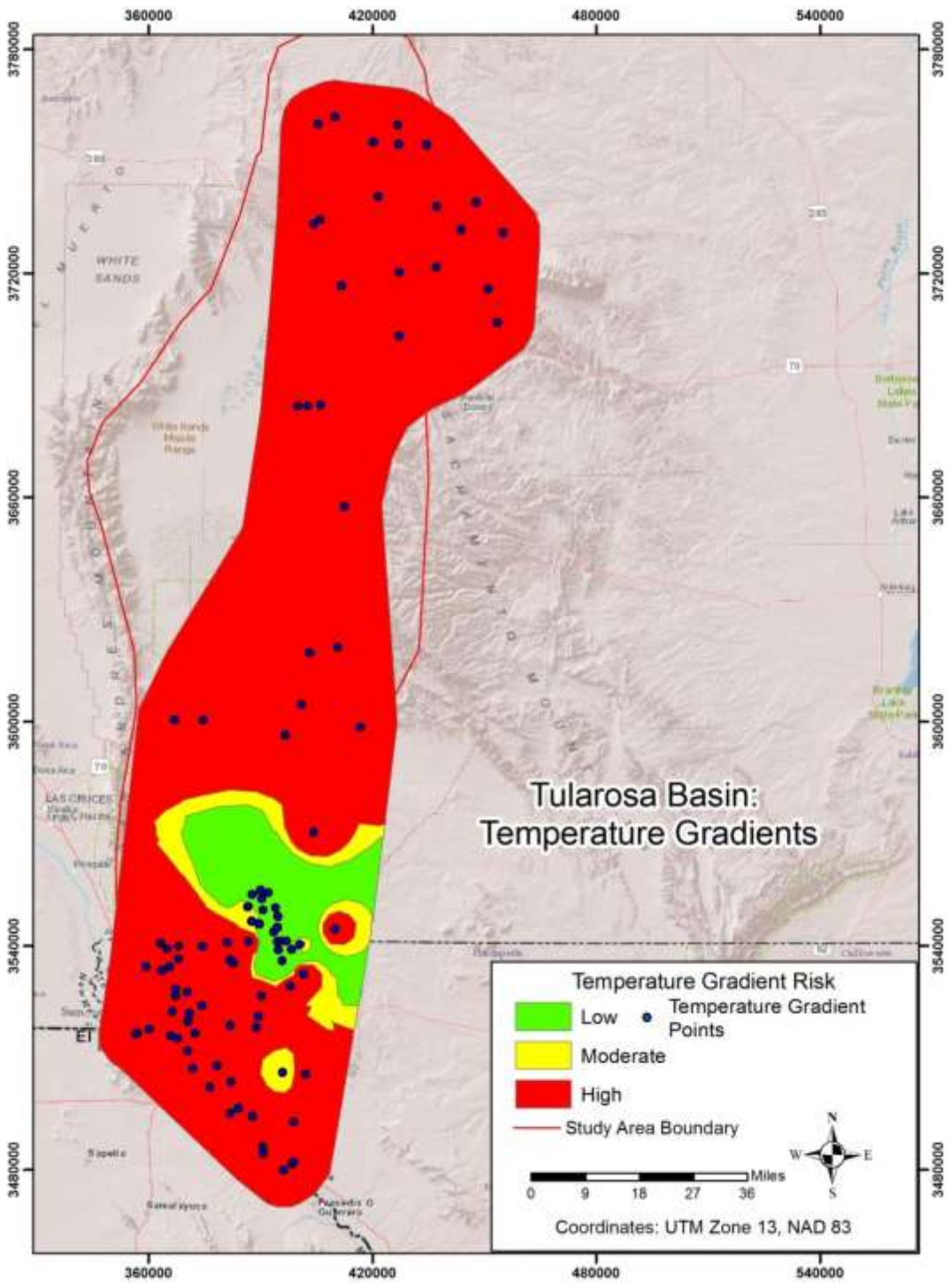

Figure 4. Heat risk -- temperature gradients.

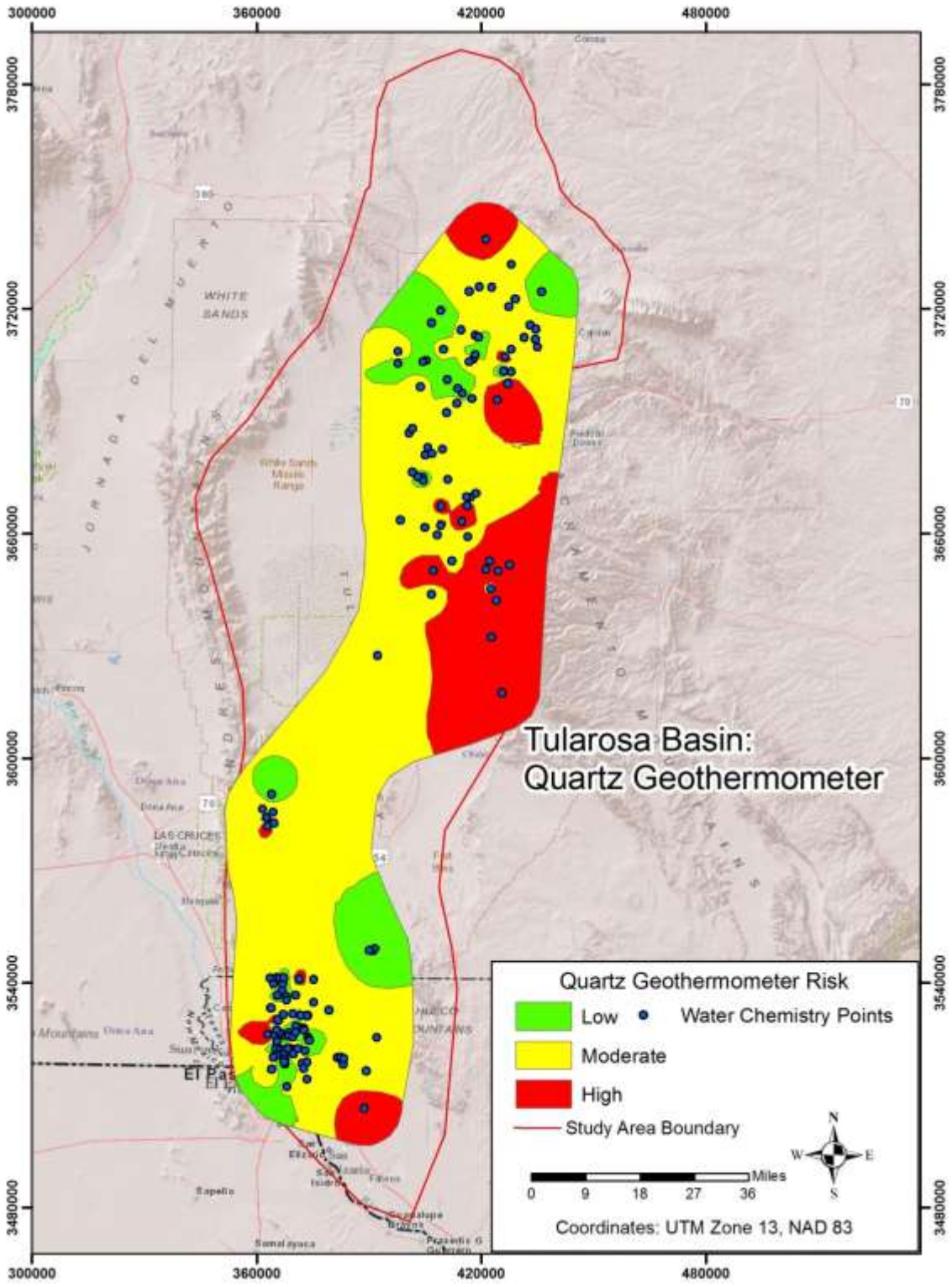

Figure 5. Heat risk – quartz geothermometers.

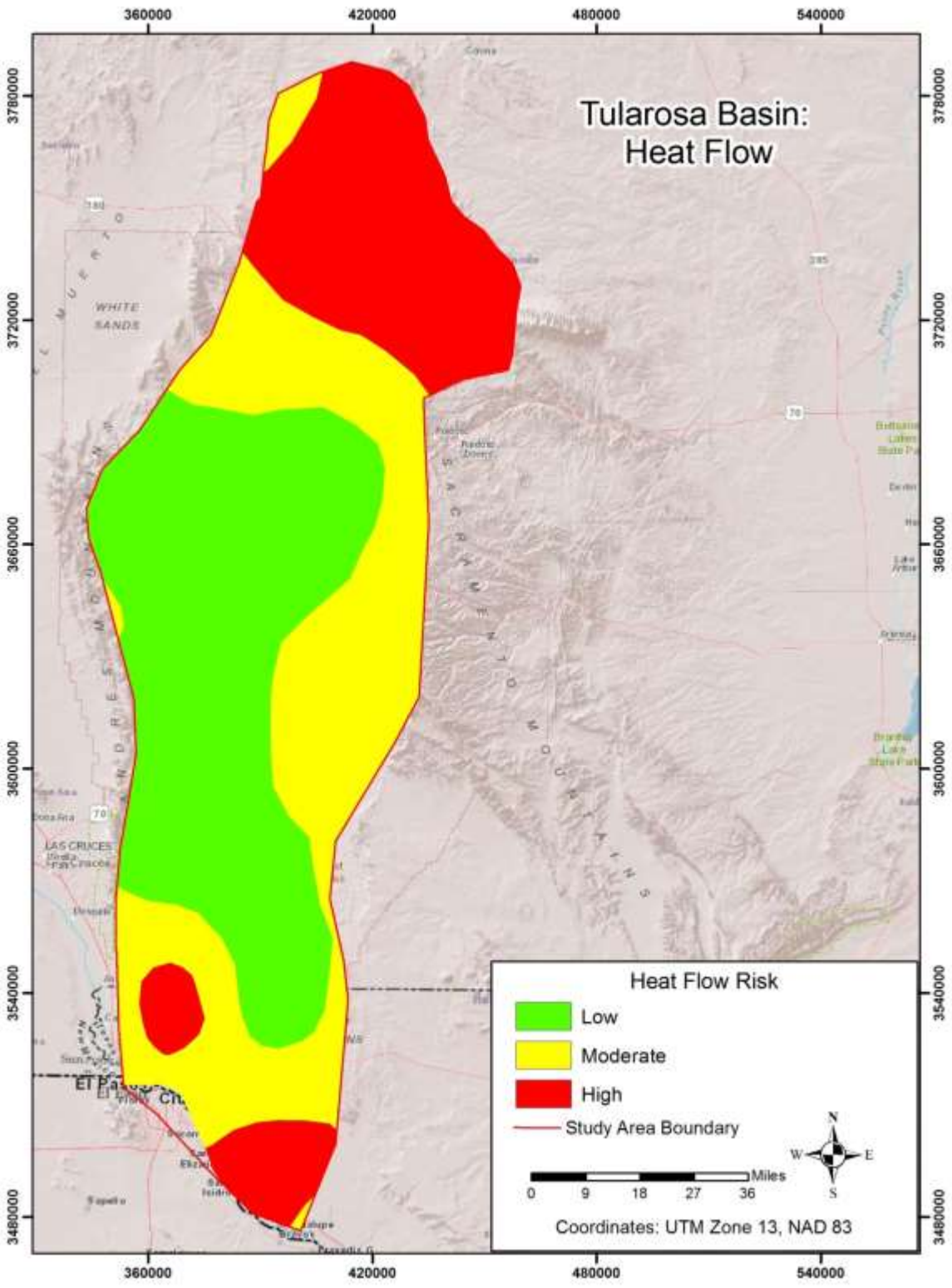

Figure 6. Heat risk – heat flow.

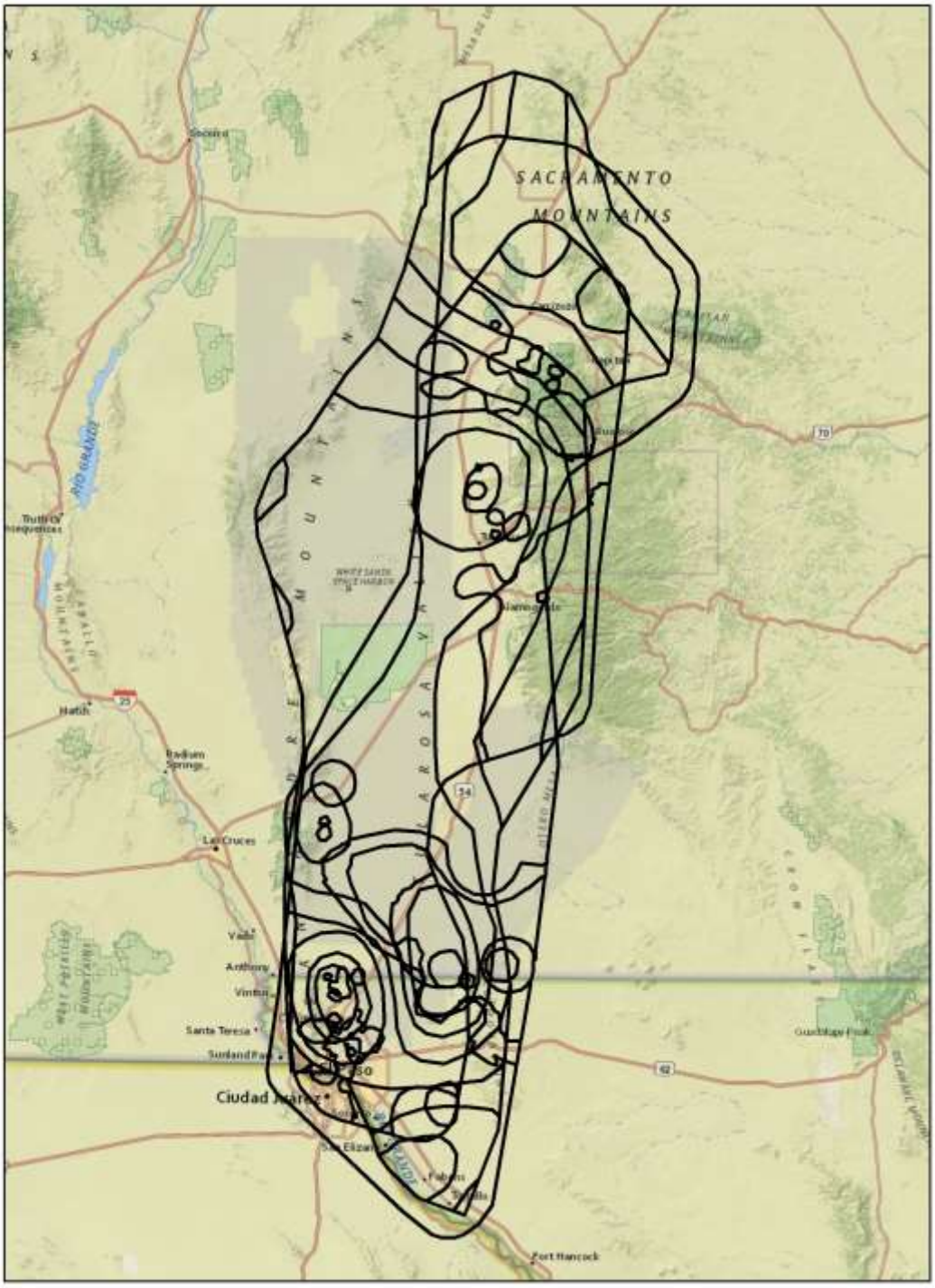

Figure 7. Graphic showing the spaghetti like polygons created using the Union overlay method.

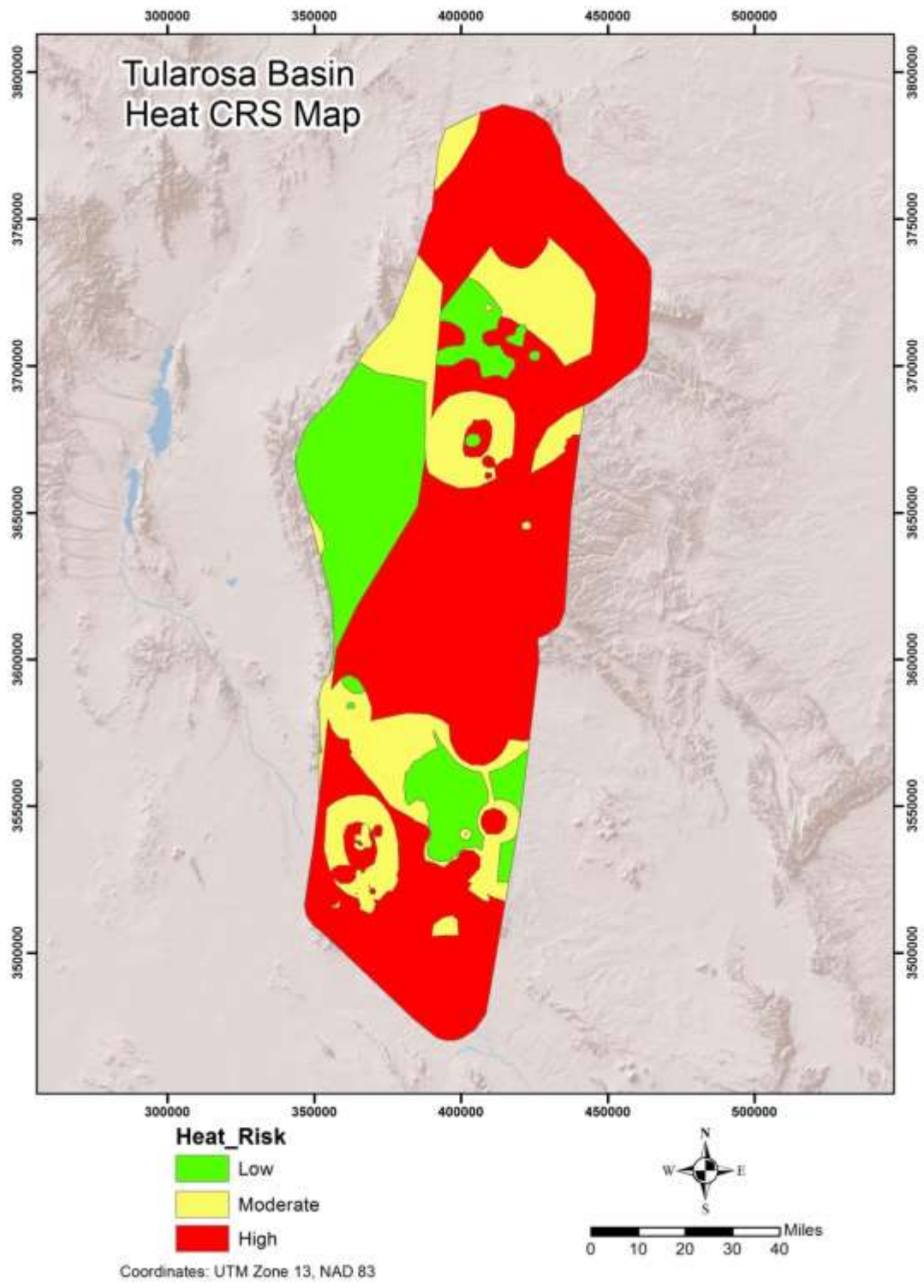

Figure 8. Final heat CRS after application of the Dissolve method.

Fracture Permeability CRS

This CRS was developed using Quaternary faults and zones of critical stress (Fig. 9) (Faulds et al., 2006, 2010, 2013). Quaternary faults were derived from the USGS Quaternary Fault and Fold Database of the United States. These were in a polyline shapefile. These data were Clipped to fit the study area (Geoprocessing>Clip) and the clipped lines were then buffered at a distance of 1 km. The resultant polygons were then all classified as Medium Risk. Quaternary faults and recent seismic actively are known to be related to permeability in geothermal systems, but fault slippage can both open and close fractures. Therefore, we believed that Quaternary faults needed to be represented, but not as Low Risk.

Zones of critical stress form in structural settings such as fault step-overs, terminations, apexes, intersections, and accommodation zones. Critical stress zones were mapped using analysis of aerial photography, Bouguer gravity, and total magnetic data. Each zone was considered to be encompassed within a 5 km diameter circle, except where evidence indicated that a larger area may be impacted. Resultant polygons were classified as Low Risk

The ArcGIS Union method was applied to the 1 km buffered Quaternary faults and the critical stress zones polygons and a new field was added to the result to hold the final classifications. The ArcGIS dissolve method was then applied to simplify the polygons, the results of which can be seen in Fig. 10.

Ground Water CRS

This CRS was developed using data from a point of diversion (POD) water shapefile obtained from the New Mexico office of the State Engineer and from drainage basin analysis in the Sacramento Mountains. Wells that had penetrated ground water and springs were extracted from the POD data and merged with water chemistry points were not redundant, and buffered at a distance of 2 km. The Pleistocene Lake Otero shoreline was also buffered at a distance of 2 km and this was Union overlain with the other water data. A trivial amount of new area was also edited in based upon the results of the drainage basin analysis. Dissolve was applied to simplify the resultant polygons. These polygons were given a class of Low Risk (Fig.11). All other areas in the basin were considered to be High Risk, although a good deal of the High Risk area may contain ground water, there is just no data to support it.

Final Petroleum Industry Logic PFA

The final deterministic PFA was created by applying a Union overlay to the three CRS layers. This was followed by Dissolve to simplify the polygons. The PFA, which identified eight plays, can be seen on Figure 12. The methodology is detailed on a flow chart located in Appendix C.

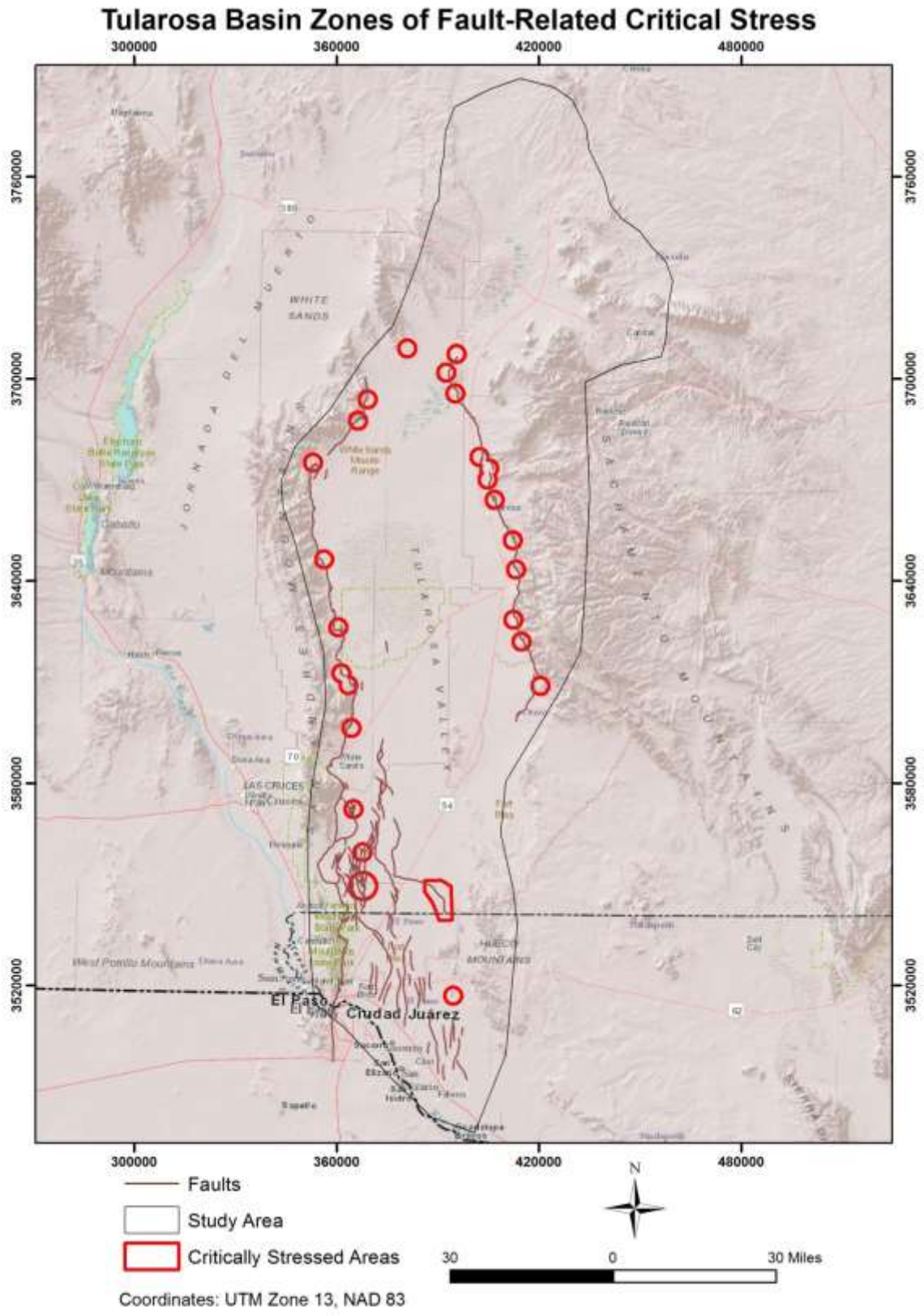

Figure 9. Study area Quaternary faults and zones of critical stress.

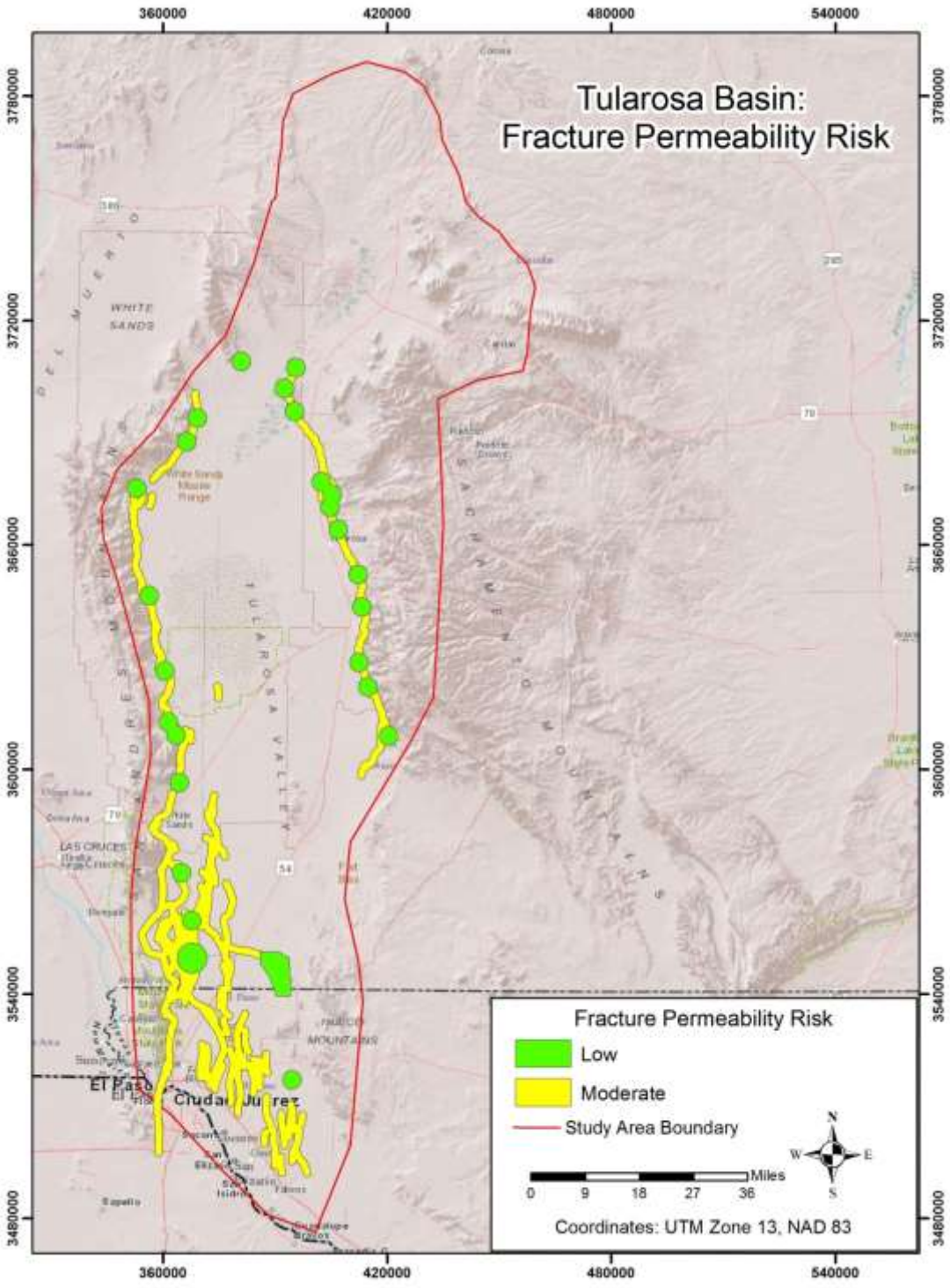

Figure 10. Fracture permeability risk CRS: Integration of Quaternary faults with a 1 km buffer (each side of fault) and 5 km diameter zones of critical stress. All areas within the study area boundary that are not colored are high risk.

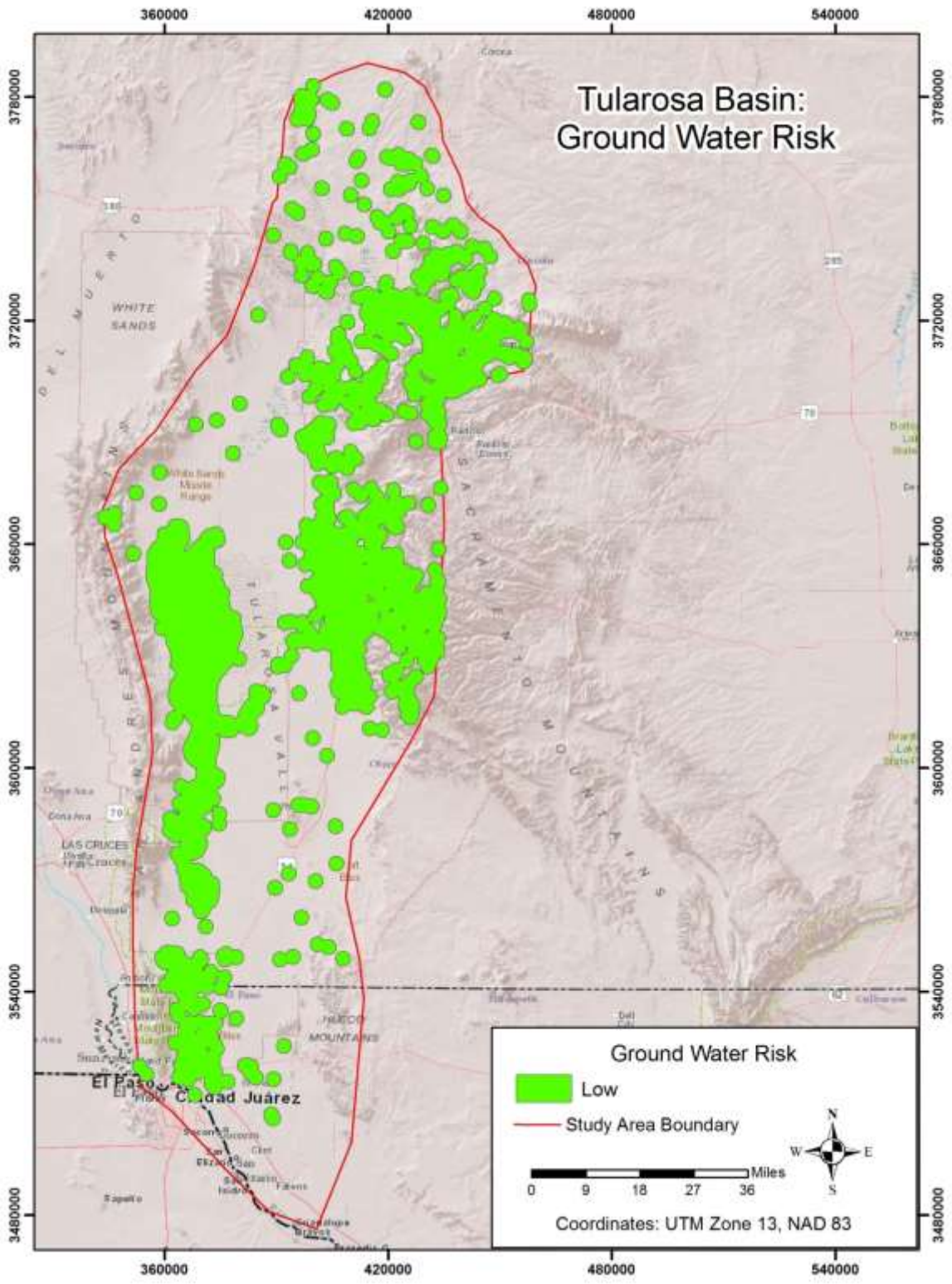

Figure 11. Ground water risk. All areas of the study area not colored in were considered to be high risk.

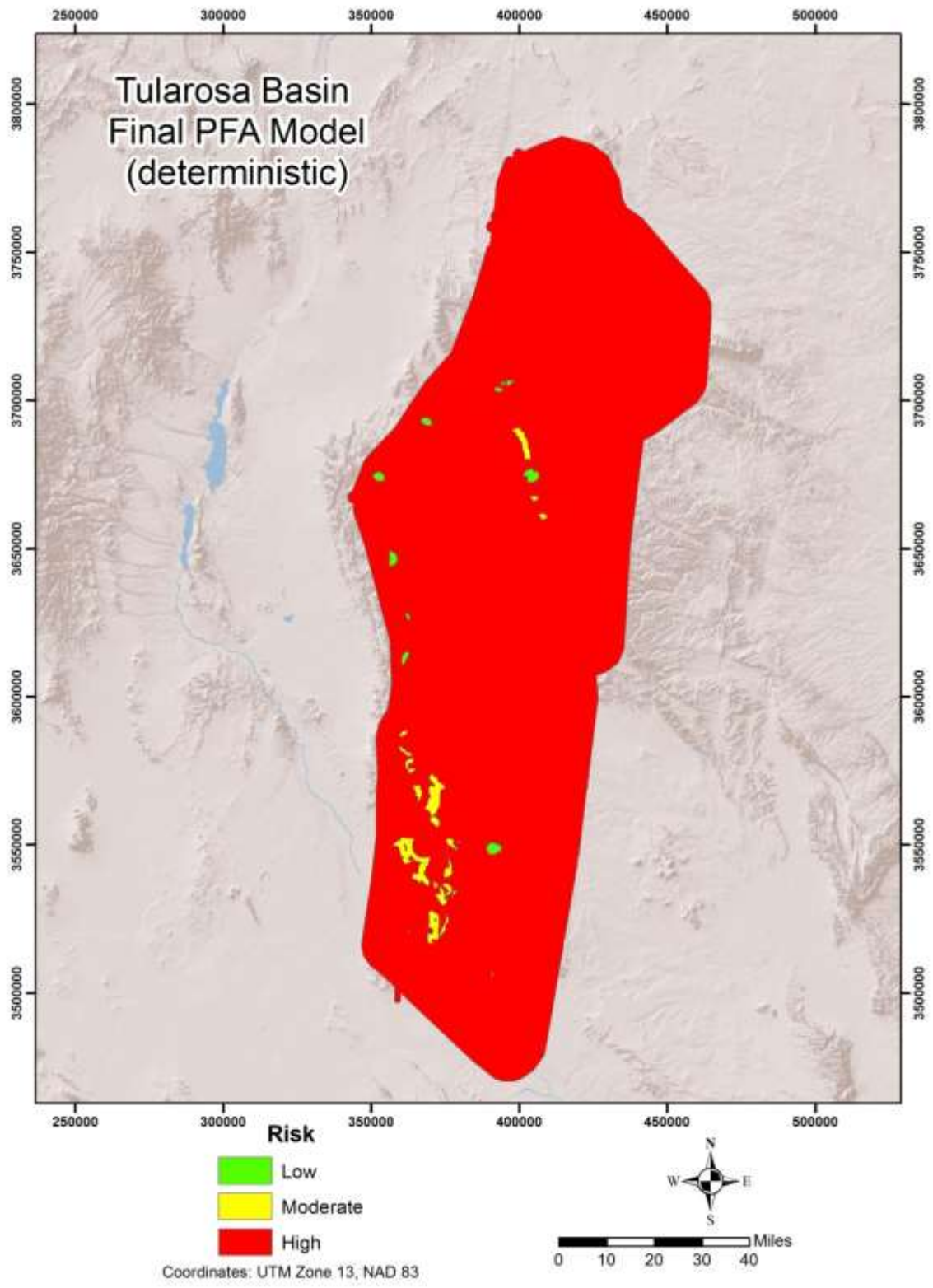

Figure 12. Final petroleum industry logic PFA. This model identified eight plays including the known geothermal system.

PFA Certainty

Certainty for this deterministic model was addressed in a deterministic way. Some data, such as fault traces, wells penetrating ground water, and zones of critical stress may have some elements of error, but this would be very difficult to ascertain in a desk-top exercise using existing data. However, there were several sources of heat data from a number of different sources and it was felt that confidence was bolstered for areas where all data sets were present.

Therefore, considering Heat CRS polygons, the following certainty classes were ascertained:

- All three heat data sets present: High Certainty
- Two heat datasets present: Moderate Certainty
- Only one heat dataset present: Low Certainty

The results can be seen on Figure 13. The low certainty areas were only represented by heat flow data because this is the only map covered the entire study.

3.2 Stochastic Play Fairway Analysis: Weights of Evidence Approach

The weights of evidence (WoE) method was used in this PFA because Moghaddam et al., 2013, found it to be the superior stochastic method, out of several tested, for geothermal exploration model development. This technique examines multiple layers of evidence, calculates weights for each evidential layer based upon the spatial relationships of training points, which are located at known geothermal systems and hot springs (in this case), and then produces a posterior probability raster surface and other related statistics.

A problem with applying this method in the Tularosa Basin was a lack of training sites. This was addressed by creating statistical surfaces for training that covered Nevada, Utah, and New Mexico. This gave access to ample known geothermal areas and hot springs for training. Spatial Data Modeler was used for the WoE analysis (Sawatzky et al., 2009)

Evidence of Heat

Water chemistry was compiled into an ArcGIS shapefile from the Great Basin Groundwater Geochemical Database from the Nevada Bureau of Mining and Geology (http://www.nbmg.unr.edu/Geothermal/GeochemDatabase.html) and additional data from the Oregon Institute of Technology Geo-Heat Center (http://www.oit.edu/orec/geo-heat-center). Redundant points were removed and the quartz (conductive) geothermometer (Fournier, 1991) was calculated. The inverse distance weighted (IDW) interpolation method was then applied to the quartz geothermometers using ArcGIS to create a raster statistical surface (Fig. 14).

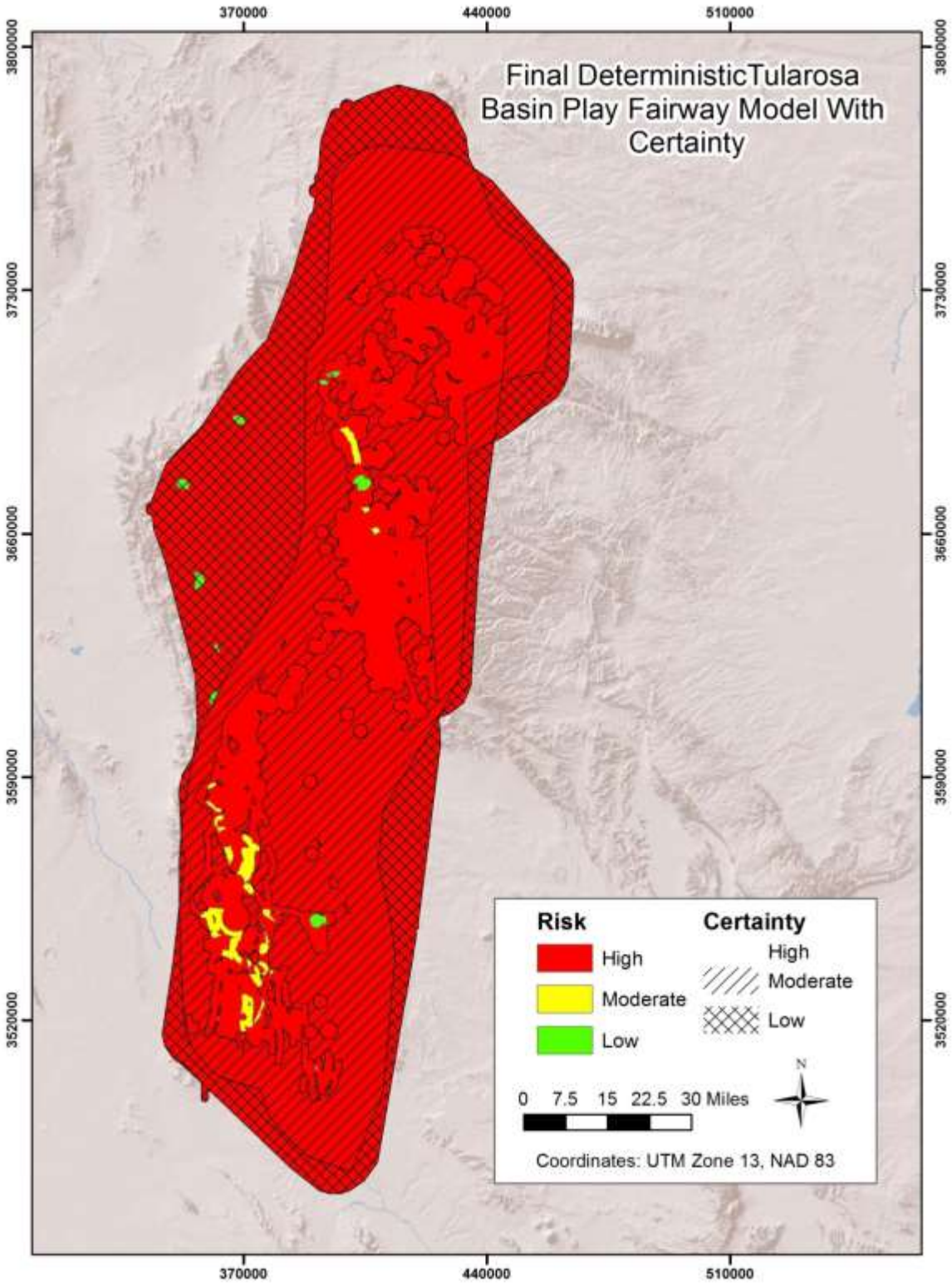

Figure 13. Deterministic certainty draped over the final deterministic PFA model.

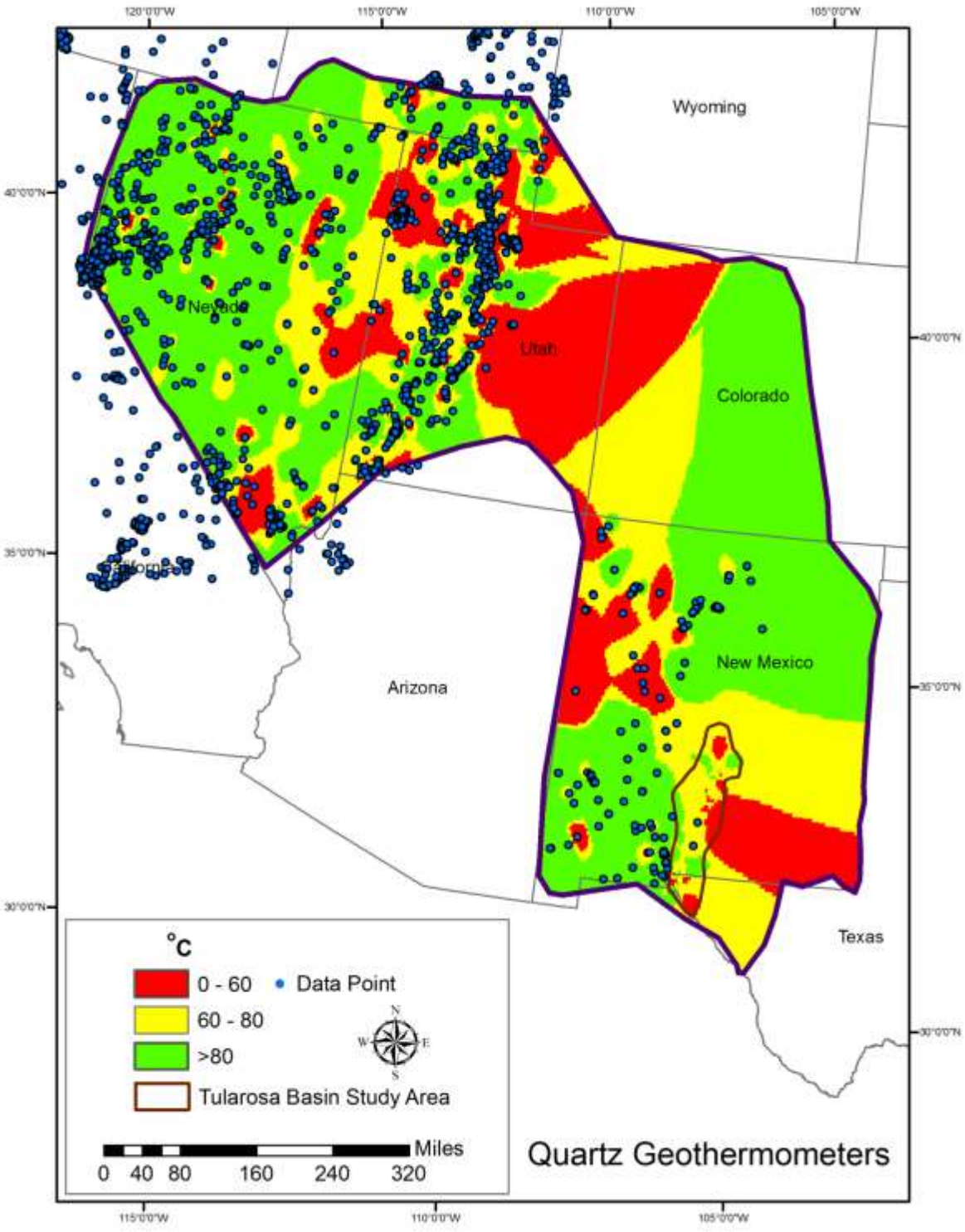

Figure 14. Quartz geothermometer evidential layer overlain with data points. Extrapolation was allowed beyond data points, but training area were all in data rich areas.

Extrapolation was allowed into areas with no data for this evidential layer. However, training sites were only chosen in data rich areas where the statistical surface was very accurate.

The same process was also applied to heat flow and temperature gradient data, originating from the SMU Geothermal Laboratory (http://www.smu.edu/dedman/academics/programs/geothermallab). The temperature gradient statistical surface produced for use in the previously discussed deterministic model, which was created with additional data, was then integrated into the new temperature gradient surface. The results of which can be seen in Figures 15 and 16.

Fracture Permeability

Evidence of fracture permeability was once again represented by the Quaternary faults from the USGS Quaternary Fault and Fold Database and the Faulds Structural Inventory of Great Basin Geothermal Systems and Definition of Favorable Structural Settings (http://en.openei.org/datasets/dataset/structural-inventory-of-great-basin-geothermal-systems-and-definition-of-favorable-structural-setti2). The Faulds data were converted into a shapefile and integrated with the critical stress zones points mapped in the Tularosa Basin. Points with unknown conducive structural settings were removed and the remaining points buffered to 5 km. This was then integrated into a training data boundary layer where zones of critical stress were classified as 1 and other areas as 0 (Fig. 17). This was then converted into a raster layer (Fig. 18).

Quaternary faults were once again buffered to 1 km on each side of the trace. The buffer polygons were then classified as one and integrated with the boundary polygon (value 0). The resultant shapefile was then converted to a raster layer (Fig 19).

Training Sites

Fifty training sites were chosen, scattered through New Mexico, Utah, and Nevada, for use in WoE analysis. Steamboat Springs and the Dixie Valley production area in Nevada were left out because it was very doubtful that a similar system exists in the Tularosa Basin. The sites that were used can be seen in Table 2, Appendix B and the points seen on a map in Figure 20.

Weights of Evidence

In weights of evidence, positive weights indicate a significant contribution by the data whereas a negative value indicates no contribution. Therefore, an examination of class weights can help give a better idea of the data relationships to geothermal systems.

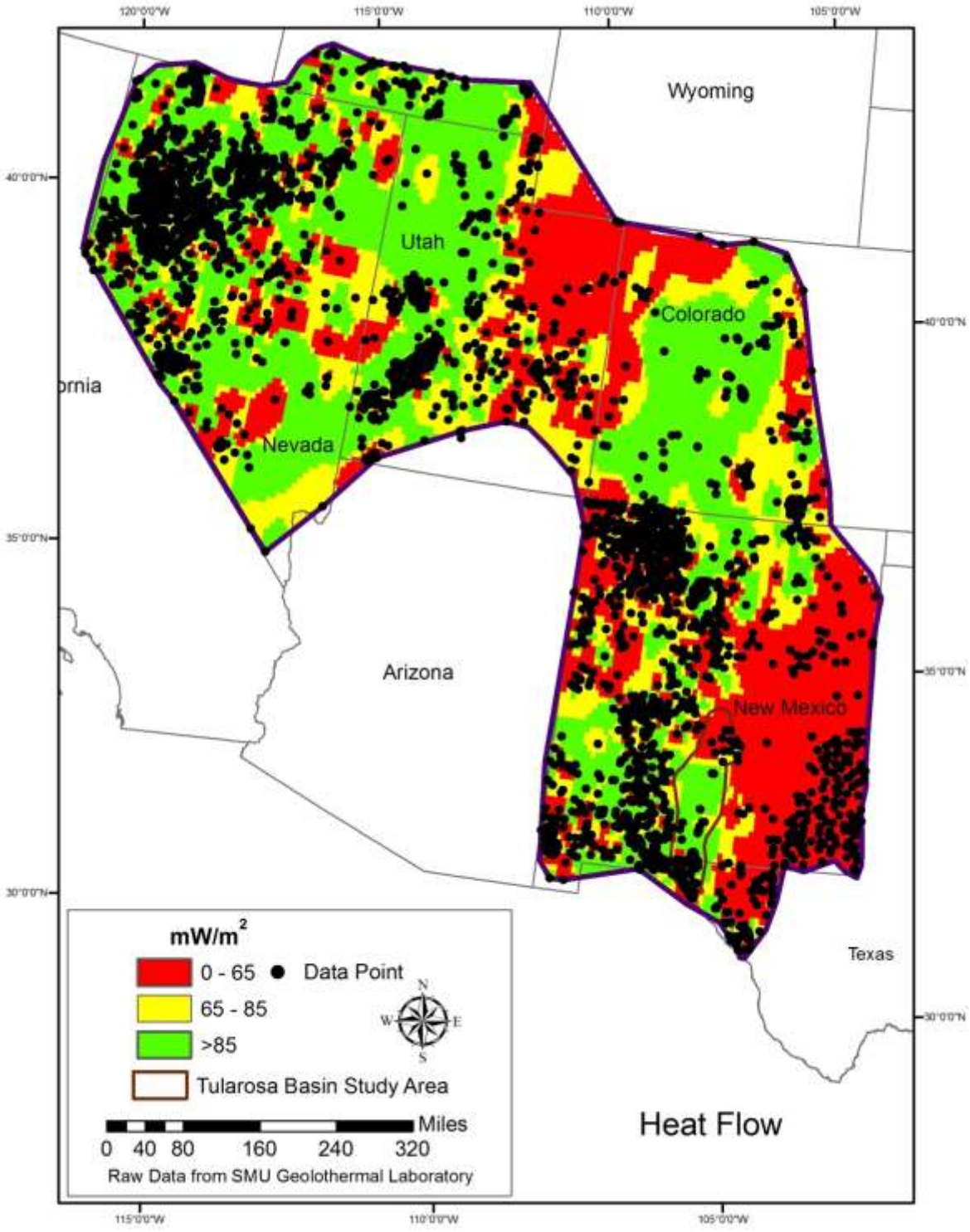

Figure 15. Heat flow evidential layer overlain with data points.

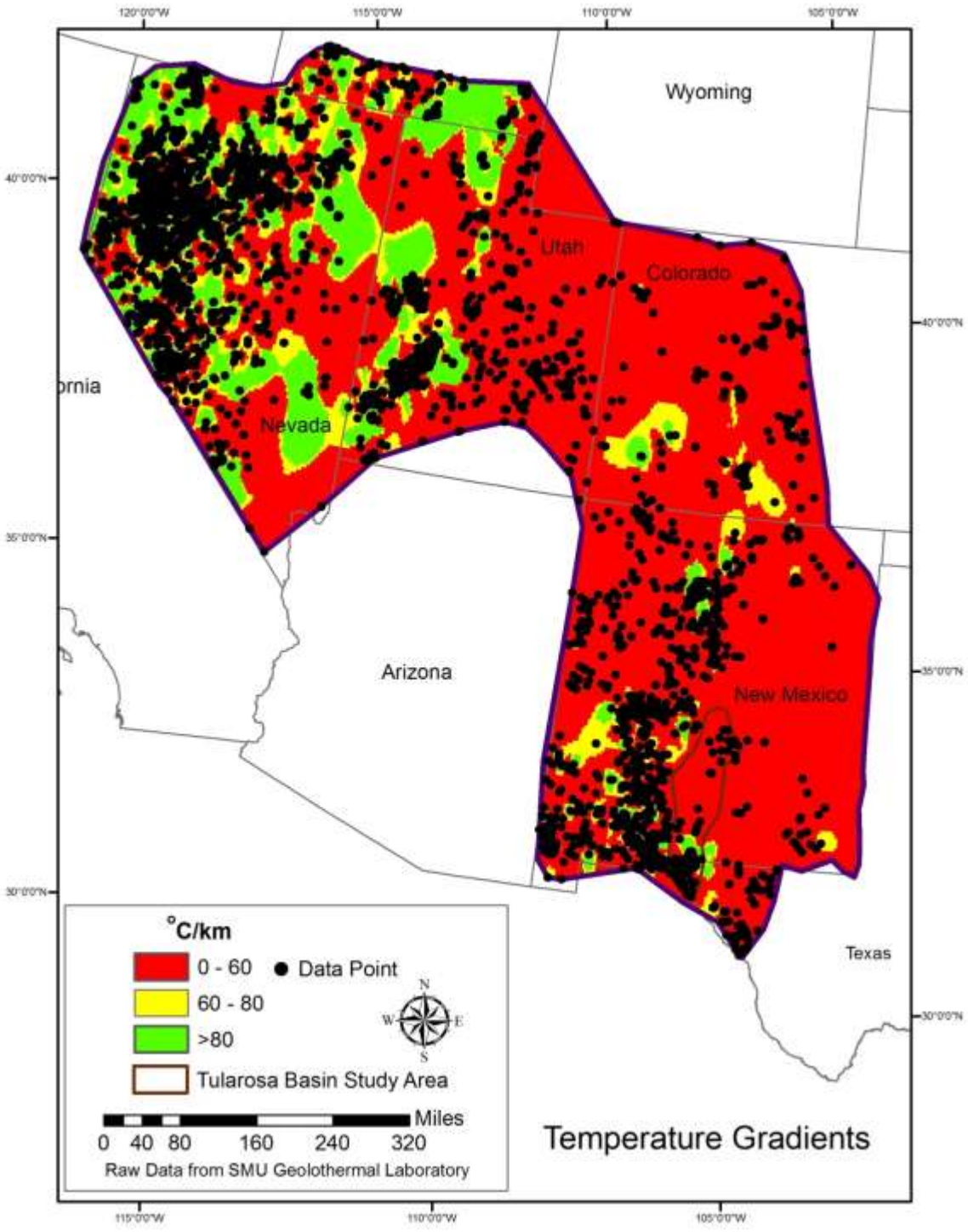

Figure 16. Temperature gradients evidential layer overlain with data points.

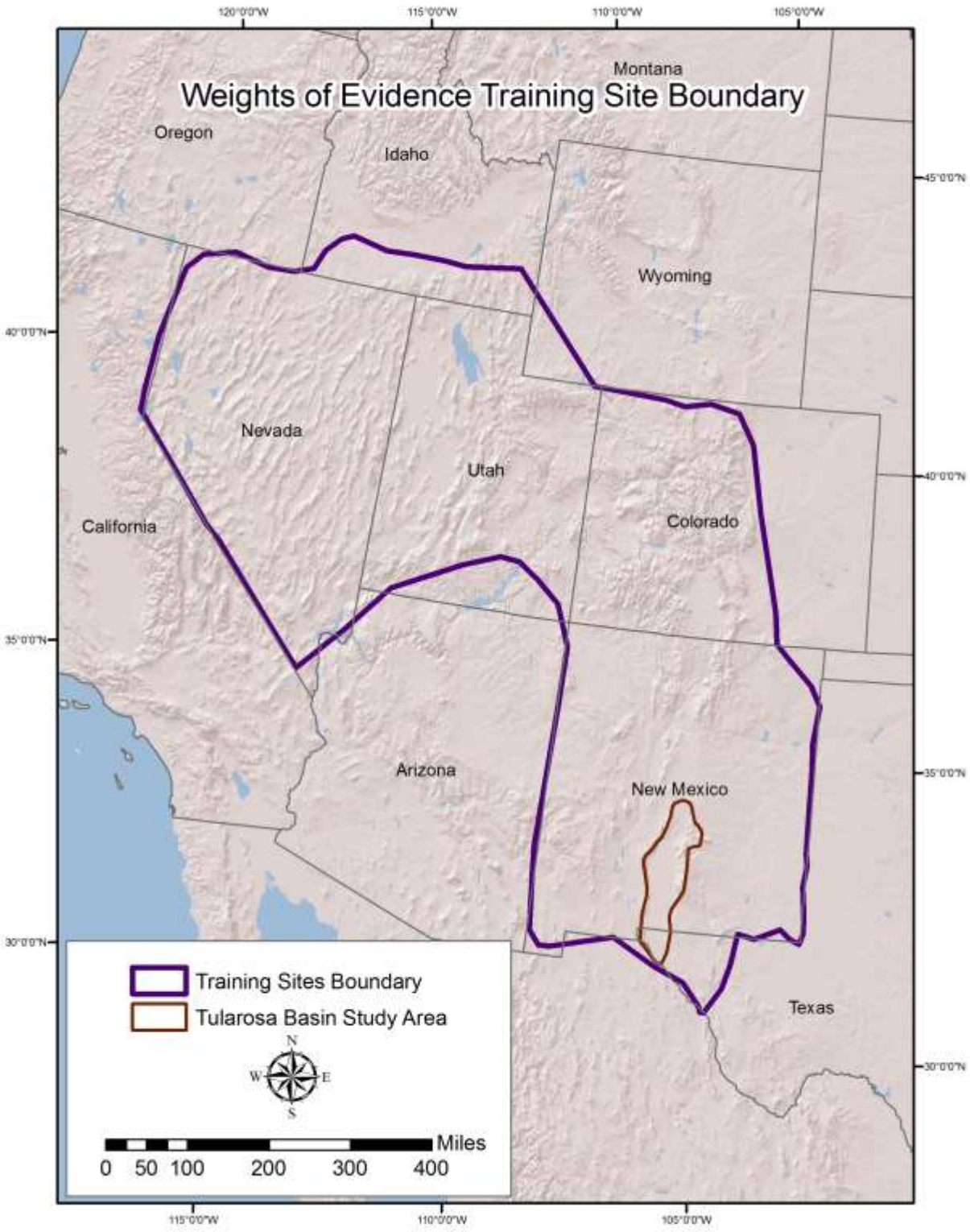

Figure 17. WoE training data boundary.

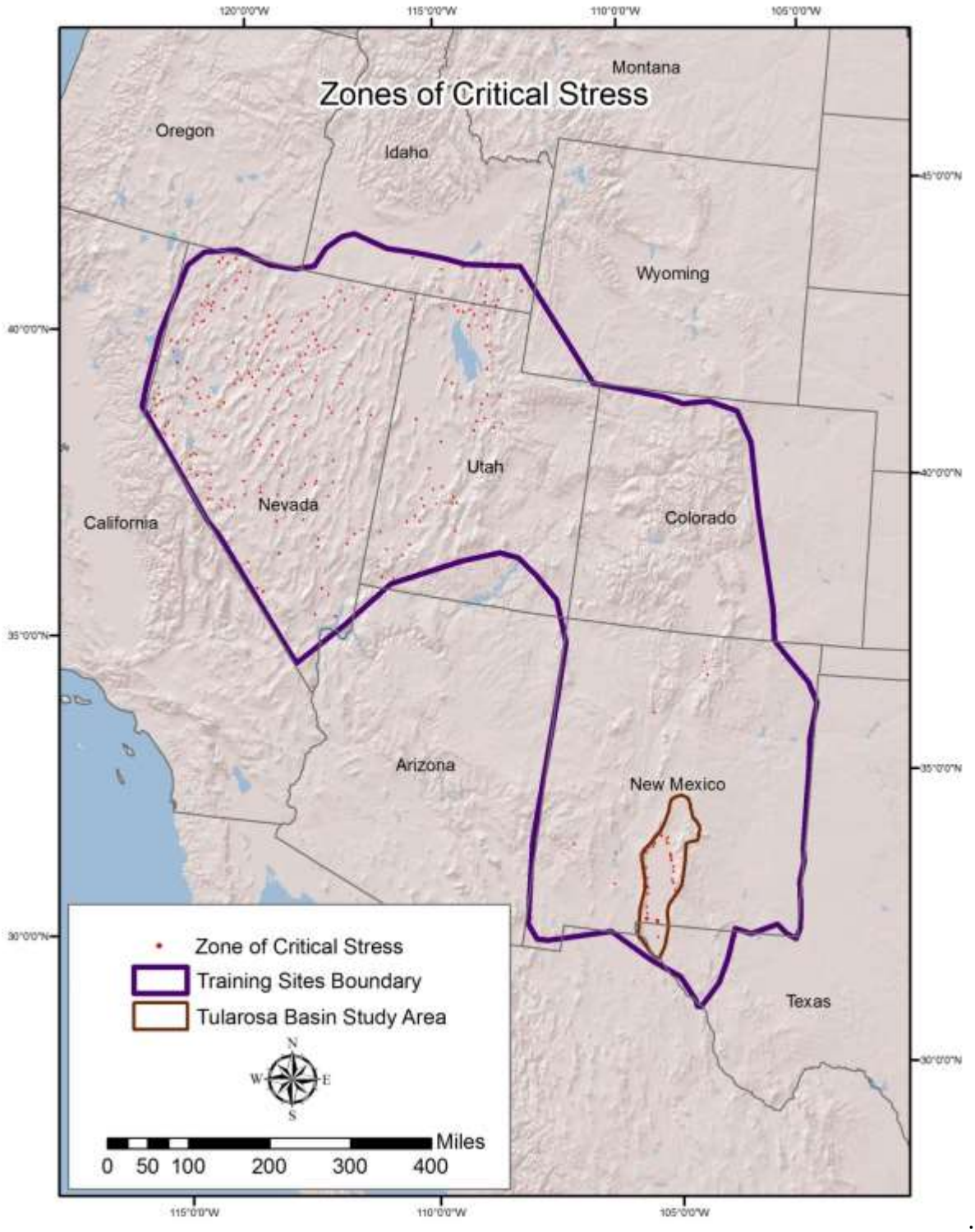

Figure 18. Zones of critical stress.

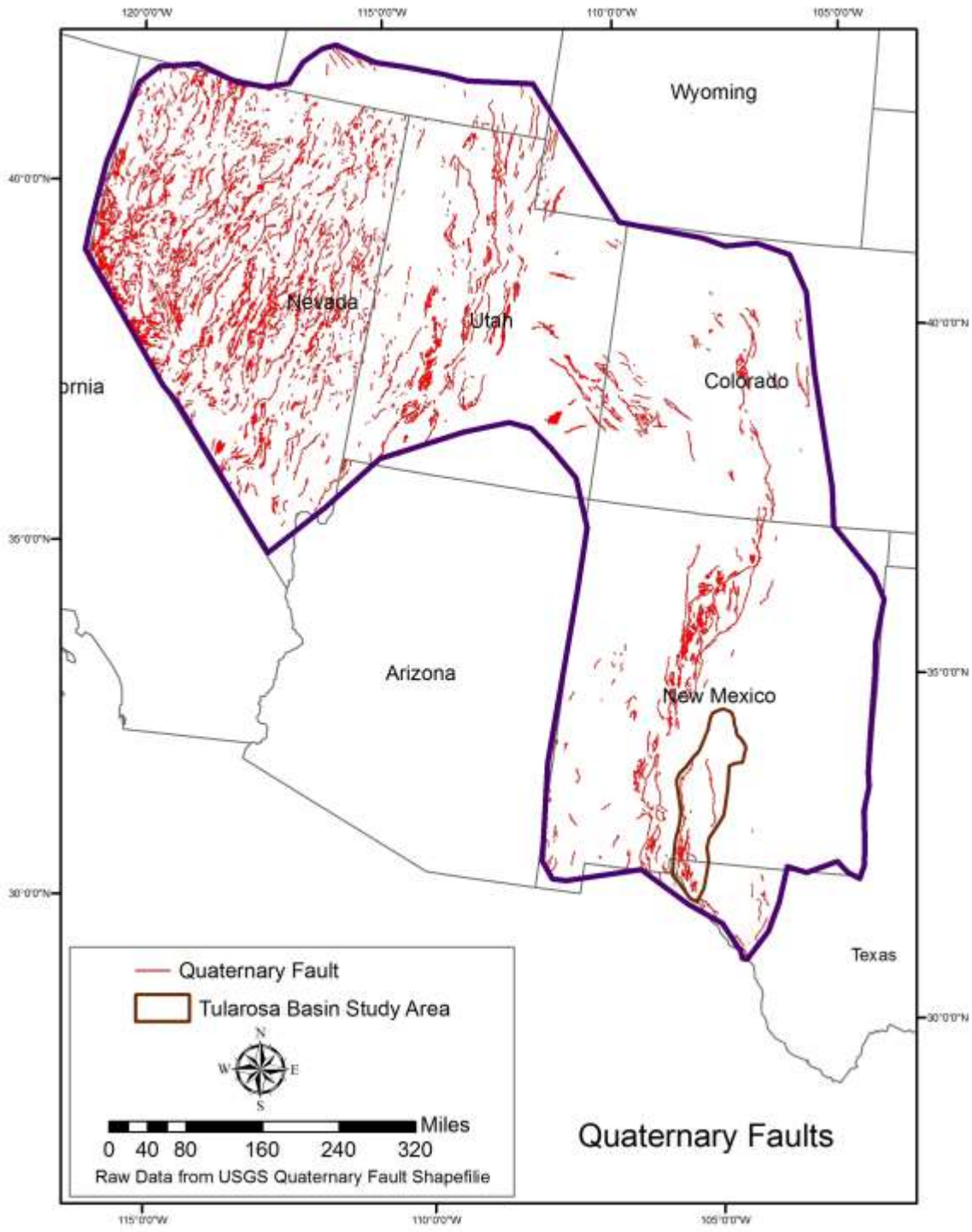

Figure 19. Quaternary faults buffered to 1 km (both sides of fault trace).

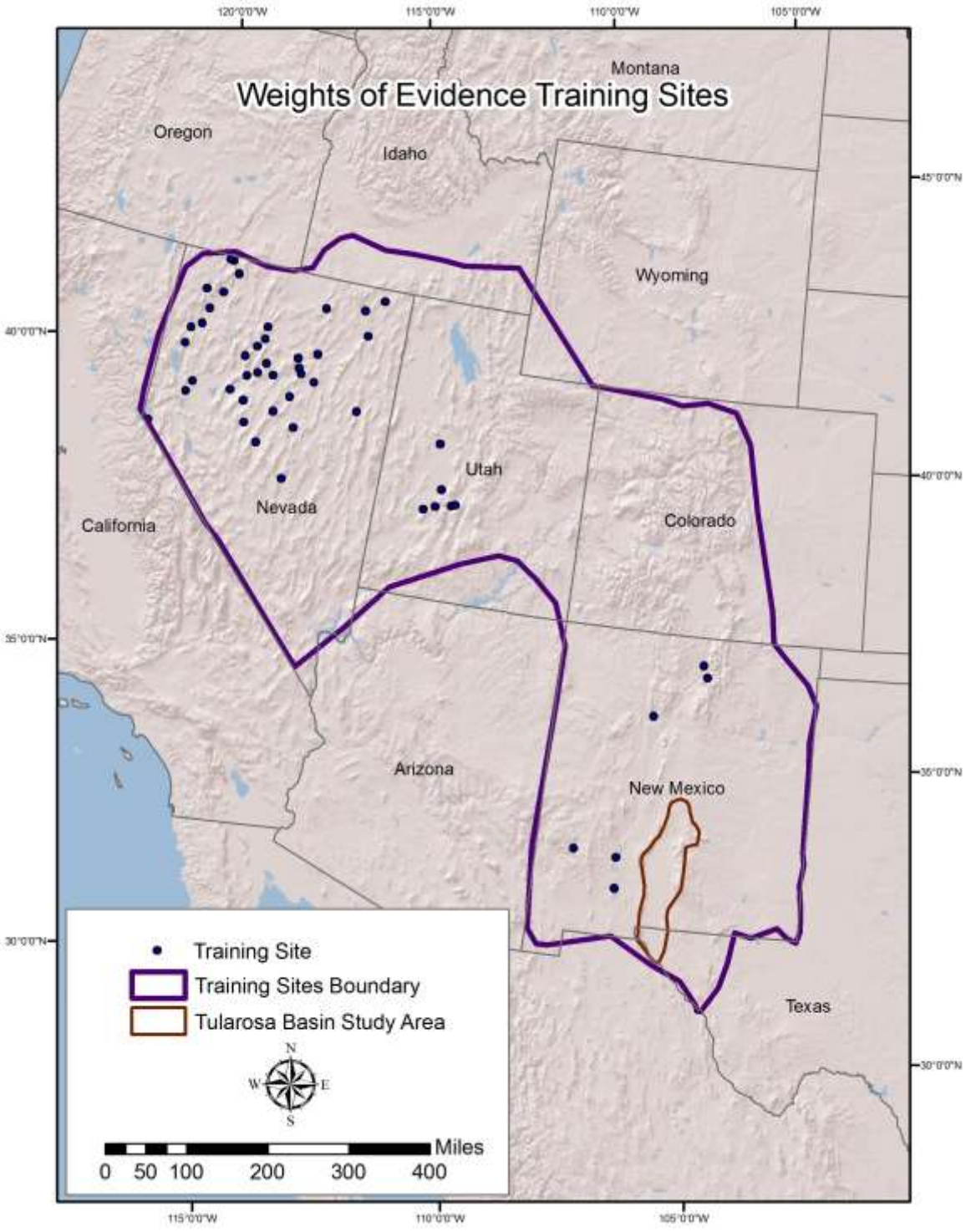

Figure 20. WoE training sites located at hot springs and known geothermal systems.

Heat Flow

The heat flow surface was divided into 15 classes using equal intervals. Positive weights were only produced for three classes:
Class 7, Range = 164 – 189 mW/m^2, Weight = 1.8805
Class 10, Range = 241 - 166 W/m^2, Weight = 2.6463
Class 13, Range = 319 – 343 W/m^2, Weight = 2.7381.

This indicates that in general, there is little relationship between hot springs and geothermal areas and temperature gradients lower than 164 mW/m^2 on the statistical surface.

Temperature Gradients

The temperature gradient surface was divided into 11 classes using equal intervals. Positive weights were generated for only four of these classes:

Class 5, Range = 80 – 100 $^oC/km$, Weight = 0.8071
Class 9, Range = 160 – 180 $^oC/km$, Weight = 1.9264
Class 10, Range = 180 – 200 $^oC/km$, Weight = 2.6685
Class 11, Range = >=200 $^oC/km$, Weight = 2.3096.

This indicates that in general, there is little relationship between hot springs and geothermal areas and temperature gradients lower than 160 $^oC/km$ on the statistical surface.

Quartz Geothermometers

The quartz geothermometers surface was divided into 5 classes using equal intervals. A positive weight was only produced for one class: Class 5, Range = >=100 ^oC, Weight = 1.0452.
This indicates that over the entire training area, hot springs and known geothermal areas generally have quartz Geothermometers higher than 100 ^oC.

Quaternary Faults
The Quaternray fault layer of evidence was a binary dataset. It produced the following weights:
Class 0 = -0.7771
Class 1 = 1.9035.

This indicates a good correlation between Quaternary faults and the training points (hot springs and known geothermal areas).

Zones of Critical Stress
The zones of critical stress layer of evidence was also a binary dataset. It produced the following weights:
Class 0 = -3.2137
Class 1 = 5.2212.

This shows that the critical stress layer of evidence had a very strong correlation with the training points (hot springs and known geothermal areas).

WoE Results

In general, based upon the WoE weightings, the Tularosa Basin would not be as likely as some areas (e.g. Dixie Valley and McGinnis Hills) elsewhere within the training data boundary, to contain a high enthalpy system. However, a new Dixie Valley was never expected and lower temperature plays, similar to the known McGregor Range system, can provide important energy to the military.

WoE identified ten plays (Fig. 21), six of which correlated with plays identified by the deterministic method and four which did not (Fig. 22). Of the four plays that were unique to the WoE method, two were given a low priority due to relatively low probabilities, and two were given medium-high priority due to relatively high probabilities, spatial relationships to input data points with permissible values, and certainty (Fig. 23). Water was also considered, although not inherently as part of the WoE. The ground water potential map created for the deterministic model was overlain on the WoE results and it was determined that all WoE plays have a good potential for groundwater (Fig. 24).

Certainty

A confidence surface was generated as a default part of the WoE analysis using Spatial Data Modeler and the result can be seen on Fig. 25, where all play areas have relatively high confidence. However, this was based upon the data for the large area used for training (Fig. 17).

Data specific to the Tularosa Basin study area boundary were also used to calculate probabilistic certainty using probability kriging on the three datasets for heat. The following thresholds were applied:
Geothermometers = 80 ^{o}C
Heat flow = 85 mW/m^{2}
Temperature Gradients = 80 ^{o}C/km

However, since the water chemistry data was clustered to three relatively specific areas, these points were split out into three separated datasets prior to kriging and probability kriging was then applied to each area. After probability kriging was completed on all of the datasets, the resultant probability raster images were classified as follows:
0.0 – 0.6 = Low Certainty
0.6 - 0.8 = Moderate Certainty
0.8 – 1.0 = High Certainty

The classified probability raster images were then vectorized. This was followed by a Union overlay and Dissolve to simplify the polygons. The results can be seen on Figure 26, where it can be seen that using localized data resulted in a more conservative layer of certainty.

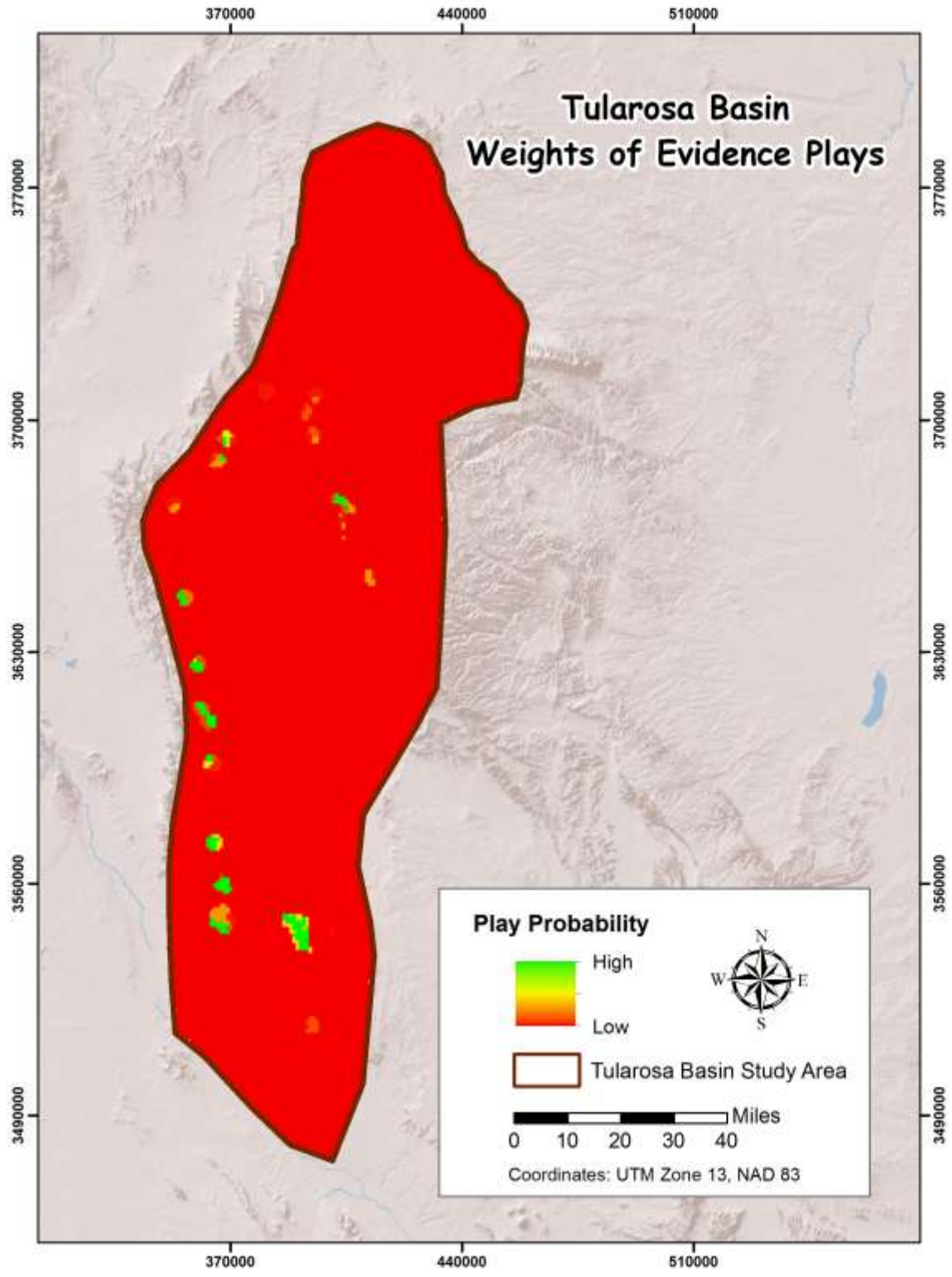

Figure 21. WoE final play probability map.

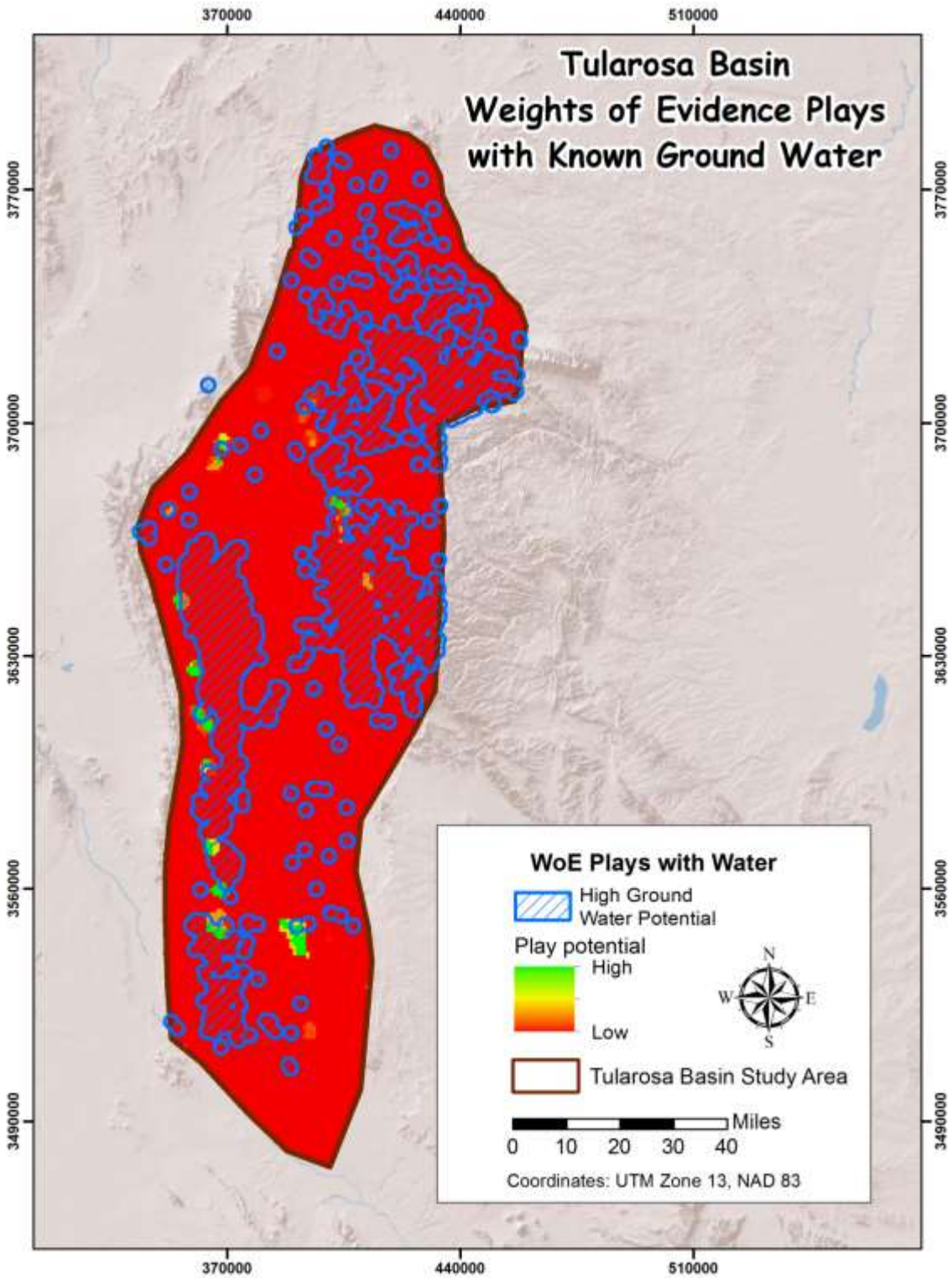

Figure 22. Ground water potential from the deterministic model overlain on WoE plays. Ground water potential is high on or bounding all plays.

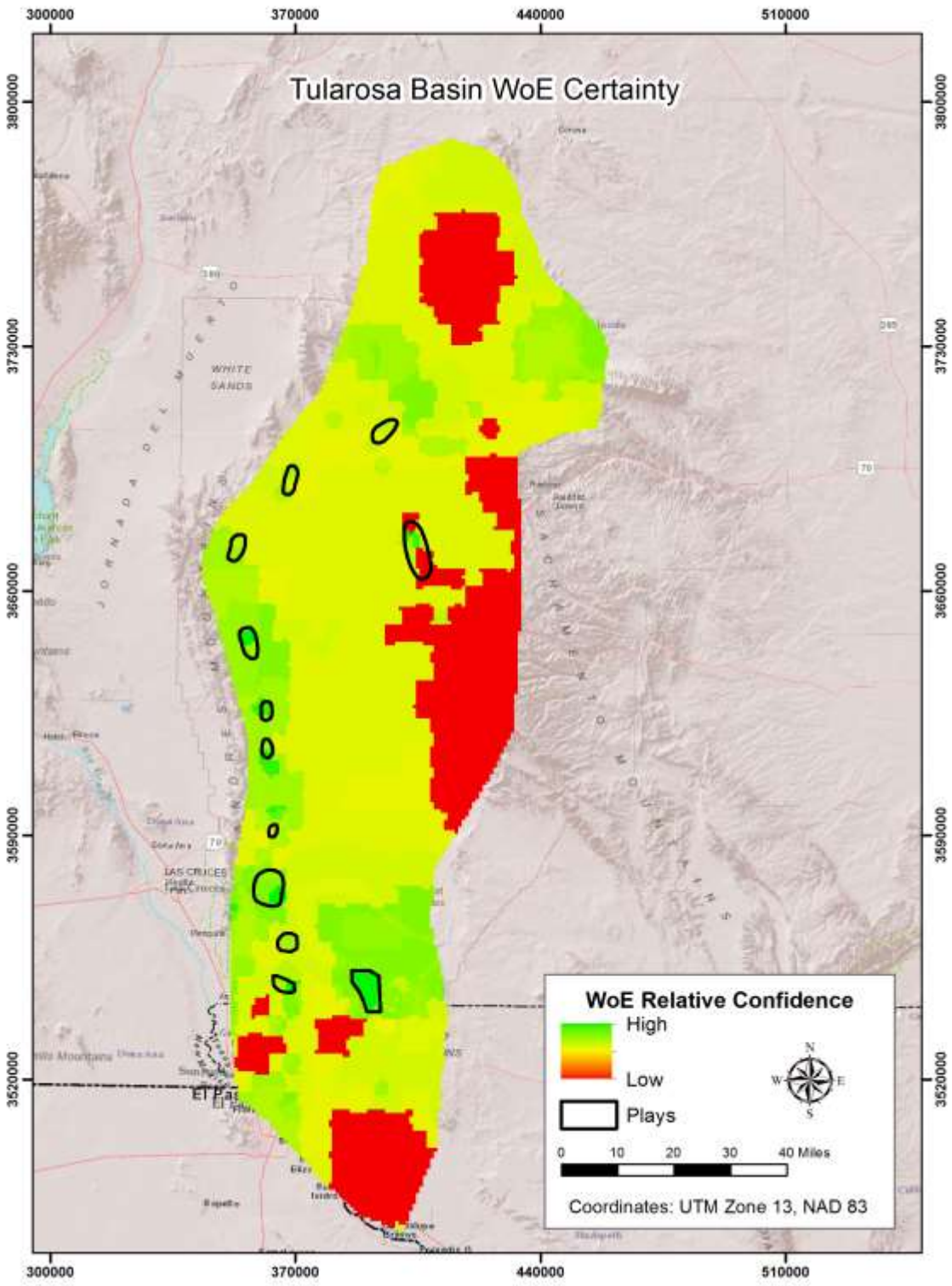

Figure 23. WoE confidence layer generated using the Spatial Data Modeler. All plays are in medium high to high confidence areas; although a single play also has low confidence areas included bounding a high confidence area.

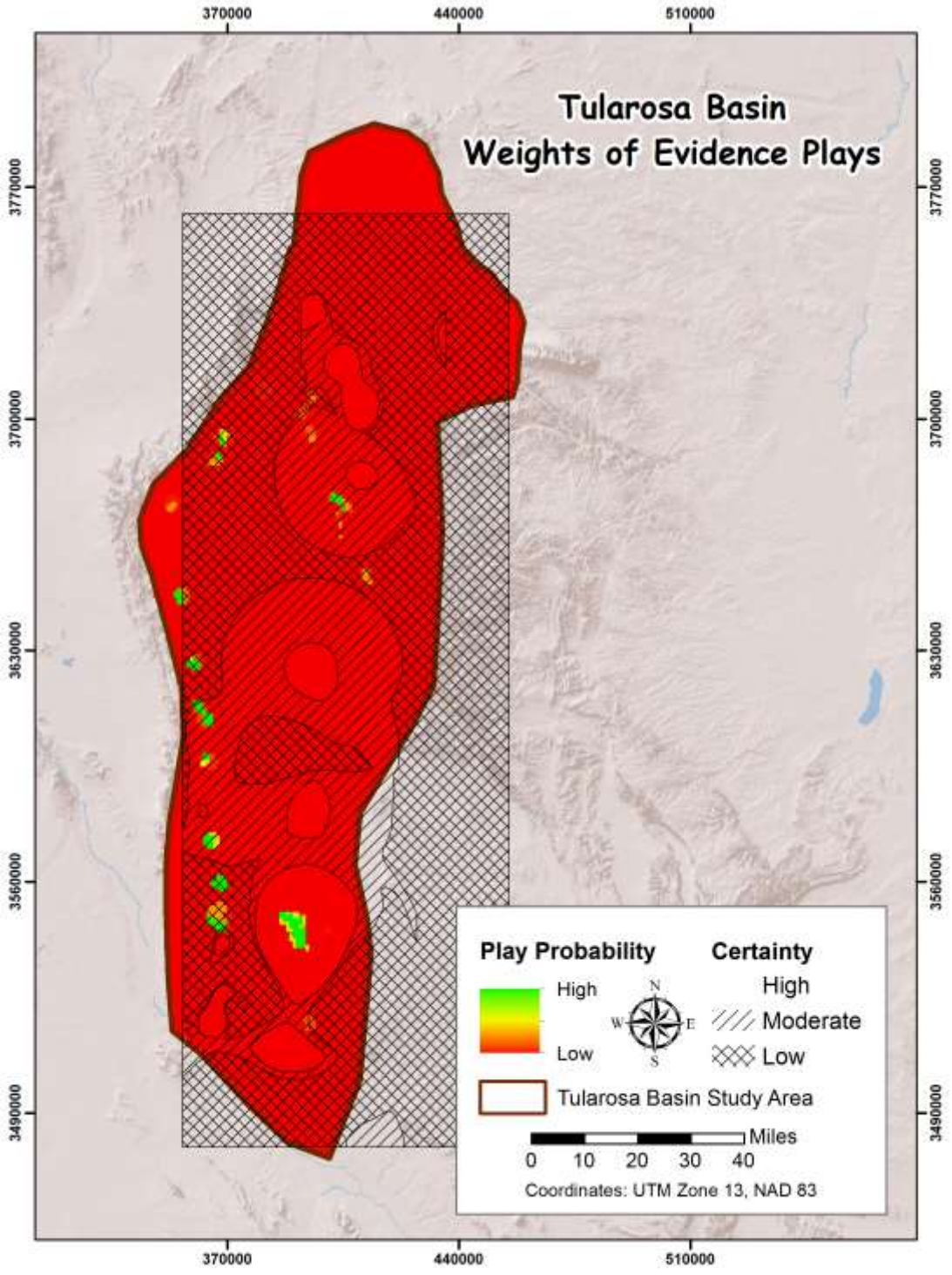

Figure 24. Certainty based upon probability kriging. Heat layers of evidence were used in this analysis, the results of which are more conservative than the WoE confidence surface with only the McGregor Range play having high certainty and three other plays having moderate certainty. Areas outside of the certainty polygon lack control data.

4.3 Compare and Contrast of Methods

Both the deterministic petroleum industry logic PFA, converted for geothermal use, and the WoE PFA methods identified potential plays. Six plays were identified by both methods with two additional plays being identified by the deterministic method and four additional plays being identified using WoE.

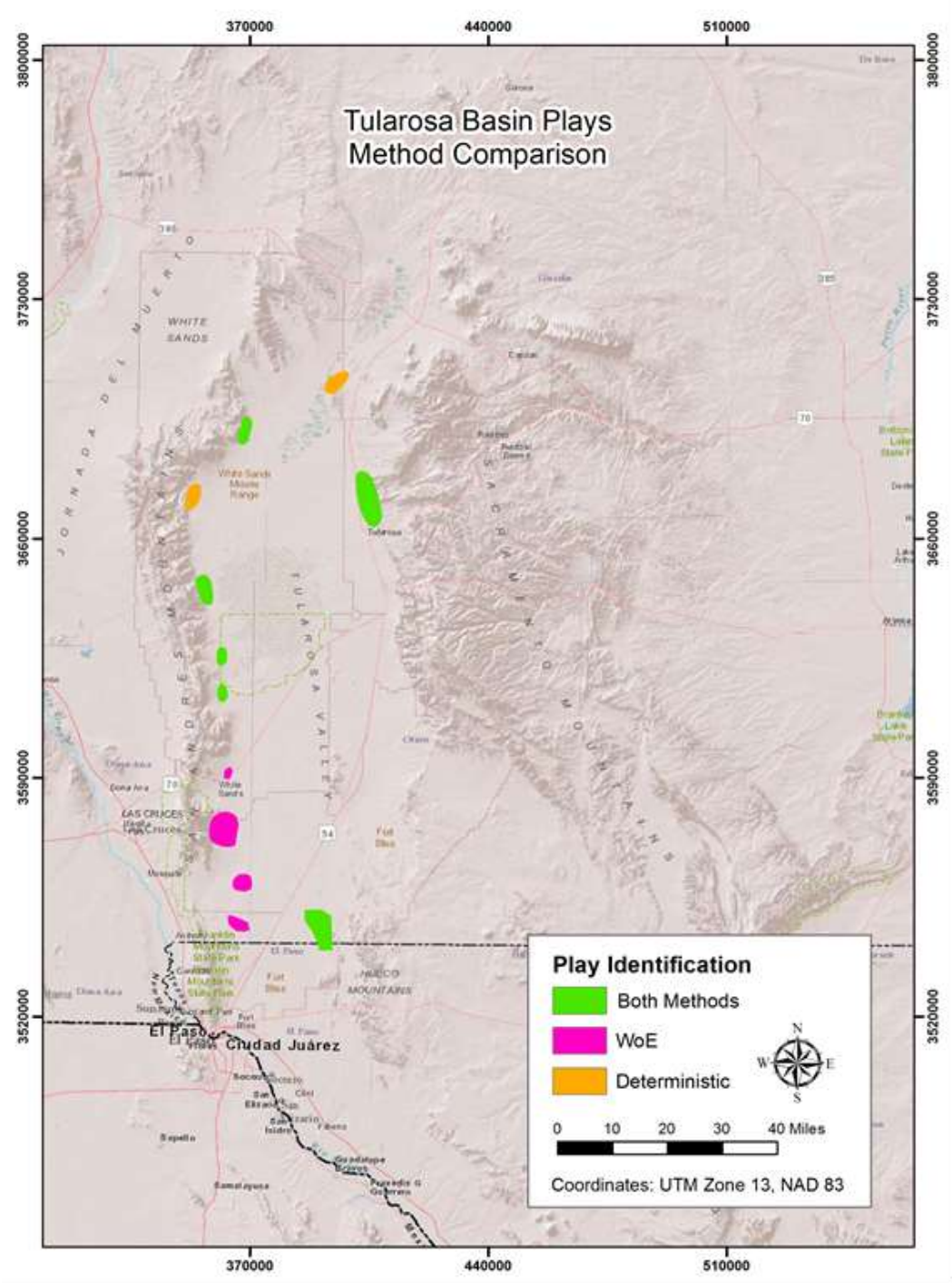

Figure 25. Plays identified by method. Twelve total plays were identified, six by both methods, two additionally by the deterministic method, and four additional by WoE.

In finality, only additional work will allow a definitive comparison of these methods. However, it is our opinion at this time that it would be prudent to apply both methods if possible. What one overlooks the other may see.

Additionally, this redundancy could give more confidence where there is agreement. However, the deterministic approach works and it would be an excellent tool in areas where adequate training sites and supporting data cannot be obtained for use in stochastic PFA.

See Appendix C for flow charts detailing the methodologies. The flow charts will also be uploaded to the GDR in larger formats for easier reading.

SECTION 4: FINAL TULAROSA BASIN PLAY RANKINGS

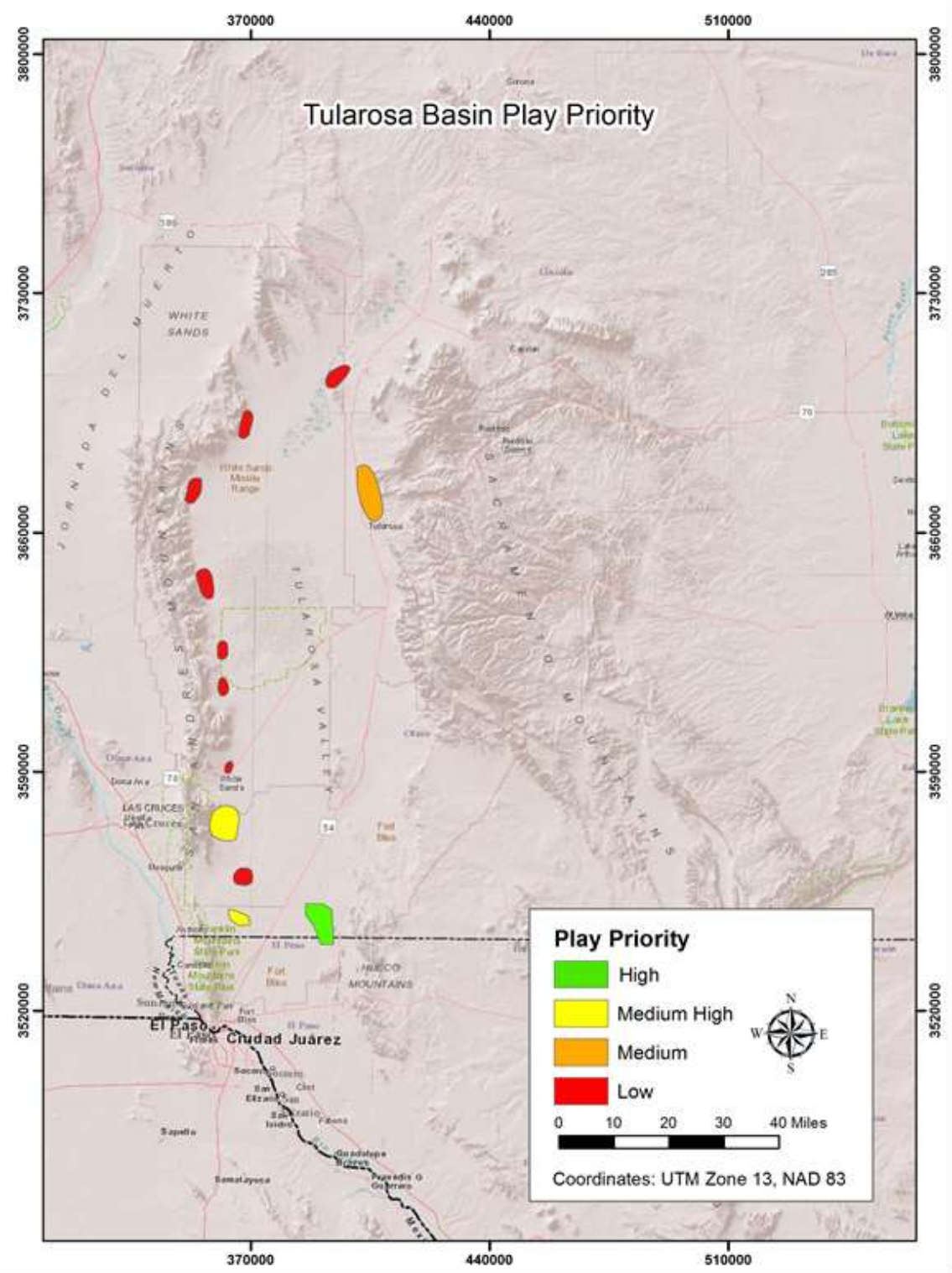

Figure 26. Play priority based upon structure, WoE probability, and proximity to permissible data points.

SECTION 5: ASSESSMENT OF RISK & REWARD FACTORS

5.1 Assessment Methodology

Background

A hallmark of the best use of PFA for effective decision making is the integration of incomplete data sets in a way that consistently weighs the uncertainty associated with the various measurements. In the petroleum industry the use of fully probabilistic geo-statistical modeling has been very successful (c.f., Journel, A.G.).

In practice, the vagaries of budget cycles, survey and drilling equipment availability, investor philosophy, and so on, mean that some mix of deterministic and probabilistic methods is almost always used. At this preliminary stage of data collection, the resources are not available to rigorously demonstrate the ideal industrial-strength analysis. This section will illustrate the analysis using largely deterministic values, with remarks on the potential for applying a probabilistic approach at key points.

This Phase 1 analysis also differs from the real world in that we are considering a scenario in which exploration data is available for analysis in a single package that would actually be acquired over a period of months or years. Iterative analysis of collected data and new data as it is discovered is the norm in industry. Most managers of the authors' acquaintance consider it essential to focusing exploration dollars on areas having the highest probability of success.

Estimation of Productive Area

Continuously processing new information allows for fluidity of the valuation of a project. In this early phase of data collection and analysis of existing data, a simpler deterministic approach to several parameters was sufficient to demonstrate the ability of PFA to identify attractive prospects in the Tularosa Basin.

The area for exploration and eventual development for production for each of the play was estimated using the following steps:

1. The total area of the play, as defined in the preliminary study of the basin, was considered to be a target for further geological, geochemical and geochemistry (GGG) studies. These are collectively referred to as surface exploration studies. As the three plays selected are of similar size, a total cost of $350k was assigned to each.

2. The surface exploration work provides the information necessary to select the portion of each play with the most favorable conditions for further expenditures. In this example we arbitrarily used 50% as the cull fraction. In practice, this fraction will be dependent on the actual results. We would, for example, expect the cull fraction to be small near Yellowstone and quite large in the Appalachians. The next step in exploration is temperature gradient well (TGW) drilling. For this example we used a TGW density of 1 well/km^2.

3. Refine the area for exploratory well drilling by eliminating areas of low temperature gradient from further consideration. This will normally be accomplished in concert with geostatistical modeling as described in the background discussion above. In the present case a simpler approximation was developed assuming normally distributed gradient values. The gradients measured in several hundred TG wells throughout the Tularosa Basin range from 25-140°C/km. If we assume this range covers about 95% of the possible values, we can construct a normal distribution curve with 25°C/km and 140°C/km assigned to probability values of -2σ and +2σ, respectively. The high risk threshold for CRS is defined as 60°C/km, so we excluded areas with a gradient ≤ 60°C/km. The cumulative probability of a gradient exceeding 60°C/km is 78% for the distribution as described, so exploratory wells will be drilled on 78% of the area passing the initial surface screening in step (2). For this example, a density of two exploratory wells per ten square kilometers was assumed.

4. Estimate the likelihood of successful exploration well drilling. This lends itself to Monte Carlo simulation if no experiential data exists for the play in question. For this example, a probability of success of 45% was used, based on the initial drilling experience reported in Indonesia (Sanyal and Morrow). The reported success rate increased to nearly 70% with experience, but the small size of the subject plays makes choosing a lesser value prudent. We acknowledge the vast geologic differences between the Tularosa Basin and Indonesia, but find that the reported drilling success rates are consistent with the proprietary domestic industrial experience of which we are aware.

To illustrate the process of this approach to narrowing the focus of the study to the most prospective area, the table below summarizes the percentages applied to each activity phase for all the plays identified.

Table 2. Percentages Applied to Each Activity Phase

Area Selected from Total Play				
	Surface Exploration	**Temperature Gradient Wells**	**Exploration Wells**	**Successful Development Wells**
Activity applies to:	**100%**	**50%**	**39%**	**18%**

5.2 Cost and Revenue Calculations

Gross Revenue

A target plant capacity of 10 MW per 10 sq. km. was used as the basis for gross revenue calculations. Plant and well field parasitic load was assumed at 25%, based on industrial experience (Verkis Consulting Engineers). Flash plants normally show records of 4% to 7% parasitic loads while binary plants' parasitic loads may range from 15% to 40%, or higher depending on the high use of pumps to flow the wells.

Net present value of future annual revenue estimate is calculated as the product of the Estimated Net Generation and the electricity price over a lifetime of 30-years. A discount rate of 2%, the average US inflation rate from 2010 to 2014, was used in the calculation.

Cost of Exploration

Well exploration cost was estimated using the formula defined in The 2011 Geothermal Well Cost Update (Mansure and Blankenship), which calculated to around US $3 million per well. The total cost of exploration for all three plays ranged from $1,360 to $1,516 per kW installed capacity.

Development and Plant Cost

An additional five (5) production wells and two (2) injection wells for a 10-MW plant capacity per 10 km^2 was used in constructing a deterministic cost profile for each play. These are representative values from existing Basin & Range plants but we would expect more sophisticated probabilistic modeling to be used when the surface exploration and TGW data are in hand.

Operating cost assumptions and plant cost estimates were provided by industry experts and validated by information taken from an Icelandic review of low temperature geothermal power plants (Verkis Consulting Engineers). The figure below summarizes the data used as assumptions in the exercise.

Table 3. Expected Value of Plays – Elements of Calculation

	Unit	**Play #1 (McGregor)**	**Play #2**	**Play #9**
Area of Play	sq. km	70.00	86.00	73.00
Reservoir Thickness	m	914.63	914.63	914.63
Minimum Temperature	°C	90.00	75.00	85.00
Maximum Temperature	°C	110.00	85.00	100.00
Depth to reach Minimum Temperature	m	909.09	727.27	848.48
Depth to reach Maximum Temperature	m	1,151.52	848.48	1,030.30
Target Depth of Wells at 400m into reservoir	m	1,309.00	1,127.00	1,248.00
Drill TG wells on 50% of Explored Area	sq. km	35.00	43.00	36.50
Area for Exploration Drilling	sq. km	27.41	33.67	28.58
Number of Temperature Gradient Wells	ea	35	43	37
Number of Exploration Wells	ea	5	7	6
Number of Production Wells	ea	6	8	6
Number of Injection Wells	ea	2	3	3
Target Capacity in Identified Play	MW	12.70	15.61	13.25
Plant Availability	%	95	95	95
Plant & Wellfield Parasitic Loads	%	25	25	25
Electricity Price	$/kWh	0.1724	0.1724	0.1724
Number of Operating Years	yrs	30	30	30
NPV Discount rate	%	2	2	2

Results

The Levelized Cost of Power (LCP) ($/kWh) was calculated as the initial capital investment, including exploration costs plus the cumulative present value of future costs discounted by the assumed inflation rate, divided by the cumulative power generation over the project life. LCP for all three plays was about $0.08/kWh.

The analysis described herein dispenses with some sophistication in modeling parameters for which reasonable values can be assigned. This is appropriate for an initial screening exercise in which the object is to learn whether there is sufficient economic attractiveness to pursue further work in a basin. The results clearly demonstrate that the unusual market conditions (i.e., $/kWh price) in the Tularosa Basin make all three plays viable candidates for exploration and development. The results are similar for all three plays identified by the PFA process. The figure below shows each has an expected net present value greater than $120 million.

Table 4. Net Present Value of Plays

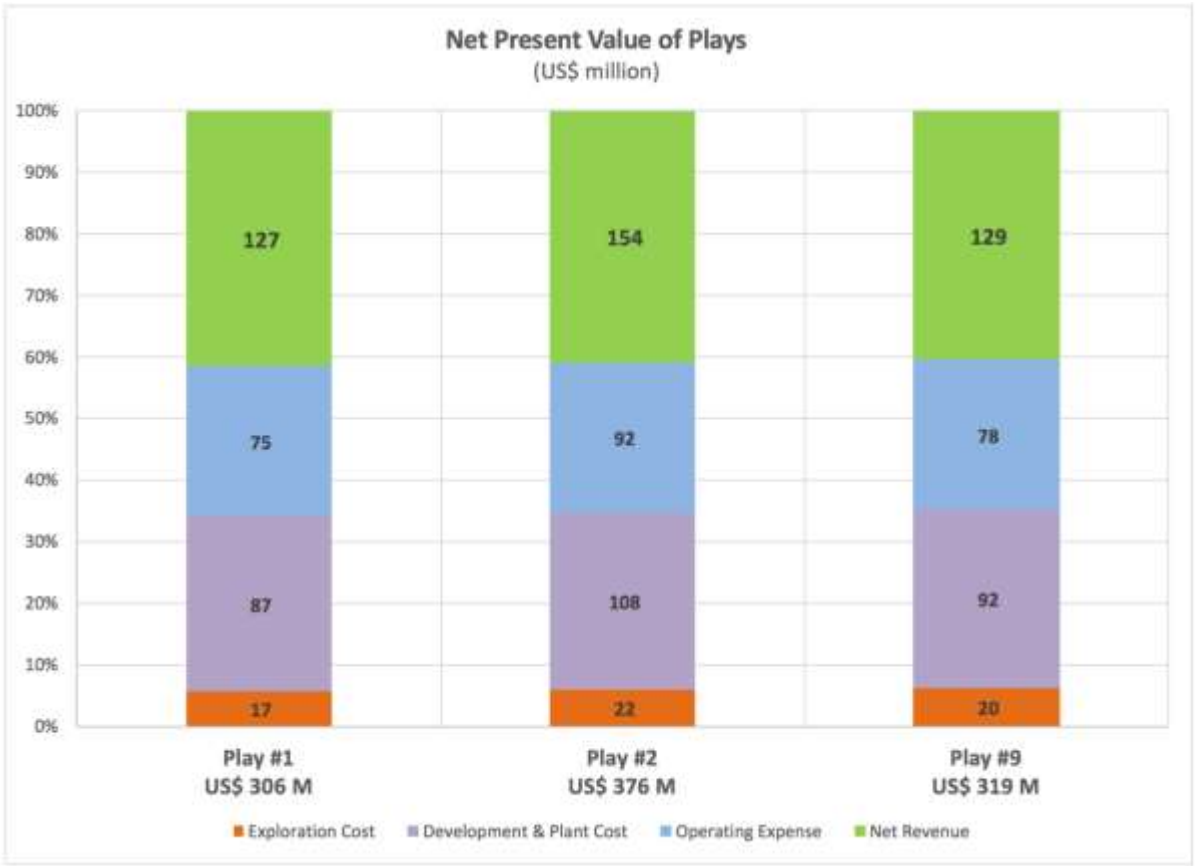

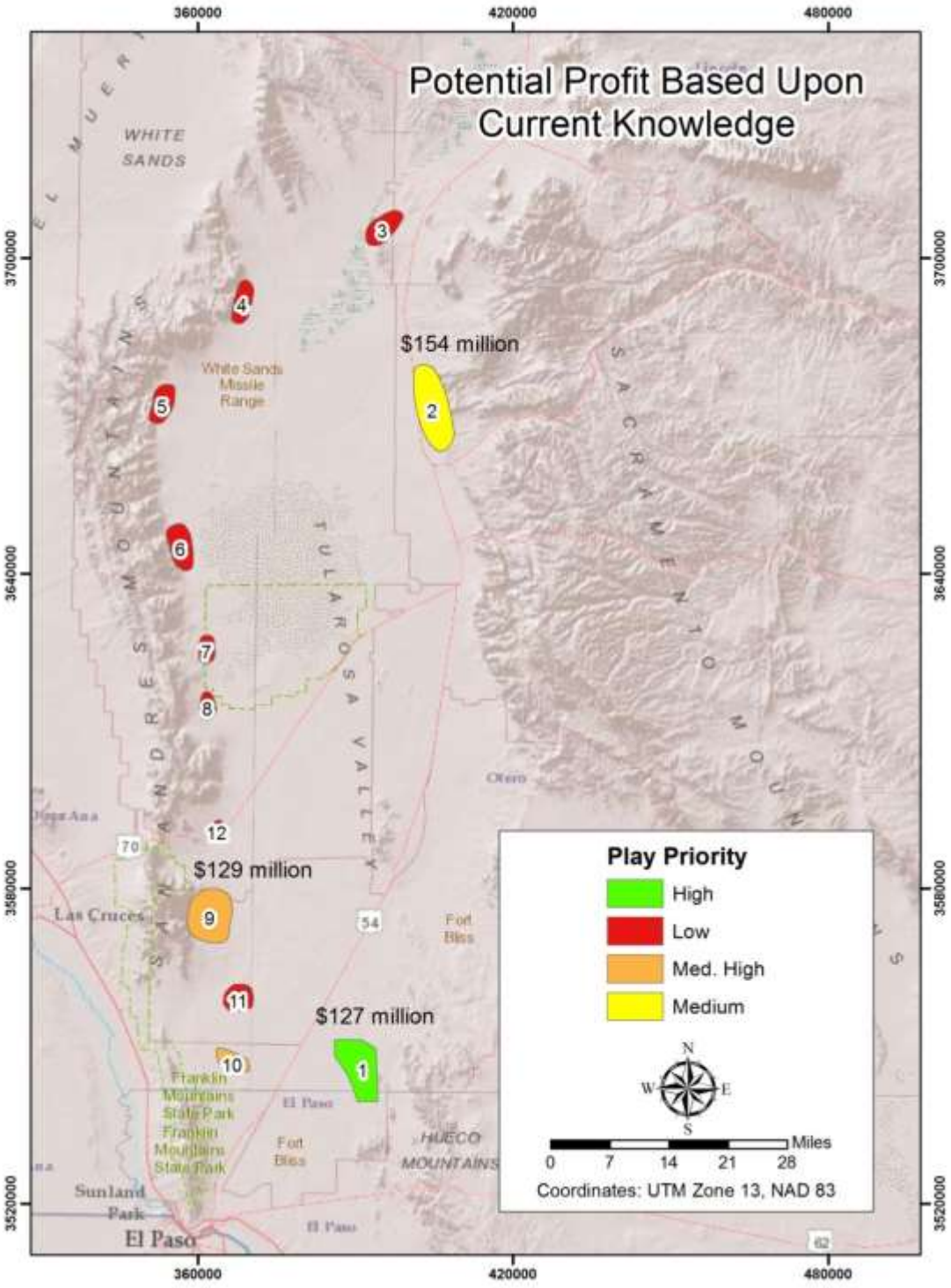

Figure 27. Profit potential of medium to high priority plays. Please note that Play 1 is the most data rich (low uncertainty), yet needs additional work to substantiate economic analysis. Plays 2 and 9 are relatively data poor and need considerably more work to facilitate refinement of this preliminary economic analysis. Please note that Play 10, although considered to be of Medium High priority, has low certainty due to critical data paucity, so no economic analysis was done for this play. Phase 2 addresses additional data needs that will allow better economic modeling.

Table 5. Levelized Cost of Power and Expected Net Present Value of Plays

	Unit	Play #1 (McGregor)	Play #2	Play #9
Area of Play	Sq. Km	70.00	86.00	73.00
Area for Development Drilling	sq. km	12.33	15.15	12.86
Target Capacity in Identified Play	MW	12.70	15.61	13.25
Annual Net Generation	MWhr/yr	79,288	97,411	82,686
Cumulative Net Generation Over Project Life	MWhr	2,378,644	2,922,334	2,480,586
Annual Gross Revenue	$/yr	13,669,274	16,793,680	14,255,100
Cumulative Net Present Value of Gross Revenue	$/project life	306,143,292	376,118,902	319,263,719
Surface Exploration & Exploration Drilling Cost		17,280,829	22,299,324	20,085,930
Surface Exploration	$	350,000	350,000	350,000
Temperature Gradient Wells	$	700,000	860,000	740,000
Exploration Well Cost based on Depth	$/ea	3,246,166	3,012,761	3,165,988
Total Cost of Exploration Wells	$	16,230,829	21,089,324	18,995,930
Surface Exploration and Expl. Drilling Cost Ratio	$/kW	1,360	1,429	1,516
Development & Plant Costs		86,945,540	108,054,001	92,083,376
Production & Injection Wells	$	25,969,326	33,140,366	28,493,896
Pipeline & Facilities	$/kW	16,514,391	20,289,109	17,222,151
Binary Plant & Pump Cost	$/kW	44,461,823	54,624,525	46,367,330
Annual Operating Expense	$	3,338,448	4,101,521	3,481,524
Cumulative Net Present Value of O&M Expense	$	74,769,396	91,859,544	77,973,799
Levelized Cost of Power	$/kWh	0.075	0.076	0.077

5.3 Next Steps

A more refined valuation using Monte Carlo Analysis will suit well Phase 2 of the project when more detailed data can be coupled with practical parameters based on the further study of the plays.

USGS Methods in the Assessment of Identified Geothermal Resources will be used as a way of evaluating reserves versus a conservative density assumption in Phase 1 of the project.

Further studies and information within the Tularosa Basin, like, financing, permitting, transmission details and a defined exploration and development strategy will add more granularity to the next valuation phase. Also, an iterative process of data input and output discussions will provide an environment where research data intersect with actual historical industry performance.

SECTION 6: MARKET TRANSFORMATION

Getting the results of this project in front of geothermal exploration/development companies and military energy decisions makers is a priority for the project team. While market transformation began with our Phase 1 reporting and presentation efforts described below, should we be funded into Phase 2, the project team will expand our efforts through targeted outreach to those two key constituencies.

6.1 Phase 1 Market Transformation Activities

As stated in our original project funding proposal, the project team initiated limited market transformation activities in Phase 1 by presenting our preliminary findings for comment to the DOE Geothermal Peer Review and the Geothermal Resources Council (GRC) in 2015.

For the 2015 Peer Review, a project summary was prepared and a presentation given for comment by the Technical Monitoring Team. The comments received were very helpful and some adjustments in PFA representation made as a result. Also, in 2015 a paper was accepted to GRC and a presentation was given by Dr. Greg Nash. Posters were presented at GRC in both 2014 and 2015. Some promising contacts were made as a result of those presentations. Specifically, during Phase 1, the following market transformation activities were completed:

- **Poster Presentation:** ***Innovative Play Fairway Modelling Applied to the Tularosa Basin***
  Authors: Gregory D. Nash, Ph.D., EGI & Carlon R. Bennett, Sr. Project Mgr., RMI
  Poster Presentation Given at the 2014 Geothermal Resources Council Annual Meeting, Portland, OR, September 2014

- **Publication:** ***Adaptation of a Petroleum Exploration Tool to Geothermal Exploration: Preliminary Play Fairway Model of Tularosa Basin***
  Authors: Gregory D. Nash, Ph.D., EGI & Carlon R. Bennett, Sr. Project Mgr., RMI
  Paper Published and Formal Presentation given at the 2015 Geothermal Resources Council Annual Meeting, Reno, NV, September, 2015

- **Presentation:** ***Preliminary Findings - Innovative Play Fairway Modelling Applied to the Tularosa Basin***
  U.S. Dept. Of Energy Geothermal Technologies Office Peer Review, Westminster, CO, May, 2015

- **Publication:** ***Adaptation of a Petroleum Exploration Tool to Geothermal Exploration: Preliminary Play Fairway Model of Tularosa Basin***
  Authors: Gregory D. Nash, Ph.D., EGI & Carlon R. Bennett, Sr. Project Mgr., RMI
  Paper Published and Formal Presentation given at the 2015 Geothermal Resources Council Annual Meeting, Reno, NV, September, 2015

- **Poster Presentation:** ***Adaptation of a Petroleum Exploration Tool to Geothermal Exploration: Preliminary Play Fairway Model of Tularosa Basin***
  Authors: Gregory D. Nash, Ph.D., EGI & Carlon R. Bennett, Sr. Project Mgr., RMI
  Poster Presentation Given at the 2015 Geothermal Resources Council Annual Meeting, Reno, NV, September, 2015

Additionally in 2015, an article regarding the Tularosa Basin PFA Project was published on EGI's "Ask EGI" website with distribution to 65 energy companies and Ruby Mountain made several presentations on the PFA methodology to military energy management staff.

Since so many agencies were involved in our data collection process at the beginning of Phase 1, Ruby Mountain is in process of planning a meeting to present the final Phase 1 Tularosa Basin PFA Model to stakeholders en masse. Military representatives, government officials, local utility staff and likely some industry representatives will be invited to the presentation which is tentatively scheduled for the first week in December 2015.

Additionally, individual separate meetings will be held with military installation energy staff located within the Tularosa Basin Study area to encourage additional collaboration, collect more information, and most importantly, address how this geothermal exploration methodology can assist them in addressing both current and future installation energy needs.

6.2 Expanded Market Transformation Activities

The project team believes that the play fairway methodology being developed by our project, that while complex, has the unique ability to be easily understood by the educated layman, makes the most of existing data, and is highly replicable. Put simply, getting valuable time in front of key civilian government officials and/or military energy staff is not an easy task, but doing so with a full complement of scientists and researchers in tow is even more difficult. Time with key decision makers is always at a premium and the methodology being proven out by this effort offers a low-cost, pragmatic approach to geothermal exploration which can be easily understood by non-industry, non-academic decision makers.

For that reason, if funded to Phase 2, the project team will develop a market transformation approach for our PFA process which, over the course of the next few years, will offer some near-term market penetration for PFA to facilitate increased geothermal exploration and/or development. Increase market transformation for PFA will require a targeted, multi-faceted approach, but in summary:

- Continued Reporting and Publication of Results through Conference Posters and Presentations;
- Outreach to Industry through EGI;
- Direct collaboration with one or more industry partners;
- Targeted outreach to military energy managers, key installation energy staff and subject matter experts; and,
- Continued exploration / validation of our PFA modelling methodology through expanded project implementation.

At this time, the project team is planning a submittal to the 2016 Stanford Geothermal Conference regarding comparison of the Weights of Evidence PFA Method and Deterministic PFA Methods, and a subsequent paper (topic not yet determined) will be submitted to the 2016 GRC for consideration. Additionally, we are contemplating recruitment of one or more industry partners to assist with validation of the Tularosa Basin methodology(ies) and identifying at least one DoD Energy Conference for which to submit a paper or make a presentation on this project.

SECTION 7: PHASE 1 CONCLUSIONS

The project team has developed the following conclusions through the end of Phase 1 of the Tularosa Basin Play Fairway Analysis Project:

Conclusion #1
The project team successfully developed and compared two methods - deterministic and stochastic – for purposes of creating a play fairway analysis for the Tularosa Basin.

Conclusion #2
Twelve total plays were identified, six by both methods, two additionally by the deterministic method, and four additionally by the WoE method.

Conclusion #3
Significantly, both methods tested identified the known McGregor Range Geothermal system, so this is an indicator that they are effective tools for geothermal exploration. New work suggested for Phase 2 will provide further proof of their veracity. It is our opinion at this time that it would be prudent to apply both methods where possible - what one method overlooks the other method may see.

Conclusion #4
The project team believes that the play fairway methodology developed by our project, while complex, has the unique ability to be easily understood by the educated layman, makes the most of existing data, and is highly replicable.

Conclusion #5
The project team incorporated economic analysis into the top plays identified by both methods finding what appear at this point to be multiple valuable and marketable plays.

Conclusion #6
Data collection efforts exceeded expectations and individual outreach to key stakeholders yielded significant results in terms of integrating previously unpublished data into the project database. Phase 1 of this study has exponentially increased the level of understanding of the basin from a geothermal resource perspective and could very well lay the groundwork for a clean energy future in the region.

Conclusion #7
DOE funding for this project facilitated the identification of geothermal resources for the first time on a basin-wide scale, bringing a substantial amount of disparate data into a common database for analysis.

Conclusion #8
A comprehensive approach to data collection, and the accompanying GIS database development, can be an effective means of assembling preexisting data (published and unpublished) to assess geothermal potential on a basin (or regional) scale.

Conclusion #9
The project team, led by Ruby Mountain Inc. and The Energy and Geoscience Institute at the University of Utah, had no significant departure from stated goals or methods and brought Phase 1 to a successful conclusion on budget and on time while substantially exceeding cost sharing targets

SECTION 8: OVERVIEW OF PHASE 2 RECOMMENDATIONS

Verifying the existence of the plays identified in this Phase 1 ("ground-truthing") was not done because field work and generation of new data were not part of the allowed work scope. However, Phase 2 will be geared toward collecting data that will provide significant confirmation. These will include (1) mapping detailed surface geology, (2) collecting additional water samples for geothermometry, and (3) measuring temperature gradients in existing wells. The project team also suggests high resolution gravity surveys over the high priority plays to facilitate enhanced structural model development and an MT survey covering the McGregor Range (Play 1) to better characterize the system, which will help us develop a better 3D geothermal system model.

Specifically, we recommend the following activities in Phase 2:

1. Geologic field work. For higher priority plays, surface geologic mapping at high resolution and a fracture study at the outcrop level. For lower priority plays, field reconnaissance to determine if any surficial evidence can be located indicating historic geothermal activity. This work often results in the discovery of subtle geothermal manifestations, as well as a better understanding of the site specific geology.

2. Additional water sample collection. Samples should be gathered from all plays where water chemistry is lacking. The samples will be used for geothermometry and isotopic analysis. Down-hole temperatures can be measured during water sampling to improve the temperature and temperature gradient data bases.

3. Gravity data infill for the highest priority plays. Phase I relied on regional-scale gravity data. Surveys on finer grids will provide additional structural information and help gain a better understanding of the relationships of basement faulting to Quaternary surface fault expressions and zones of permeability.

4. An MT survey on the highest priority play, McGregor Range. This will help characterize the system and identify up-flow. This will be integrated into a 3D geothermal model with existing lithologic and new structural data.

5. A flow test of well RMI 56-5 at the McGregor Range. A comprehensive flow test will determine its viability for power production, will indicate resource volume, and may detect boundaries. A concerted effort is under way to obtain a portion of funding for this test (50-75 percent) from other sources.

6. Update the GIS database and PFA models and upload all new data to the GDR.

7. Conduct advanced probabilistic economic modeling in high priority plays based upon Phase 2 results.

8. Develop a market transformation approach for our PFA processes. The objective is to facilitate the early adoption of effective PFA methods by the geothermal industry. Near-term market penetration for PFA will be encouraged by a successful project.

Specific tasks as they relate to prioritized plays and other factors, such as property ownership and land access, can be seen in Figures 28 - 31 below.

Total Estimated Phase 2 Cost: $889,000 *

* Estimate above includes all coordination and preparation for, as well as supervision of, on the ground testing on 2-3 separate military facilities, coordination with relevant state & federal agencies, ongoing military liaison, travel costs to test site, as well as mandatory conference and meeting expenses.

Alternative to Phase 2 Estimated Cost: If the flow test cost on well RMI 56-5 can be obtained from other sources (in whole or in part) the Phase 2 costs could be reduced by as much as $145,000. Other options include reducing the size of the gravity survey and/or MT survey. All other work suggested above would take place.

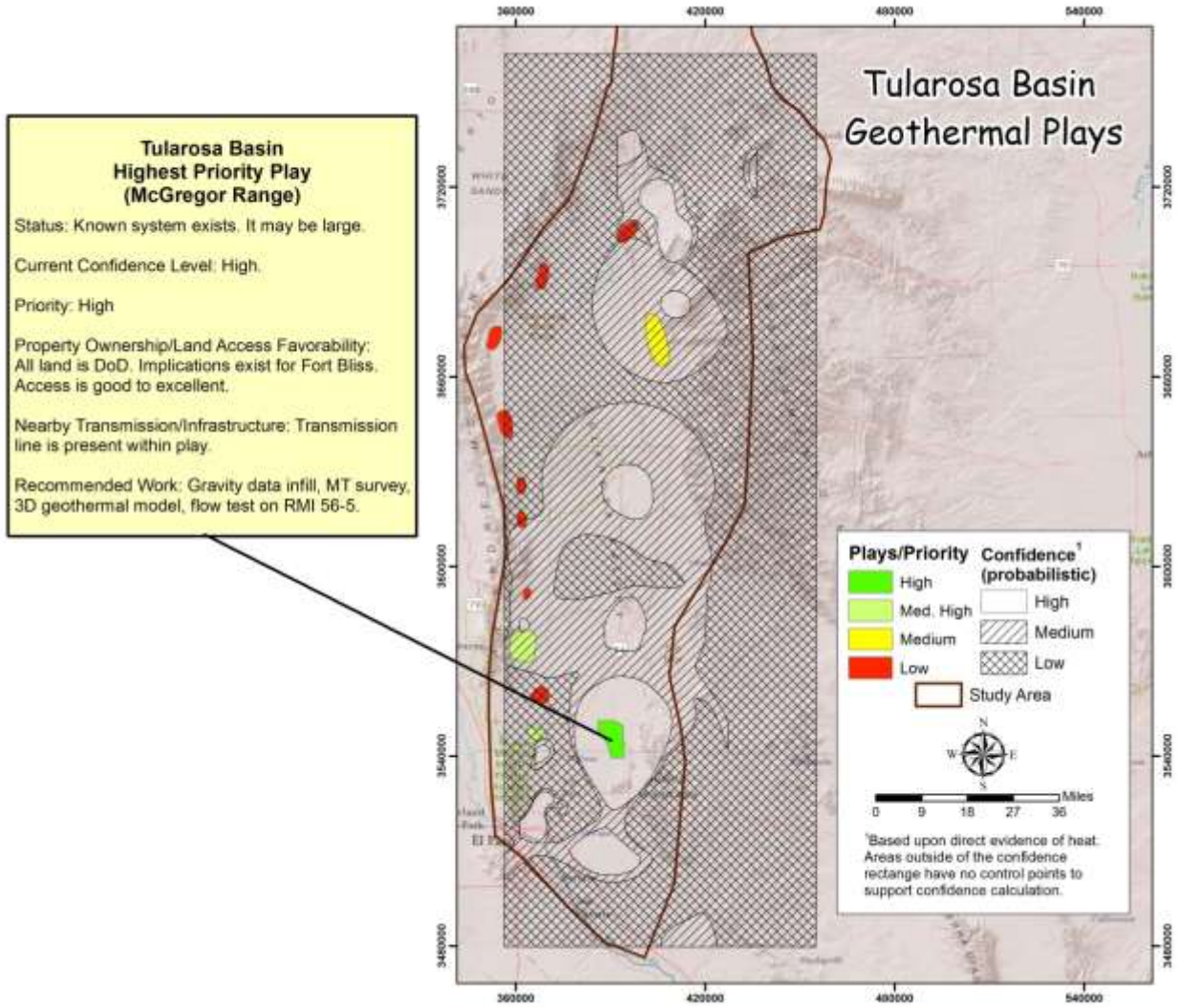

Figure 28. Phase 2 work suggested for the highest priority play.

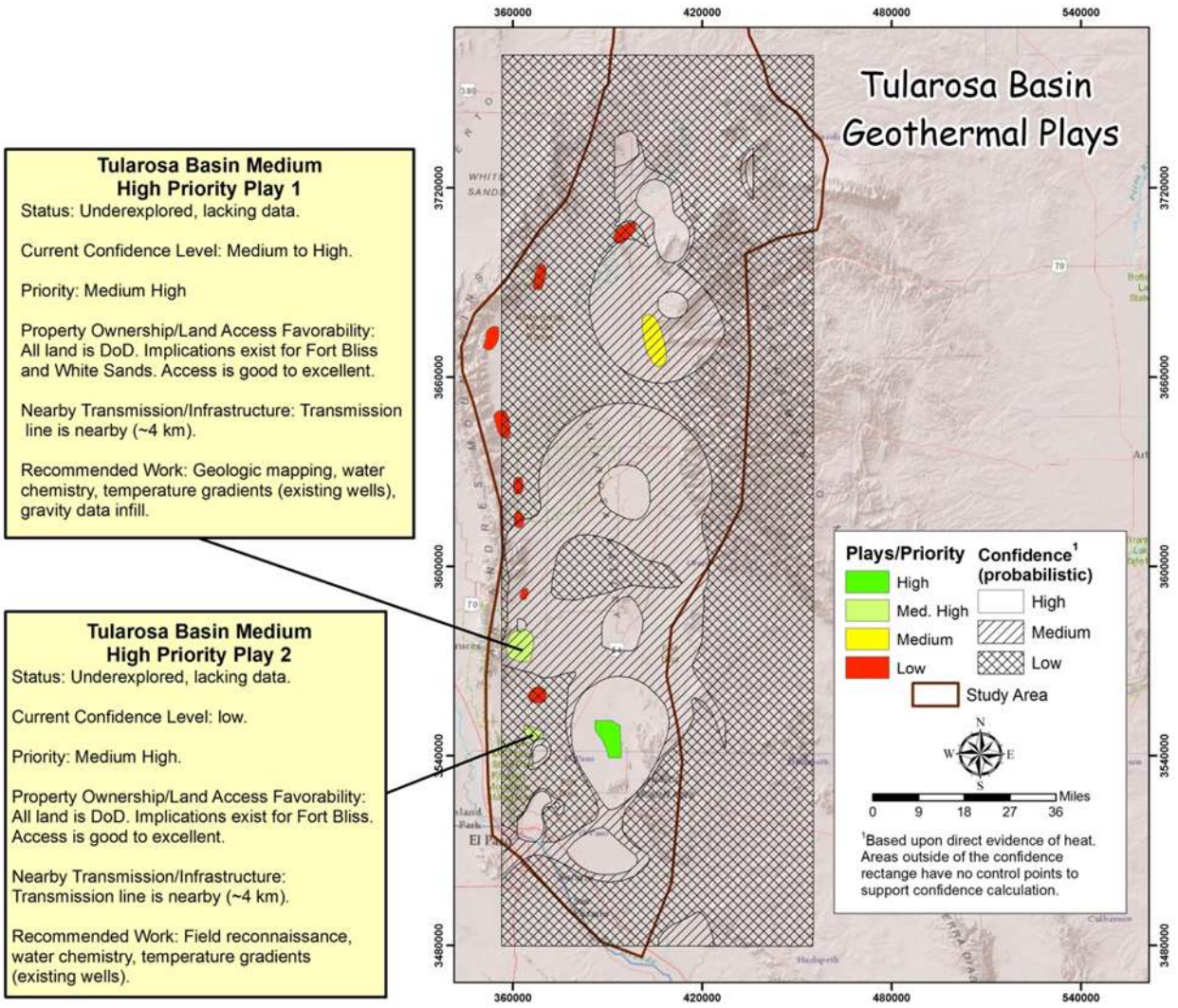

Figure 29. Suggested Phase 2 work for medium-high priority plays. Note that the southernmost play has low certainty which is largely due to a lack of data in the immediate area, so collecting more evidence of heat here would be recommended to raise certainty.

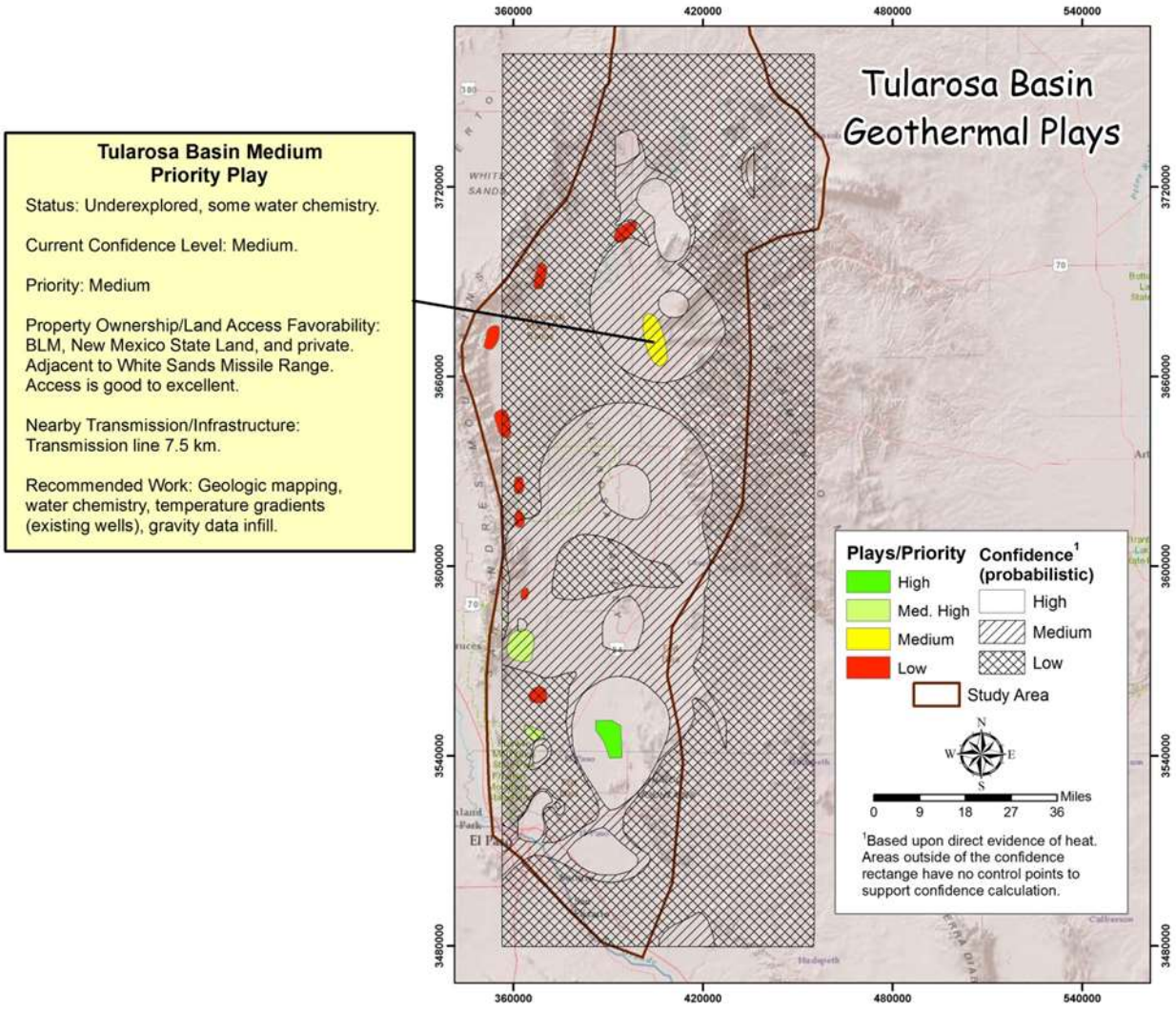

Figure 30. Suggested Phase 2 work for the medium priority play.

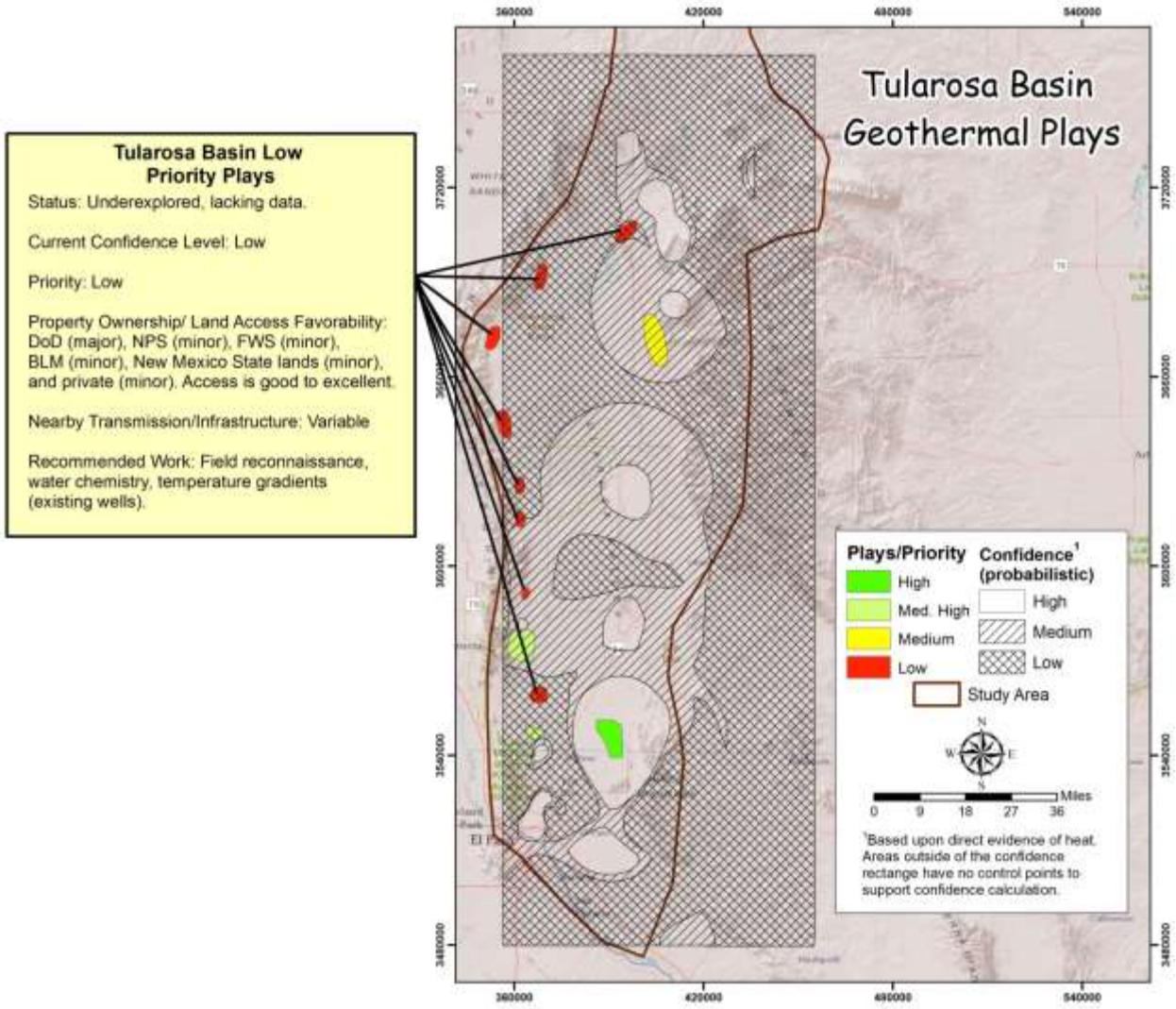

Figure 31. Suggest Phase 2 work for low priority plays.

REFERENCES

Barker, B., Nash, G., Moore, J., and Bennett, C., 2015, Multimodal geothermal development in the Tularosa Basin, NM: Proceedings, 40th Workshop on Geothermal Reservoir Engineering Stanford University, Stanford, California, January 26-28, 2015, SGP-TR-204.

Blackwell, D. D., M. C. Richards, Z. S. Frone, J. F. Batir, M. A. Williams, A. A. Ruzo, and R. K. Dingwall, 2011. SMU Geothermal Laboratory heat flow map of the coterminous United States.

Bonham-Carter, G., 1994. Geographic information systems for geoscientists: modelling with GIS. Pergamon press.

Coolbaugh, M. F., 2003: the prediction and detection of geothermal systems at regional and local scales in Nevada using a geographic information system and thermal infrared imagery. Dissertation, University of Nevada, 172 p.

Coolbaugh, M, C. Kratt, A. Fallacara, W. M. Calvin, and J. V. Taranik, 2007. Detection of geothermal anomalies using Advanced Spaceborne Thermal Emission and Reflection Radiometer (ASTER) thermal infrared images at Bradys Hot Springs, Nevada, USA, *Remote Sensing of Environment*, v. 106, i. 3, p. 350-359.

Cronin, V., Olds, S., Pratt-Sitaula, B., Resor, P., West, N., Hammond, W., & Kreemer, C. (2014). Infinitesimal Strain Analysis Using GPS Data: Module for Structural Geology or Geophysics Course. *UNAVCO, Geodetic Education Resources.* Retrieved from http://www.unavco.org/education/resources/educational-resources/lesson/majors-gps-strain/majors-gps-strain.html#development.

Powell, T and W, Cumming 2010. Spreadsheets for Geothermal Water and Gas Geochemistry. Thirty-Fifth Workshop on Geothermal Reservoir Engineering, Stanford University, Stanford, California, February 1-3, 2010. SGP-TR-188.

Dudley, E.A. and G.D. Nash, 2003. **"**Using Thermal Infrared (TIR) Data to Identify Geothermal Anomalies." Geothermal Resources Council *Transactions* vol. 27, 645-647.

Eneva, M, M. Coolgaugh, S. Bjornstad, and J. Combs, 2007. In search for thermal anomalies in the Coso Geothermal Field (California) using remote sensing and field data, *Proceedings*, Thirty-Second Workshop on Geothermal Reservoir Engineeing, Stanford University, SGP-TR-183.

Faulds, J., M. Coolbaugh, G. S. Vice, and M. L. Edwards, 2006. Characterizing structural controls of geothermal fields in the northwestern Great Basin: A Progress Report, GRC *Transactions,* v. 30, p. 69-76.

Faulds, J., M. Coolbaugh, V. Bouchot, I. Moeck, and K. Oguz, 2010. Characterizing Structural Controls of Geothermal Reservoirs in the Great Basin, USA, and Western Turkey: Developing Successful Exploration Strategies in Extended Terranes, *Proceedings*, World Geothermal Congress, Bali, Indonesia, p. 1-10.

Faulds, J. E., N. H. Hinz, C. Kreemer, and M. Coolbaugh, 2012. Regional patterns of geothermal activity in the Great Basin region, western USA: Correlation with strain rates, GRC *Transactions*, v. 36, p. 897- 901.

Faulds, J. E., N. H. Hinz, G. M. Dering, and D. L. Siler, 2013. The hybrid model – the most accommodating structural setting for geothermal power generation in the Great Basin, western USA: *GRC Transactions*, 37, 3-10.

Federal Register, v. 79, no. 55, Friday, March 21, 2014, p. 15732–15733.

Flyn, T. and P.K. Buchanan, 1993, Pleistocene origin of geothermal fluids in the Great Basin, western United States: *Resource Geology*, v. 16, p. 60-68.

Formento-Trigilio, M. L. and F. J. Pazzaglia, 1998, Tectonic Geomorphology of the Sierra Nacimiento: traditional and new techniques in assisting long-term landscape evolution in the Southern Rocky Mountains, *The Journal of Geology*, v. 106, p. 433-453.

Fournier, R. O., 1991, Water geothermometers applied to geothermal energy: in Applications of Geochemistry in Geothermal Reservoir Development, UNITAR-UNDP (ed. F. D'Amore), p. 37-69.

Fraser, A. J., 2001, Vining, B.A. & Pickering, S. C. (eds) Petroleum Geology: From Mature Basins to New Frontiers – Proceedings of the 7th Petroleum Geology Conference, 791–800. DOI: 10.1144/0070791# Petroleum Geology Conferences Ltd. Published by the Geological Society, London, p. 791-800.

Garg, S. K. and J. Combs, 2010. Appropriate ues of volumetric “heat in place” method and Monte Carlo calculations, Proceedings, Thirty-Fourth workshop on Geothermal Reservoir Engineering, Stanford Unicersity, California, SGP-TR-188.

Giggenbach, W. F., 1991, Chemical techniques in geothermal exploration: in Applications of Geochemistry in Geothermal Reservoir Development, UNITAR-UNDP (ed. F. D'Amore), p. 119-144.

Grant, S., N. Milton, and M.Thompson, 1996. Play fairway analysis and risk mapping: an example using the Middle Jurassic Brent Group in the northern North Sea, *Norwegian Petroleum Society Special Publications*, v. 6, Elsevier, p. 167-181.

Hulen, J.B., Nash, G.D., and Deymonaz, J., 2005. Geology of the Emigrant geothermal prospect, Esmeralda County, Nevada, Geothermal Resources Council, *Transactions*, v. 29, 15 p.

Journel, A. G., *Combining knowledge from diverse sources: An alternative to traditional data independence hypotheses*, MATHEMATICAL GEOLOGY, 2002; 34 (5): 573-596.

Mansure, J. and D. A. Blankenship, *The Geothermal Well Cost Update*, GRC Transactions, Vol. 35, 2011.

Mamer, E. A., B. T. Newton, D. J. Koning, S. S. Timmons, and S. A. Kelly, 2014. Northeastern Tularosa Basin Regional Hydrogeology Study, New Mexico, New Mexico Bureau of Geology and Mineral Resources, Open-File Report 562, 78 p.

Mars, J. C. and Rowan, L. C., 2006, Regional mapping of phyllic- and argillic-altered rocks in the Zagros magmatic arc, Iran, using Advanced Spacebourne Thermal Emission and Reflection Radiometer (ASTER) data and logical operator algorithms, *Geosphere*, v. 2, p. 161-186.

Moghaddam, M. K., Y. Noorollahi, F. Samadzadegan , M. A. Sharifi, and R. Itoi, 2013: Spatial data analysis for exploration of regional scale geothermal resources, *Geothermics*, Elsevier, p. 69–83.

Nash, G. D. and P. M. Wright, 1996. Remote sensing and geographic information systems (GIS) - tools for geothermal exploration in the Great Basin, U. S. A.: Sandia National Laboratories, Final Report, Contract #AB-6807, 74 p.

Nash, G. D. and G.W. Johnson, 2003. "Conceptualization and implementation of a tectonic geomophology study for geothermal exploration in the Great Basin, U. S. A." Geothermal Resources Council *Transactions* v. 27, 663-667.

Purelsy, J., S. L. Bilek, and C. J. Ruhl, 2013. Earthquake catalogs for New Mexico and bordering areas: 2005–2009, *New Mexico Geology*, vol. 35, no. 1, p. 3–12.

Rowan LC, Hook SJ, Abrams MJ & Mars JC. 2003. Mapping hydrothermally altered rocks at Cuprite, Nevada, using the Advanced Spacebourne Thermal Emission and Reflection Radiometer (ASTER), a new satellite-imaging system. Economic Geology 98:1019–1027.

Rowan L. C. & Mars J. C. 2003. Lithologic mapping in the Mountain Pass, California area using Advanced Spaceborne Thermal Emission and Reflection Radiometer (ASTER) data, *Remote Sensing of Environment* v. 84, p. 350–366.

Ruby Mountain, Inc., electricity cost data reported by Fort Bliss, 2015

Sabins, A. E., D. J. Walker, J. Unruh and F. C. Monastero, 2004. Toward the Development of Occurrence Models for Geothermal Resources in the Western United States: Geothermal Resources Council *Transactions*, vol. 28, p. 41 – 46.

Sanyal, Subir K. and James W. Morrow, *Quantification of Geothermal Resource Risk—A Practical Perspective*, GRC Transactions, Vol. 34, 2010.

Sawatzky, D.L., Raines, G.L., Bonham-Carter, G.F., and Looney, C.G., 2009, Spatial Data Modeler (SDM): ArcMAP 9.3 geoprocessing tools for spatial data modelling using weights of evidence, logistic regression, fuzzy logic and neural networks. http://arcscripts.esri.com/details.asp?dbid=15341.

Verkis Consulting Engineers, *Geothermal Binary Power Plants: Preliminary Study of Low Temperature Utilization,* Reykjavik, 2014, Retrieved from http://www.verkis.com/media/pdf/iceida-geothermal-binary-overview.pdf

Williams, C. F., M. J. Reed, R. H. Mariner, *USGS Assessment of Identified Geothermal Resources*; Open-File Report 2008-1296

Younes Noorollahi, Ryuichi Itoi, Hikari Fujii, Toshiaki Tanaka, 2007a. GIS model for geothermal resource exploration in Akita and Iwate prefrctures, northern Japan: *Computers and Geosciences*, vol. 33, Issue 8, Pergamon Press, Inc, p. 1008 – 1021.

Younes Noorollahi, Ryuichi Itoi, Hikari Fujii, Toshiaki Tanaka, 2007b. GIS integration model for geothermal exploration and well siting: *Geothermics*, vol 37 issue 2, Elsevier, p. 107-131.

Yousfi, H., S. Ehara, Y. Noorollahi, 2007. Geothermal potential site selection using GIS in Iran: *Proceedings*, Thirty-Second Workshop on Geothermal Reservoir Engineering Stanford University, Stanford, California, SGP-TR-183.

Yousfi, H., S. Ehara, Y. Noorollahi, 2010. Developing the Geothermal Resources Map of Iran, *Geothermics*, vol. 30, issue 2, Elsevier, p. 140-151.

Zehner, R. E., M. F. Coolbaugh, L. Shevenell, 2006. Regional groundwater geochemical trends in the Great Basin: implications for geothermal exploration, GRC *Transactions*, v. 30, p. 117-124.

.

APPENDICES

Appendix A – Supporting Work and Data

Appendix B – PFA Associated Data

Appendix C - Methodology Flow Charts

Appendix A
Supporting Work and Data

Geochemistry

Waters from the play fairway display a broad range of chemical compositions. The chemical analyses are compiled in an ArcGIS shapefile that will be uploaded to the NGR. As an initial check on the analytical quality of the data, the charge balance for each sample was calculated using the Powell and Cummings (2010) geochemical spreadsheet. Charge balances that exceeded 5% were removed from further consideration to minimize the possibility of misinterpreting the data. We consider the most important analyses to be the anions, Cl, SO_4, and HCO_3, which are major constituents of the fluids and thus most likely to be a major contributor to the poor charge balances, and SiO_2. A total of 1644 samples were evaluated and of these, 414 were considered to have acceptable charge balances.

The anion contents of the samples are shown on Figures 1-3. The data are divided into three regions. The northern region lies along the eastern side of the play fairway north of Alamogordo. Mamer et al. (2014) provide a detailed discussion of the hydrology and geochemistry of this area and their work is summarized below. The central and southern regions are located on the western side of the play fairway. Fort Bliss lies within the southern region and data from this site are summarized by Barker et al. (2015). For each region, the compositions of the fluids in terms of their relative contents of Cl, HCO_3 and SO_4 were plotted on a ternary diagram (Figs. 4-6) to determine the dominant water types and to evaluate possible mixing relationships among the waters.

Northern Region

The dominant anions in waters from the northern region are HCO_3 or SO_4 (Figs. 1-4). Cl is a minor component. Ca is the dominant cation, followed by Na and then Mg. Most of the waters can be classified as Ca-SO_4 in composition. SO_4 concentrations are higher in the well waters (mean of 1040 mg/L) compared to the springs (mean of 797 mg/L) and streams (mean of 666 mg/L) but the mean HCO_3 values are similar in all three sample types (mean values range from 209 mg/L for wells to 230 mg/L for springs). Although there is some scatter in the analyses, the waters generally define a linear trend on Figure 4, indicating mixing between two end member waters; one enriched in HCO_3 and the other in SO_4.

Figures 2 and 3 indicate there are systematic changes in the HCO_3 and SO_4 across the region. Overall, HCO_3 contents decrease from east to west whereas the SO_4 contents increase in this direction. The lowest SO_4 contents are found on the western slope of the Sacramento Mountains. These waters have SO_4 contents less than about 650 mg/L. Water from the Tularosa Basin contain up to approximately 3000 mg/L SO_4.

The origins of the waters from the northern Tularosa Basin and the effects of water-rock interactions were examined by Mamer et al. (2014). They concluded the HCO_3 and SO_4 resulted from interactions with limestone and gypsum respectively. Gypsum is common in the evaporate deposits of the basin and is a likely source of the SO_4 occurring in the basin waters. Interactions with limestone, which is present in the range and beneath the basin floor, are considered to be the source of the HCO_3.

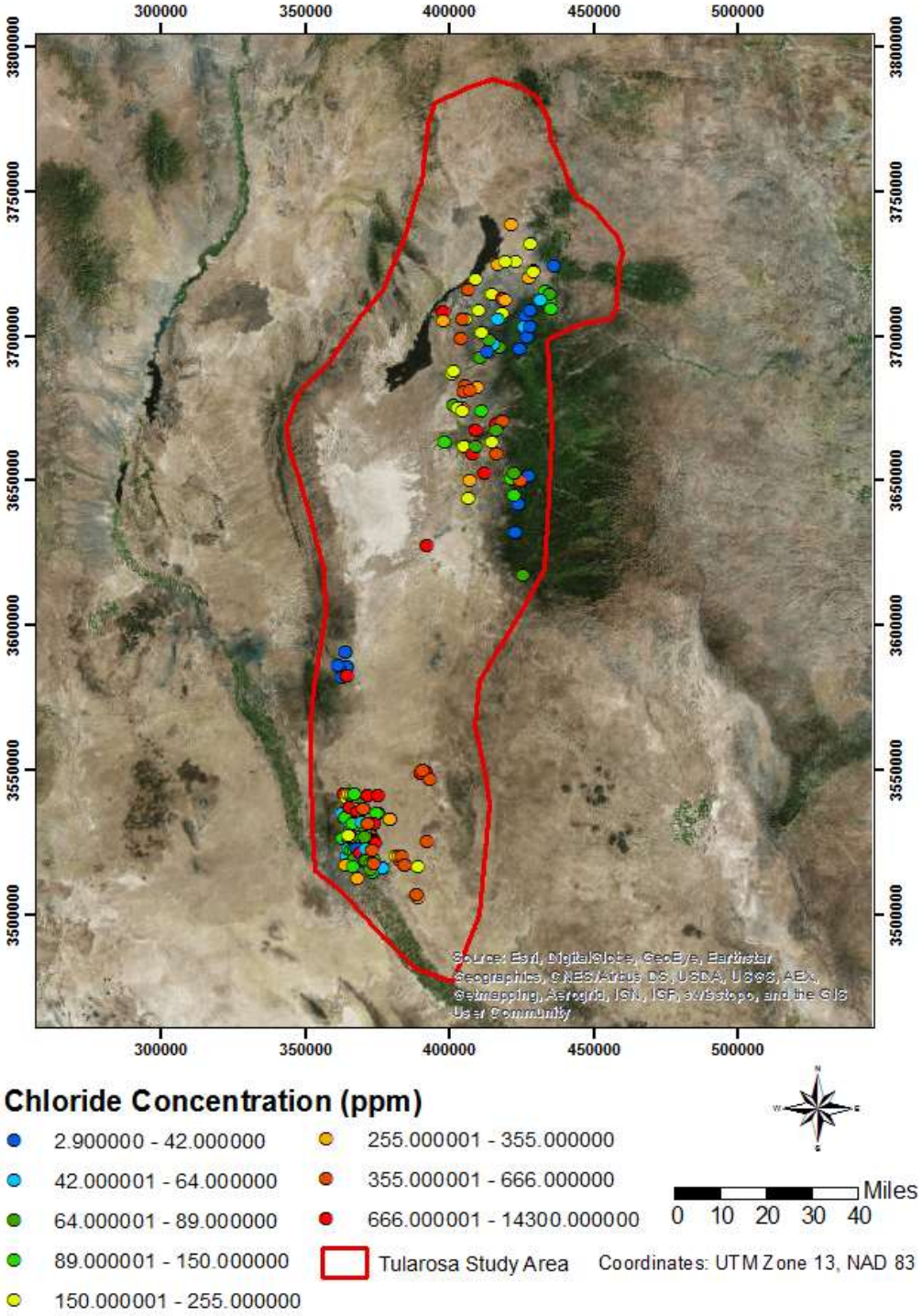

Figure 1. Chloride (Cl) contents of play fairway waters.

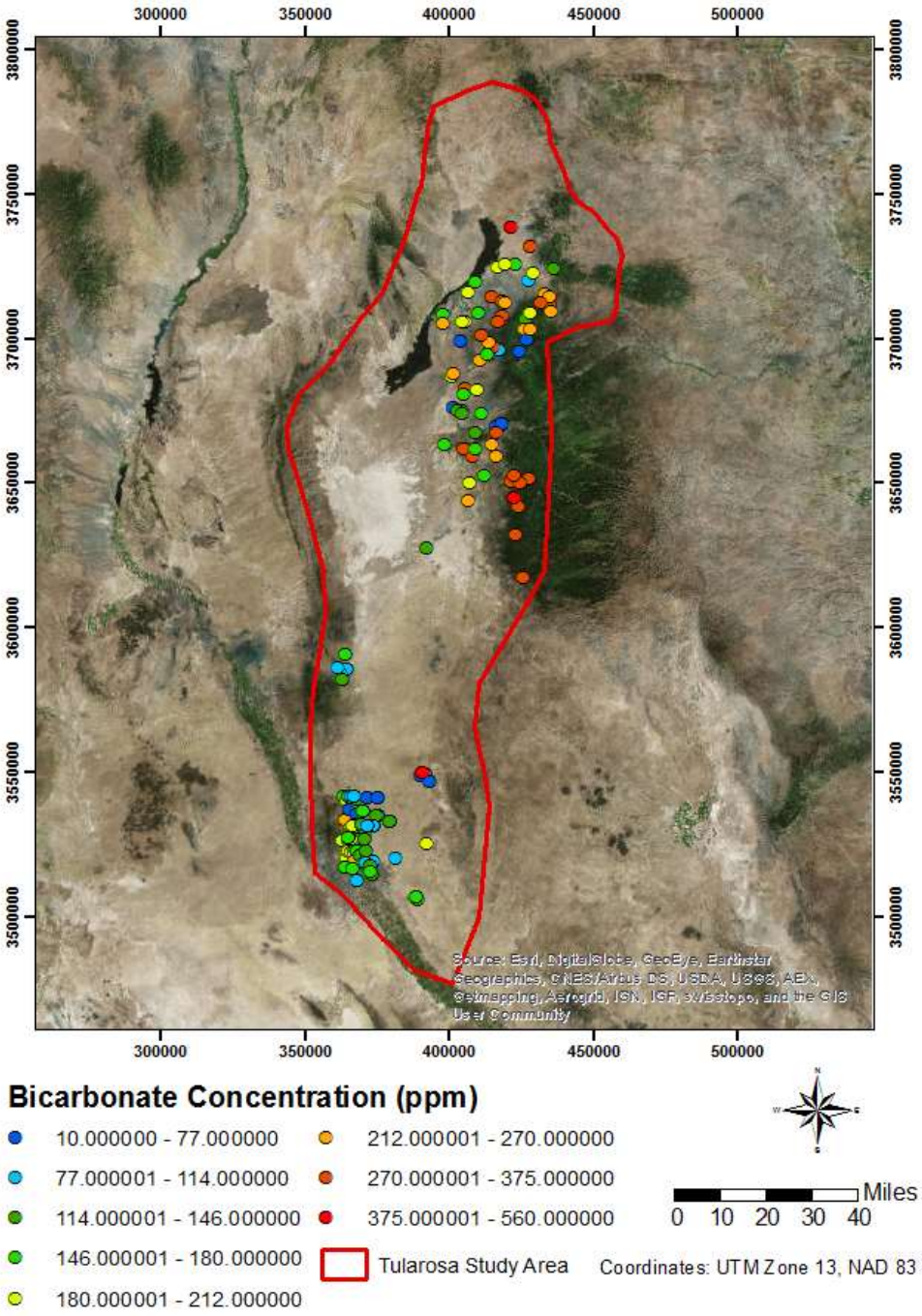

Figure 2. Bicarbonate (HCO_3) contents of play fairway waters.

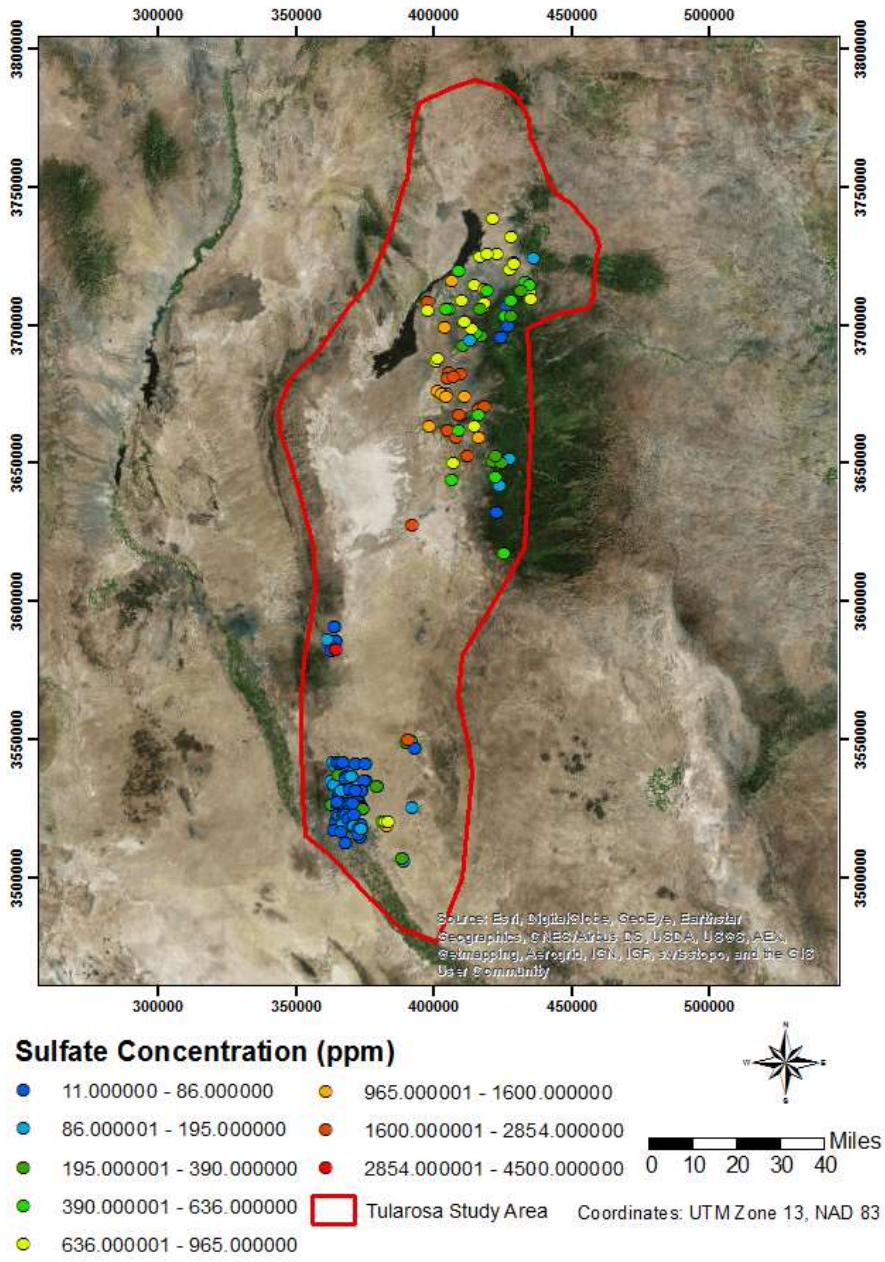

Figure 3. Sulfate (SO_4) contents of play fairway waters.

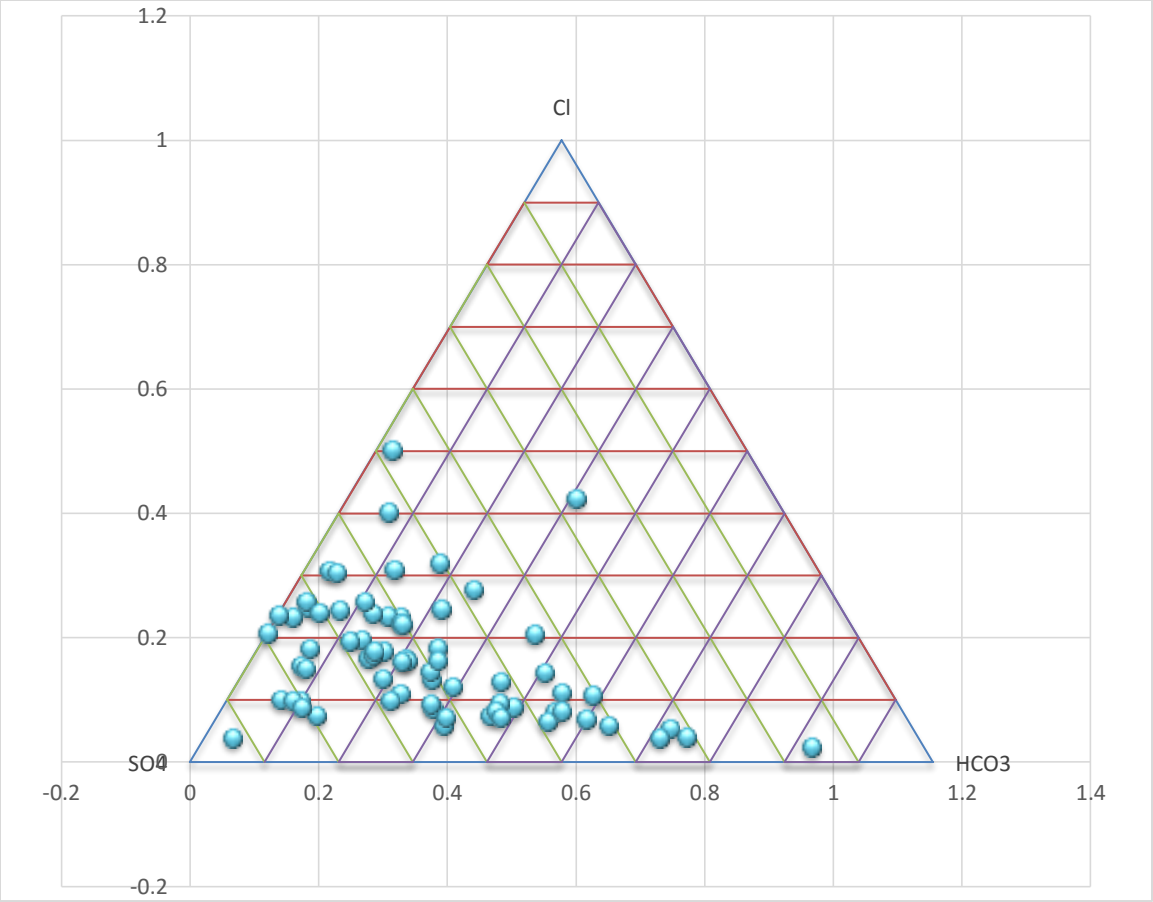

Figure 4. Relative Cl-SO_4-HCO_3 contents of waters from the northern region of the play fairway.

The Cl contents of the waters typically range up to several hundred mg/L, with most samples having a Na/Cl molar ratio of 1. The Cl concentrations display a spatial trend similar to that shown by SO_4, with the lowest Cl contents in the range and the highest in the basin. Mamer et al. (2014) suggested dissolution of halite was the primary source of the Cl and much of the Na based on the Na and Cl ratios.

Mamer et al. (2014) used tritium, ^{14}C and CFC data to assess the residence times of the waters. They concluded that most of the waters recharged hundreds to thousands of years ago and that there is no correlation between the age of the waters and their location.

Central Region

Water samples from the central region are primarily dilute HCO_3 waters with HCO_3 contents up to 150 mg/L, although one brine containing nearly equal amounts of SO_4 (4500 mg/L) and Cl (4100 mg/L) was analyzed (Fig. 5). The dominant cations are Na and Ca or K and Ca. The linear trend defined by the samples suggest they represent mixtures of HCO_3 and SO_4 rich waters, similar to the waters from the northern region.

Southern Region

In contrast to water from other portions of the fairway, the dominant anions in samples from the southern region are HCO_3 and Cl (Fig. 6). Na, followed by Ca, is the dominant cation. With the exception of the samples from the Ft. Bliss wells, waters from the southern region are relatively dilute, with total

dissolved solid contents of 1000-2000 mg/L. The linear relationship displayed on Figure 6 suggests they represent mixtures of Cl- and HCO_3-rich end members. Figures 1 and 2 show that the highest HCO_3 and lowest Cl concentrations are found in the western part of this area, whereas the highest Cl and lowest HCO_3 concentrations occur within the basin to the east. SO_4 concentrations tend to be relatively low, with concentrations less than 100/mg/L in most samples.

In contrast to the remainder of the southern region, Ft. Bliss well waters have total dissolved solids contents close to 10,000 mg/L (1 wt %) (Barker et al., 2015). These waters contain 4000-5500 mg/L Cl and concentrations of SO_4 close to 1000 mg/L. The high SO_4 contents suggest interactions with evaporate deposits; a conclusion consistent with fluid-mineral equilibrium calculations suggesting the water sampled at a depth of 1290 ft in well 56-5 is supersaturated with respect to barite (Barker et al., 2015). In contrast, water from 2960 ft is undersaturated in barite even though both the shallow and deep water contain similar concentrations of Cl and SO_4 (4220 vs 4270 mg/L and 846 vs 834 mg/L respectively). However, no SO_4 deposits (e.g. deposits containing barite, gypsum, or anhydrite) were observed in the cuttings samples from the Ft. Bliss wells. Thus, interactions with evaporate deposits may have occurred in the near-surface environment during wetter climates when lakes were present in the basin.

These chemical relationships suggest the compositions of the HCO_3-rich waters in the southern region are dominated by interactions with limestone beneath the western edge of the fairway whereas the composition of the Cl-rich waters is strongly influenced by evaporate deposits in the basin.

Geothermometry

Cation geothermometers are widely used to estimate reservoir temperatures but can yield inappropriate results if not interpreted with care. This is especially true for low- to moderate-temperature resources. To assess their applicability, standard geothermometer temperatures were calculated for the Ft. Bliss waters by Barker et al. (2015). These waters are appropriate for testing the reliability of the geothermometers because thermal data from Ft. Bliss indicates the wells were drilled into a convecting hydrothermal system. Barker et al. (2015) concluded that the quartz (conductive) geothermometer (Fournier, 1991) temperatures most closely matched the measured well temperatures, which ranged from 78^o to approximately 100^{o}C, and thus, could be considered “reliable”. The chalcedony geothermometer, which is often appropriate for low- to moderate- temperature waters (Fournier, 1991), yielded temperatures that are significantly lower than the measured temperature. In contrast, the Na/K and K/Mg geothermometers yielded values that were 80^o to >100^{o}C and 20^o to 30^{o}C hotter, respectively, than the measured temperatures (Giggenbach, 1991). The chalcedony, Na/K and K/Mg geothermometers were all considered unreliable.

Figure 7 presents the SiO_2 contents of the fairway waters. Quartz geothermometer temperatures are shown in Figure 8. The highest geothermometer temperatures, ranging from 100^o to 121^{o}C, are found in the northern and southern regions. However, geothermometer temperatures ranging from 80^o to 100^{o}C are found throughout the fairway, suggesting potential targets are present in all three regions.

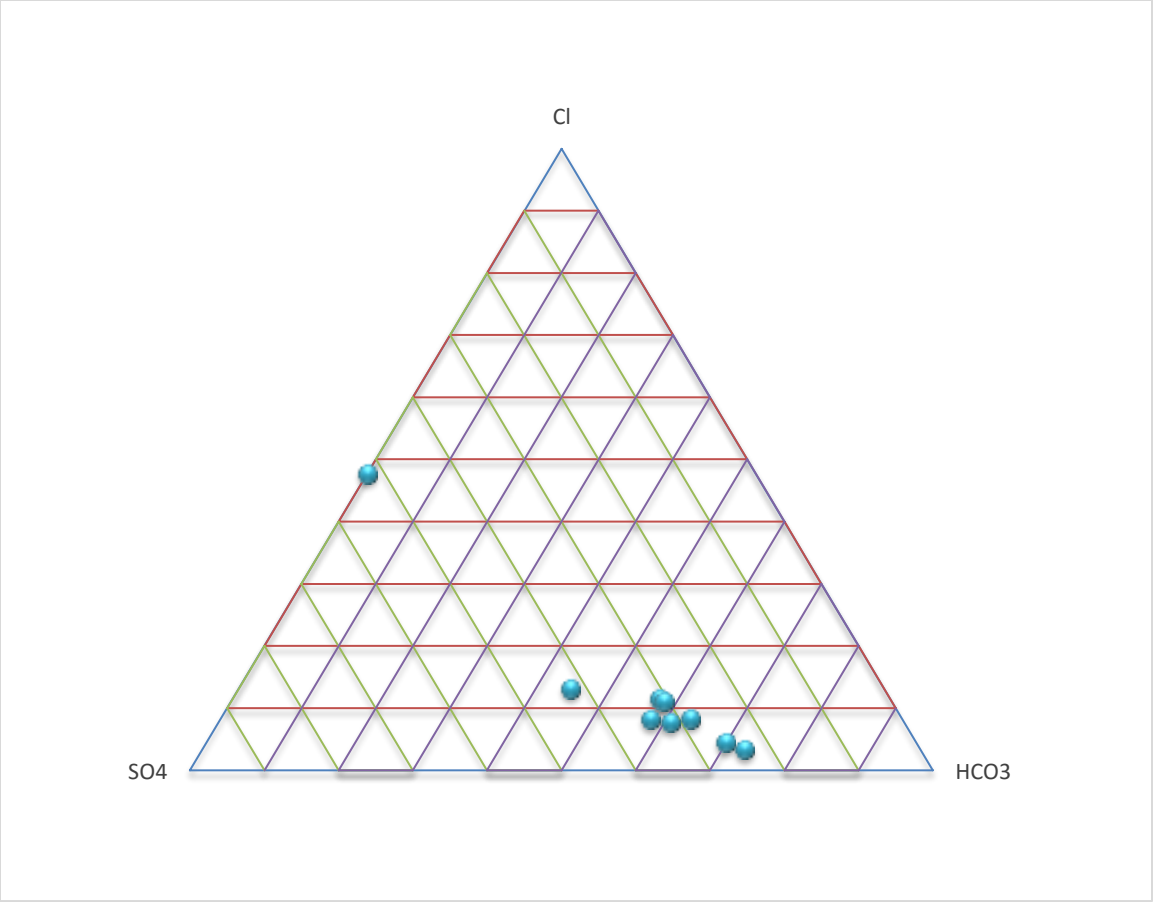

Figure 5. Relative Cl-SO_4-HCO_3 contents of waters from the central region of the play fairway

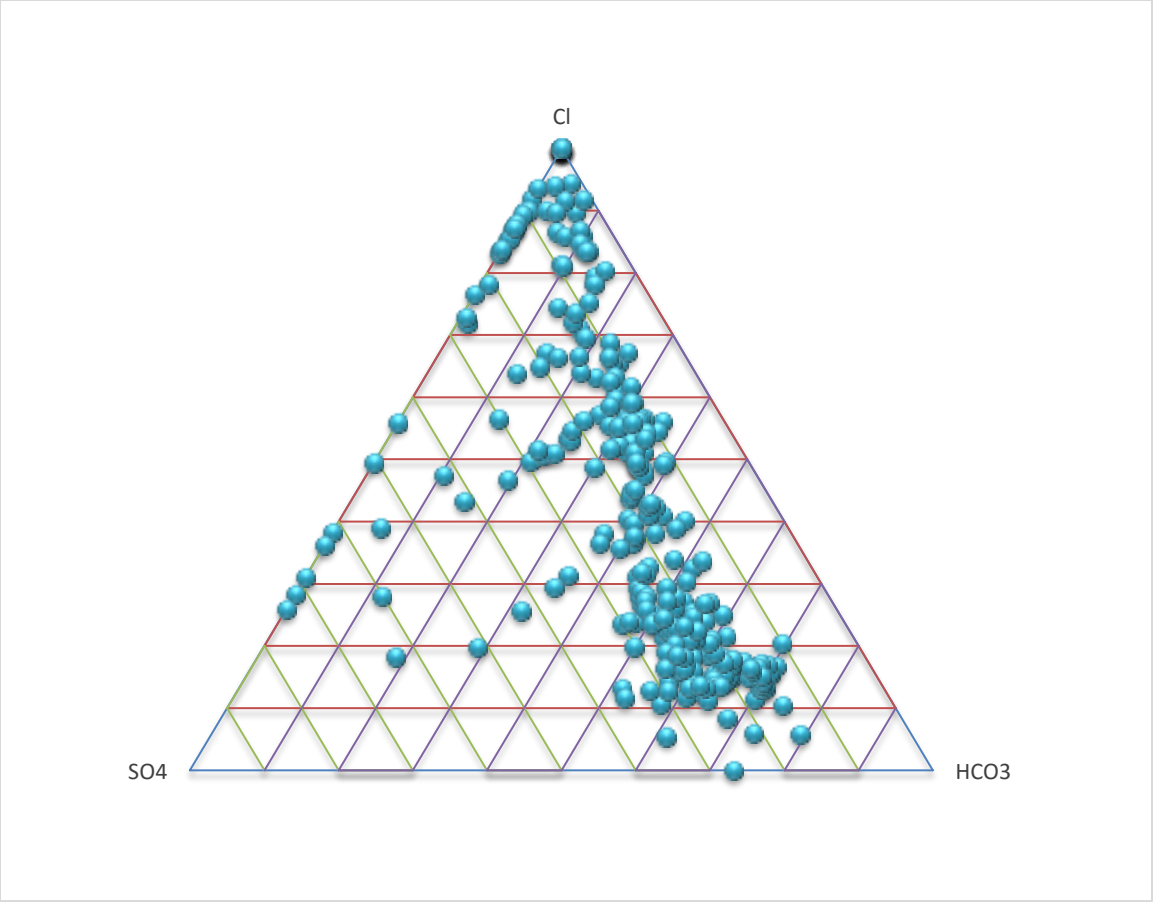

Fig. 6. Relative Cl-SO_4-HCO_3 contents of waters from the southern region of the play fairway.

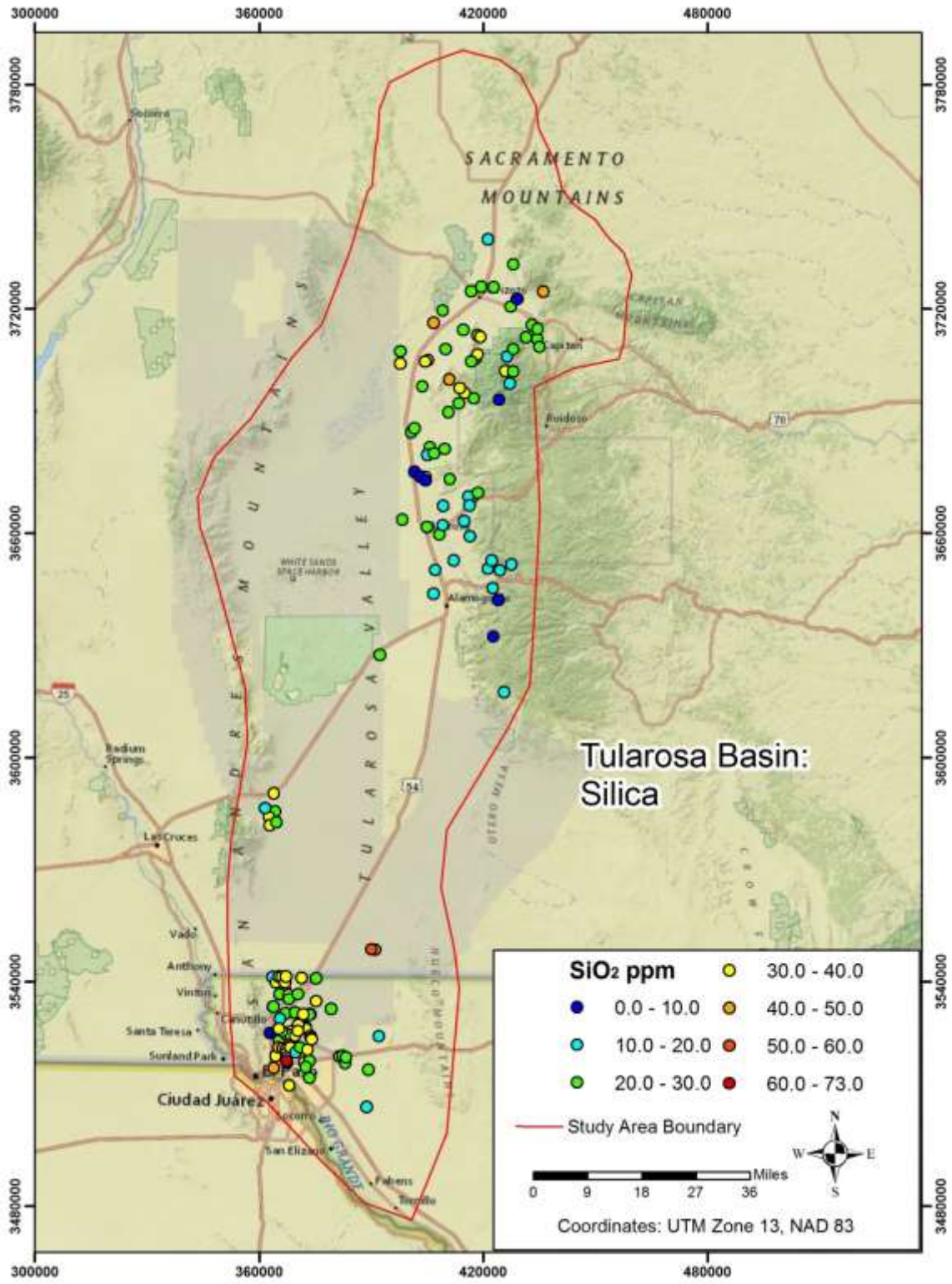

Fig. 7. Silica (SiO_2) contents of play fairway waters.

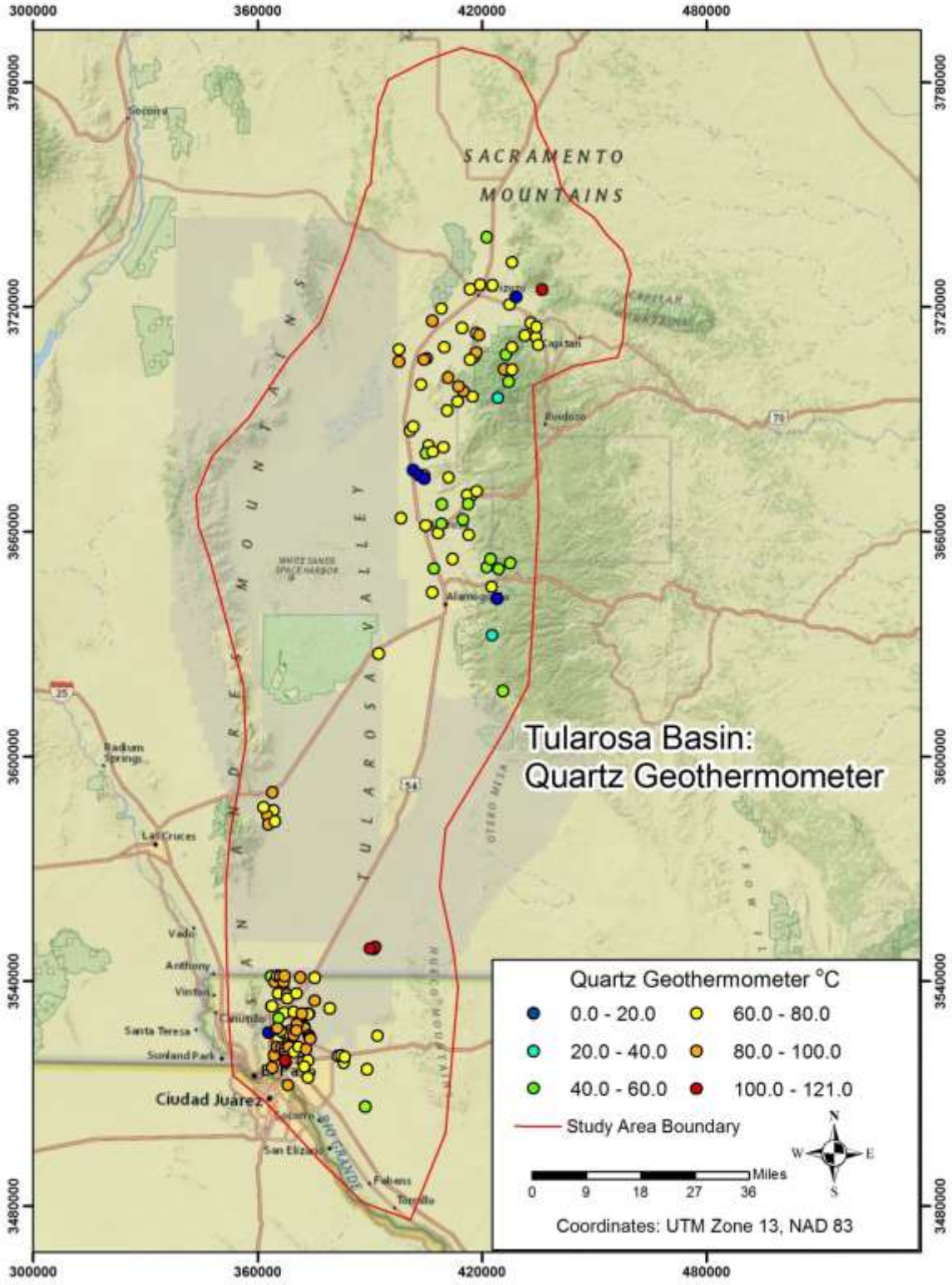

Fig. 8. Quartz (conductive) geothermometer temperatures.

Strain

Strain is an important consideration in PFA and was considered in this project. However, few GPS stations were available. Therefore, the ZR Ratio was applied to produce surrogates of strain within given areas of the study area.

Geothermal systems in the Great Basin are commonly related to relatively high strain rates (Faulds et al., 2012) and this should apply throughout the Basin and Range. The ZR ratio of Formento-Trigilio and Pazzaglia (1998) can be used to predict strain rates. In order to calculate ZR ratios, a large 10 m resolution DEM of the Tularosa basin was divided into twelve zones, shown in Figure 1, and then calculations proceeded as follows, for each zone.

Calculate local mean elevation (Ź), where $\sum_n Z_r$ is the sum of elevation values within a zone *r* and *n* is the number of elevation values within the zone.

$$\acute{Z} = \sum_n Z_r/n$$

Calculate the local mean relief ($\acute{R}$).

$$\acute{R} = (Z_{max} - Z_{min})$$

Calculate the ZR ratio.

$$ZR = \frac{\acute{Z}}{\acute{R}}$$

The results are shown on Figure 2. A minimum ZR ratio is 0.75 (Zone 4), and maximum is 1.92 (Zone 8). The mean ZR ratio is 1.146035 and the standard deviation is 0.35. Zone 8 is nearly two standard deviations greater the mean, while Zone 10 is about one and a half standard deviation greater. These zones have very high strain relative rates. Zones 1, 2 and 11 also have above average strain rates, though they are less than one standard deviation from the mean. That leaves Zones 3, 4, 5, 6, 7, 9, and 12, which are all below average and within one standard deviation of the mean.

The Tularosa Basin is large, roughly 30,000 sq. km, and so it is likely that strain rates vary throughout the basin. By clipping the basin into twelve equal zones, the variation in strain can be seen with better resolution than the infinitesimal strain rate calculations that can be made from GPS velocity vector triangles given the few stations available. It is permissible that the zones with relatively high strain rates will be more likely to have zones of high permeability, and therefore are more accommodating to geothermal systems. This analysis suggests that the northern and southern parts of the basin are the areas of greatest strain. This was taken into consideration, among many factors, in play prioritization.

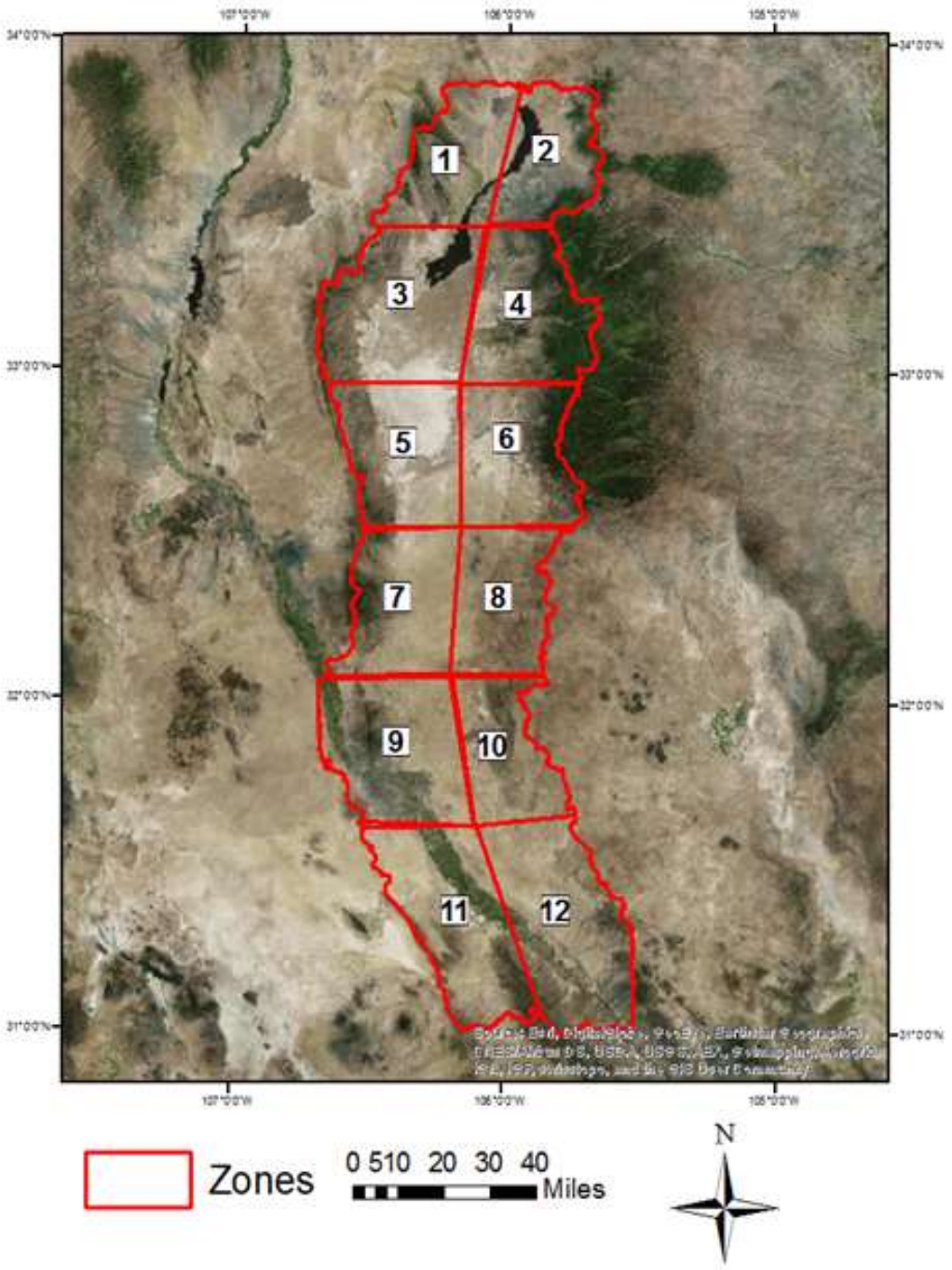

Figure 1. Tularosa Basin, divided into 12 zones for ZR ratio comparisons. Zone 8 and 10 have relatively high strain rates.

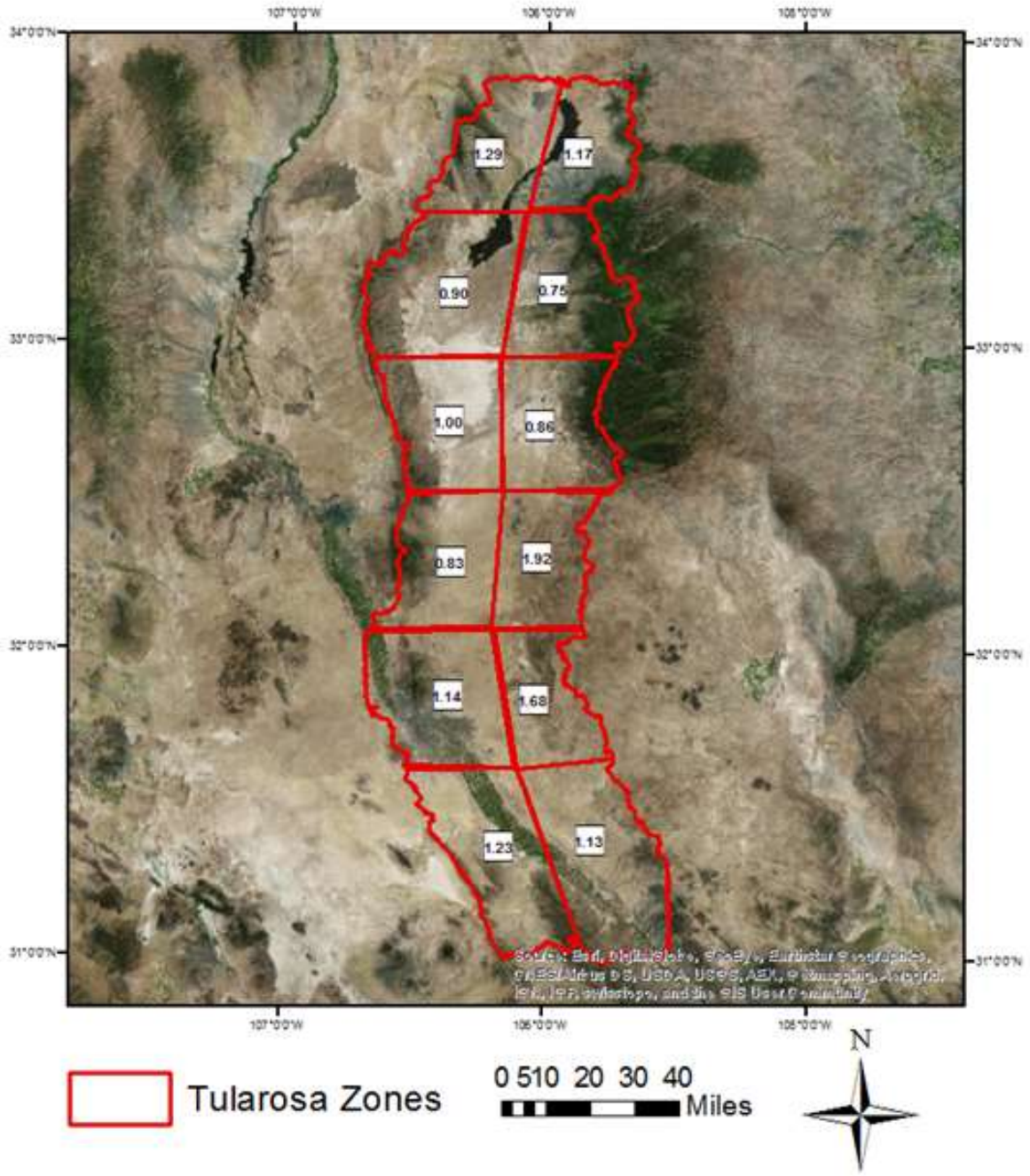

Figure 2. ZR Ratio values per zone. Higher values suggest greater strain and potentially better zones of permeability.

Basement Structure

Remote Sensing

Day and night time Advanced Spaceborne Thermal Emission and Reflection Radiometer (ASTER) data, covering most of the study area, was obtained to (1) map surface temperature anomalies, (2) map mineralogy as related to rock brittleness to support possible future EGS, and (3) map areas of hydrothermal alteration. The properties of this data are shown in Figure 1. These data have been shown to be useful for general geological mapping (Hulen et al., 2005); lithologic mapping (Rowan and Mars, 2003); hydrothermal mineralogy mapping (Rowan et al., 2003; Mars and Rowan, 2006); and temperature anomaly mapping (Eneva, 2007).

First surface temperatures were calculated from ASTER emissivity data. These 90 m spatial resolution data were used to determine if any anomalous temperatures could be found along the fault-bounded basin margins. Figure 1 show the results. A few areas show up along the base of the Sacramento Range, but they are not associated with plays. However, on the west side of the valley there are anomalies that either are or could be associated with plays. Field work is needed for verification.

To map the mineralogy that can affect EGS (fracing), band ratios, using diagnostic absorption features in the shortwave and thermal infrared, were used to highlight calcite and silica (brittle rocks) and clay (softer rocks) and gypsum representing evaporite beds that can be problematic in fracing. Relative concentrations of these minerals were recorded in a shapefile per mapped rock unit. The results can be seen in Figure 2. The classification was conservative and a large percentage of the rock in the area was rated as high risk. This was often the result of potential evaporite beds. Where this was not the case high risk was due to high clay content. This data, however, has not been field verified.

Hydrothermal alteration was not found to be prevalent in the study area. It was mapped in the Jarilla Mountains near Orogrande, in a small area in the Sacramento Mountains south-southeast of Oscura, and it was suggested in Mesoproterozoic granite alone the eastern margin of the San Andreas Range (Fig. 3), but this could be from weathering or hydrothermal alteration or both and needs to be field verified to determine if any alteration related to geothermal activity.

Table 1. ASTER VNirSwir band characteristics. Band numbers are in parentheses.

Spectral Region	Bandwidth (microns)	Spatial Resolution	Quantization Level
Visible Green (1)	0.52-0.60	15 m	8 bits
Visible Red (2)	0.63-0.69	15 m	8 bits
Near Infrared (3)	0.78-0.86	15 m	8 bits
Shortwave (4)	1.60-1.70	30 m	8 bits
Shortwave (5)	2.145-2.185	30 m	8 bits
Shortwave (6)	2.185-2.225	30 m	8 bits

Shortwave (7)	2.235-2.285	30 m	8 bits
Shortwave (8)	2.295-2.365	30 m	8 bits
Shortwave (9)	2.360-2.430	30 m	8 bits
Thermal infrared (10)	8.125-8.475	90m	12 bits
Thermal infrared (11)	8.475-8.825	90m	12 bits
Thermal infrared (12)	8.925-9.275	90m	12 bits
Thermal infrared (13)	10.25-10.95	90m	12 bits
Thermal infrared (14)	10.95-11.65	90m	12 bits

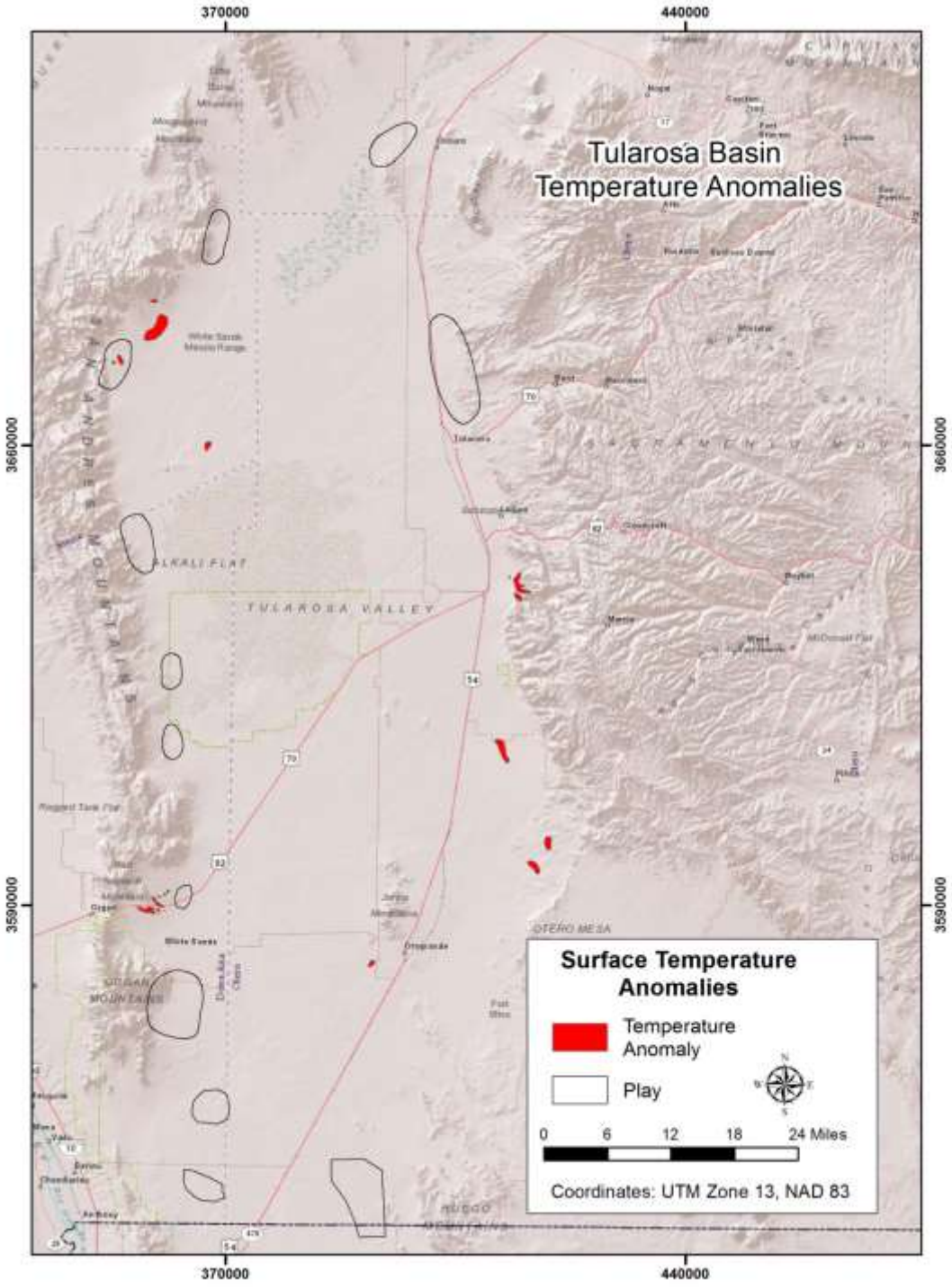

Figure 1. Surface temperature anomalies mapped from ASTER nighttime surface temperature data.

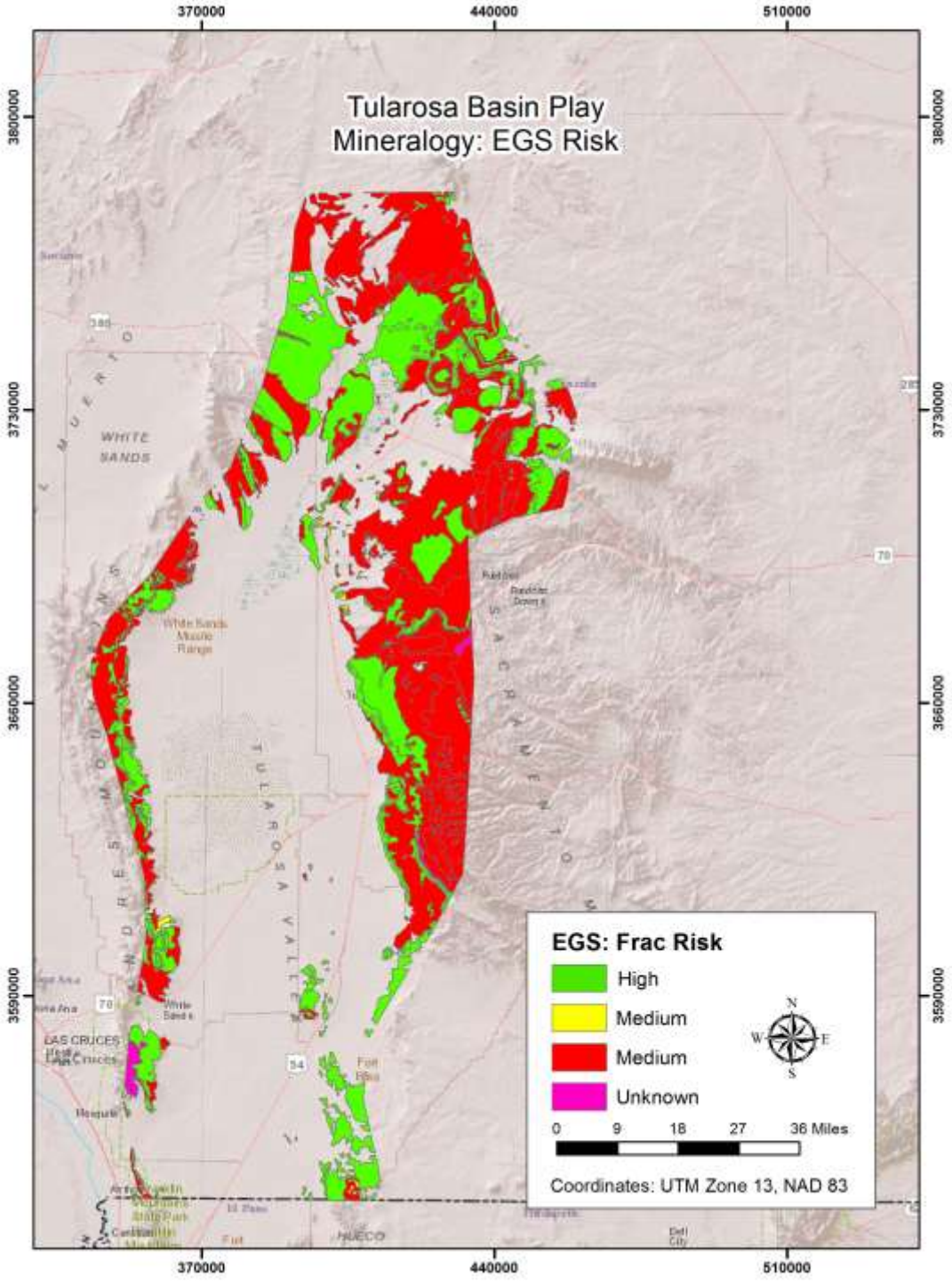

Figure 2. EGS risk based up rock brittleness suggested by ASTER multispectral image analysis.

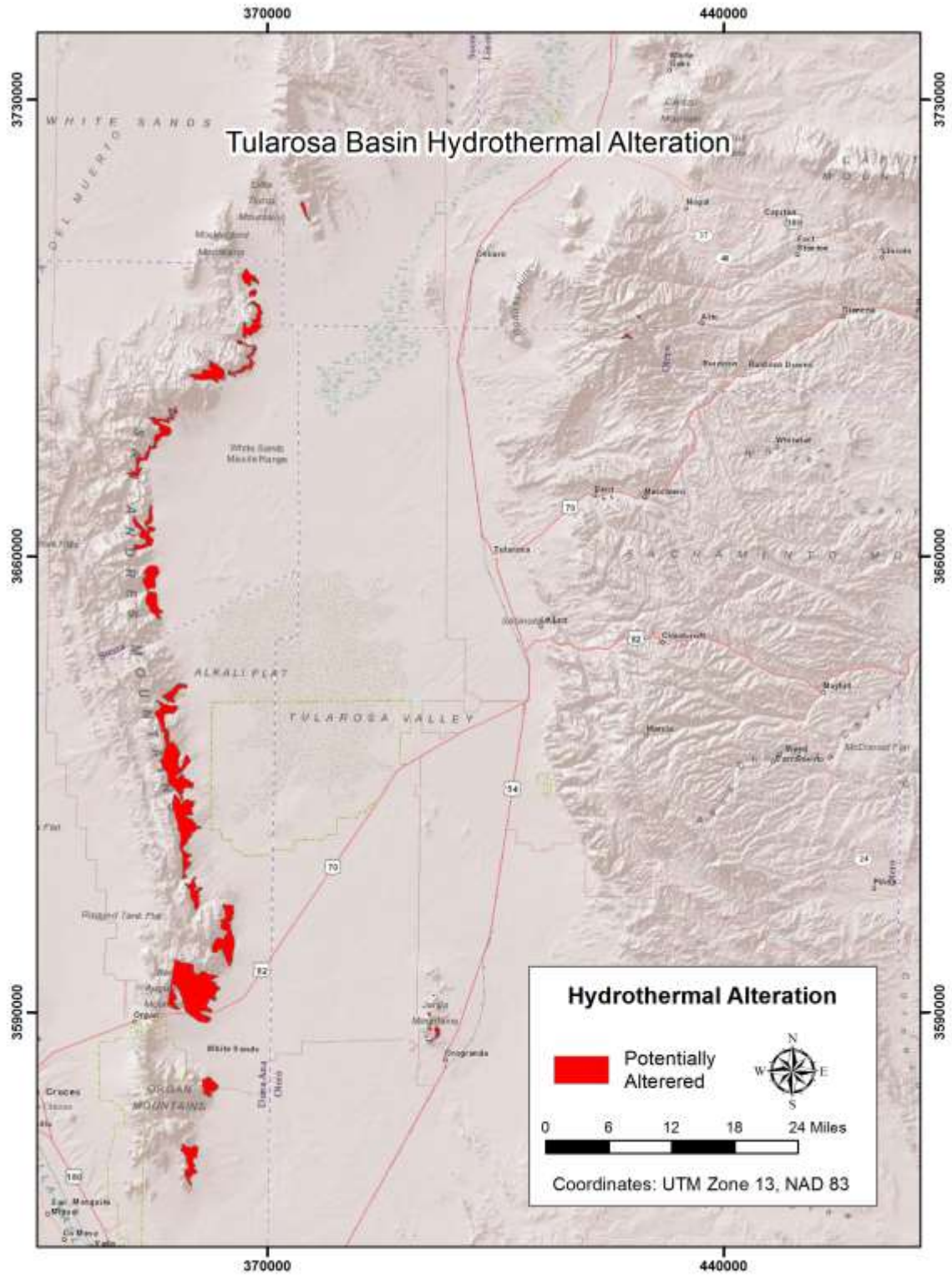

Figure 3. Hydrothermal alteration suggested by ASTER multispectral image analysis. The extensive areas on the west side of the valley are related to Mesoproterozoic granite, and may be from weathering or hydrothermal alteration or both.

Geophysical Profiles of the Tularosa Basin

Basement Structure

In order to achieve a general understanding of the basins structure we constructed 12 east-west cross sections (across the basin) and one longitudinal cross-section (north-south) using contours created from regional magnetic intensity and Bouguer gravity anomaly data obtained from PACES, University of El Paso, Texas. The locations of these geophysical profiles are shown in Figures 1 and 2.

These profiles show relative highs and lows in the geophysical properties across and along the Tularosa basin. These geophysical highs and lows indicate heterogeneities in the basin arising from rock properties (density and magnetic differences) and/or fault-bounded structural highs. In other words, a simplistic view of the Tularosa basin merely as a Tertiary rift graben filled with sediments and bounded by structural highs on the east and west margin of the basin is not realistic. This region has experienced a long and complex geological history with different thermo-tectonic episodes, and the following Figures exhibit some of this complexity.

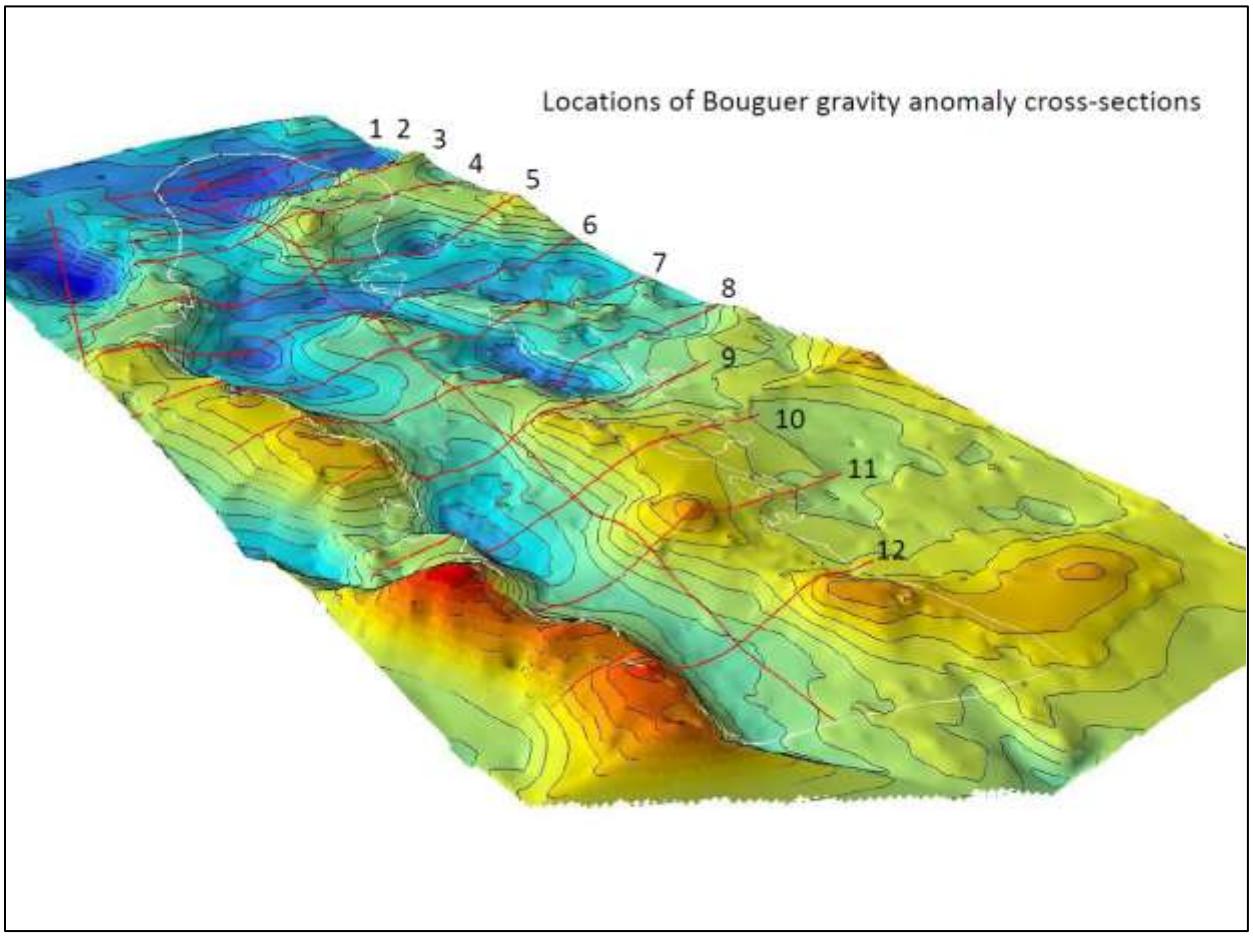

Figure 1. Locations of east-west cross sections for Bouguer gravity anomaly contours. Several sub-basins can be noted in this graphic.

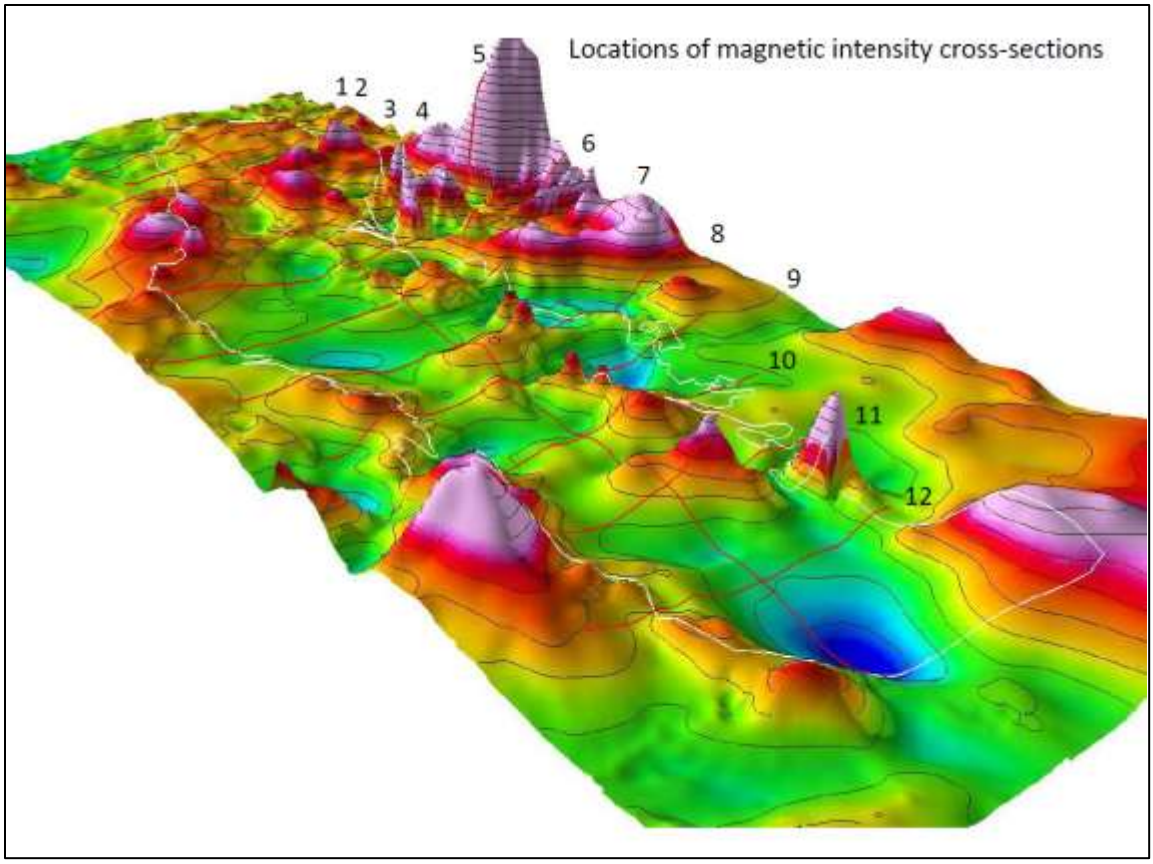

Figure 2. Locations of east-west cross sections for magnetic intensity contours, again indicating the presence of several sub-basins.

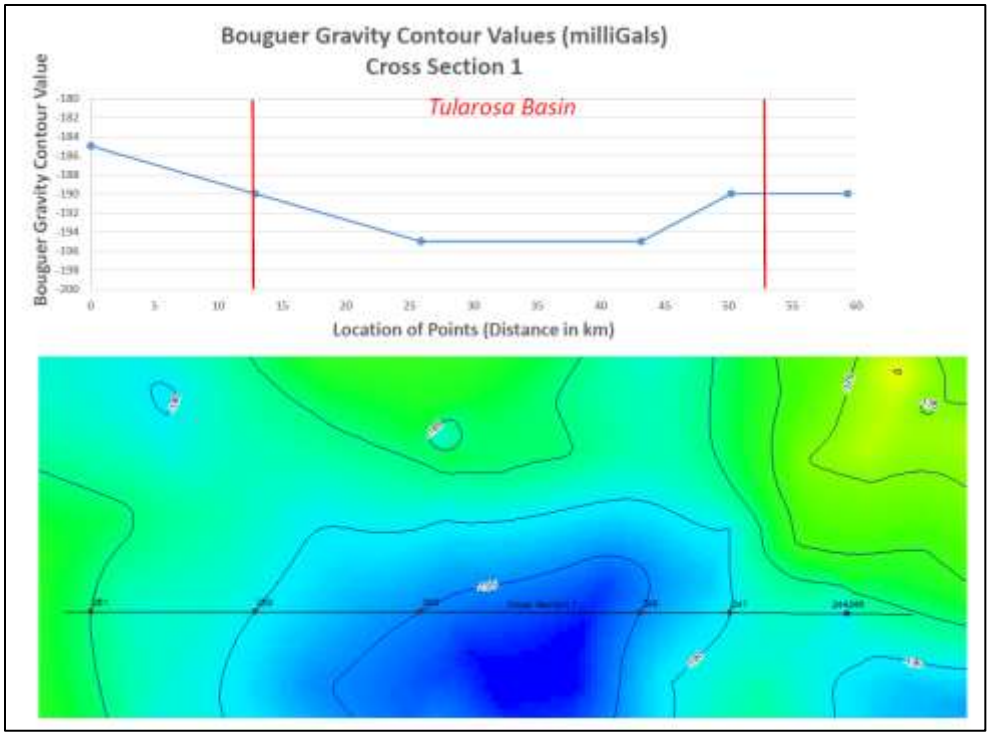

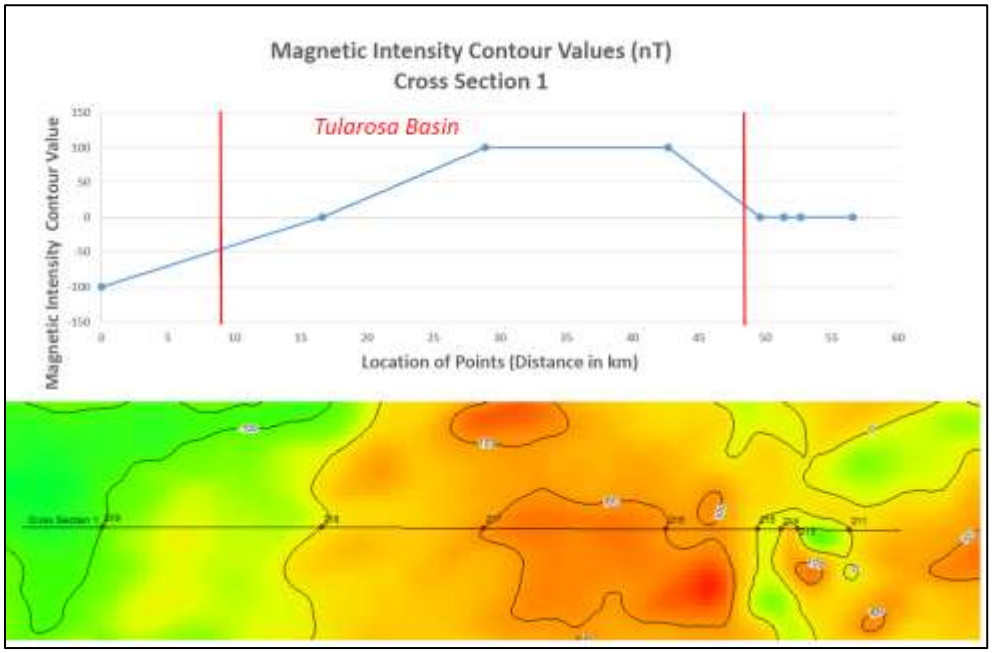

Figure 3. The east-west gravity cross-section (top) shows a relatively simple extensional basin profile. The bottom magnetic cross-section shows a high that is the inverse of the gravity profile, perhaps indicating a down-dropped tertiary intrusive.

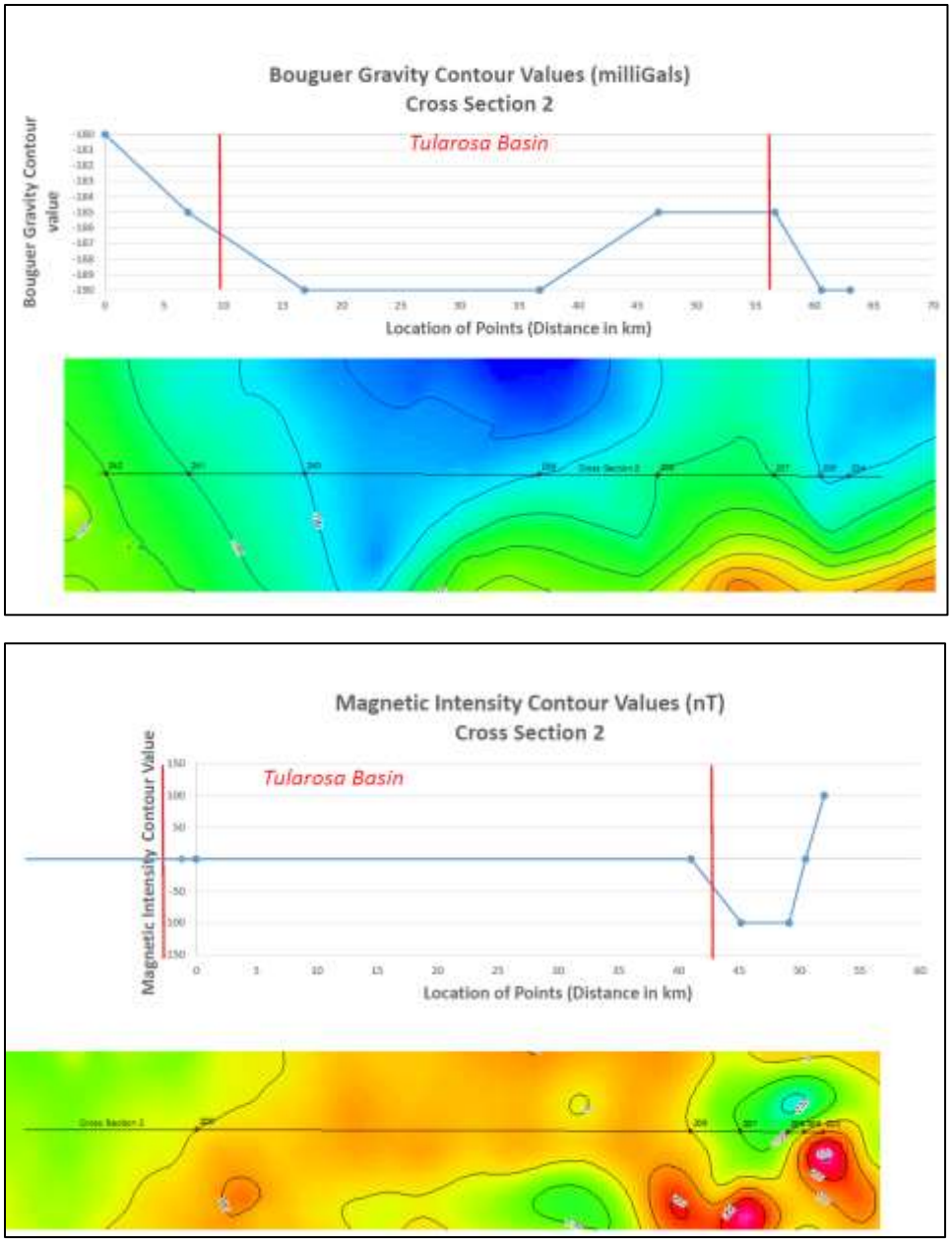

Figure 4. A gravity high (top) on the east side of the basin suggests a horst-like structure just outboard of the northern Sacramento Range that may be buried glide-block of primarily low-magnetic mineral sedimentary rock as suggested by the magnetic low covering part of the same area (bottom). The generally flat nature of the magnetic profile suggests a paucity of magnetic minerals and a sedimentary section in this part of the basin.

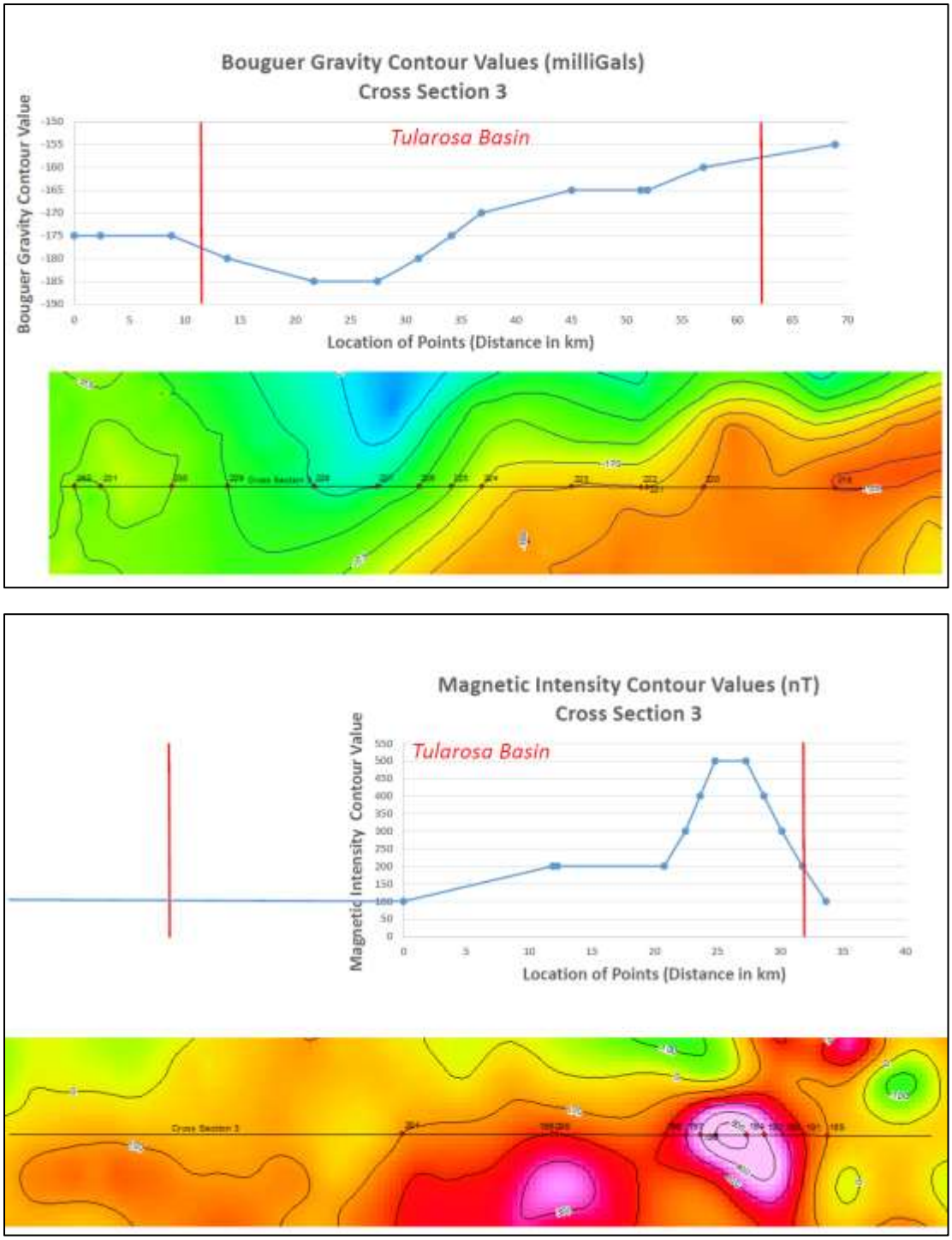

Figure 5. The gravity profile (top) suggest two west-dipping normal faults, one bounding the Sacramento Range and one out-board of the range, as well as an east-dipping normal fault bounding the basin on the west. The magnetic data (bottom) once again peaks on the east side of the cross-section suggestion intrusive rock, which is faulted (fault correlates with gravity fault). As the magnetic data cross-section slopes to the west it crosses a Quaternary basalt flow which may cause the moderate high prior to dropping off to the west.

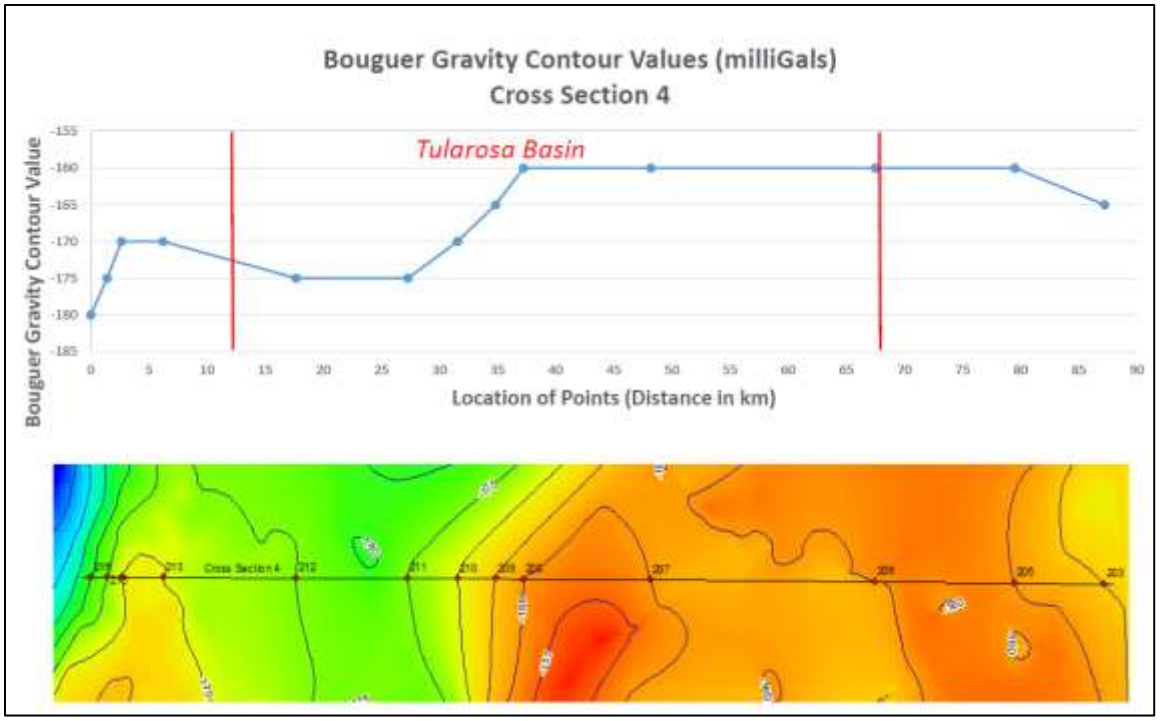

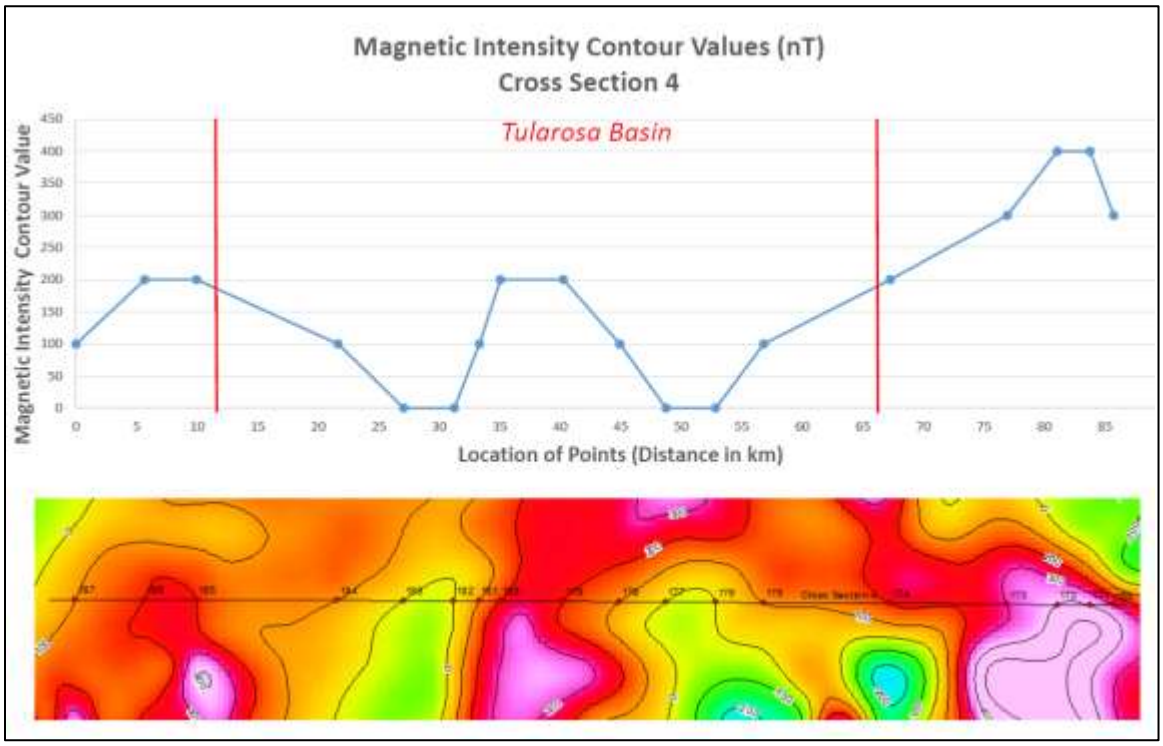

Figure 6. The gravity profile (top) shows a narrowing of the basin with a distinctive west-dipping fault bounding the east side of the valley and possibly another west-dipping fault on the western margin of the profile. The Magnetic data show a prominent high that may represent mafic magma chamber rocks related to the Quaternary basalt flow that this profile crosses.

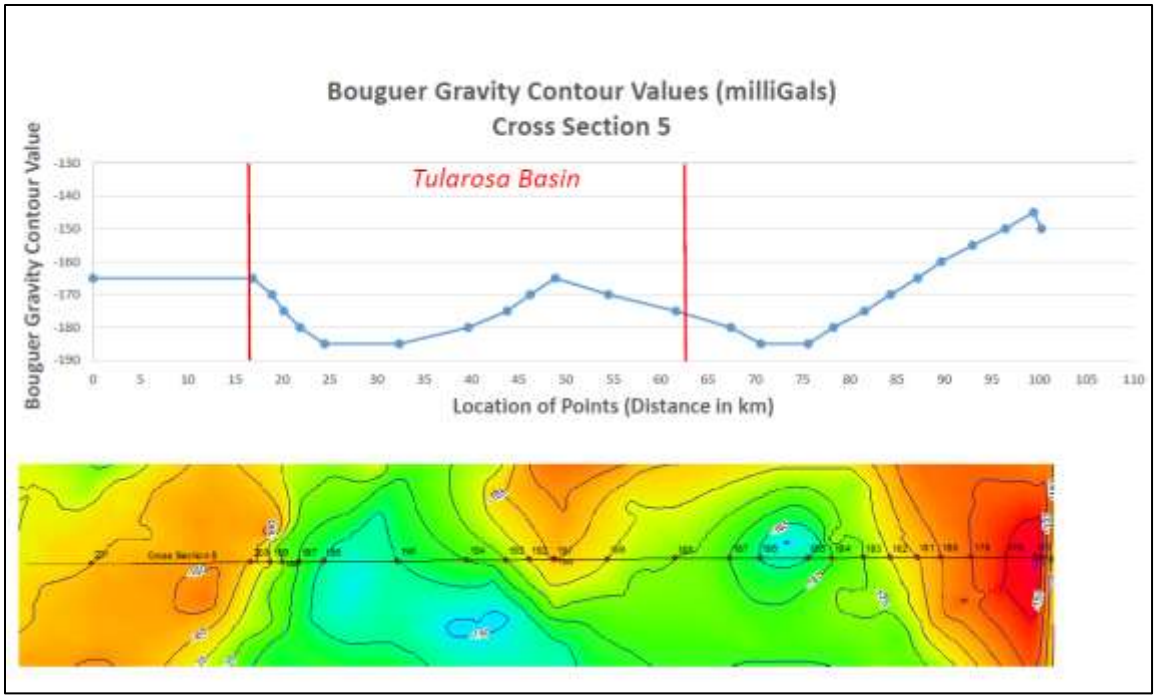

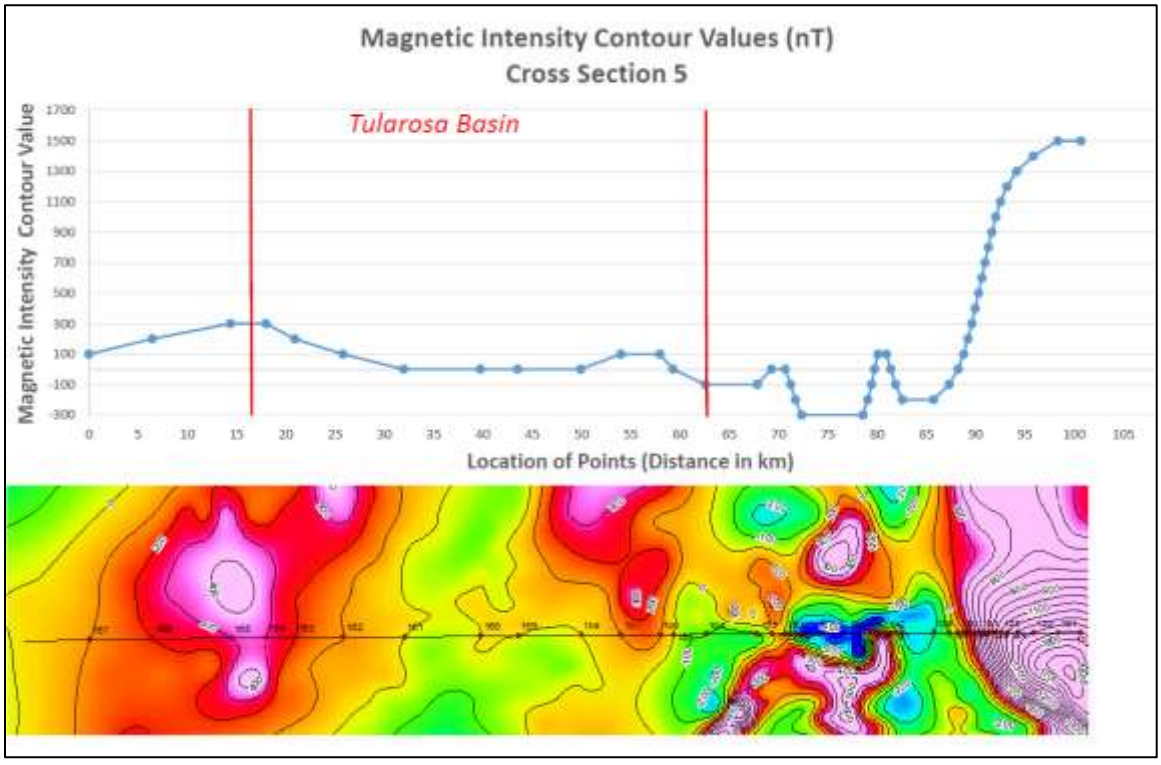

Figure 7. Both the gravity (top) and magnetic data (bottom) suggest the location of basin-bounding faults and what may be the southern margin of the mafic magma chamber related to the Quaternary basalt flow.

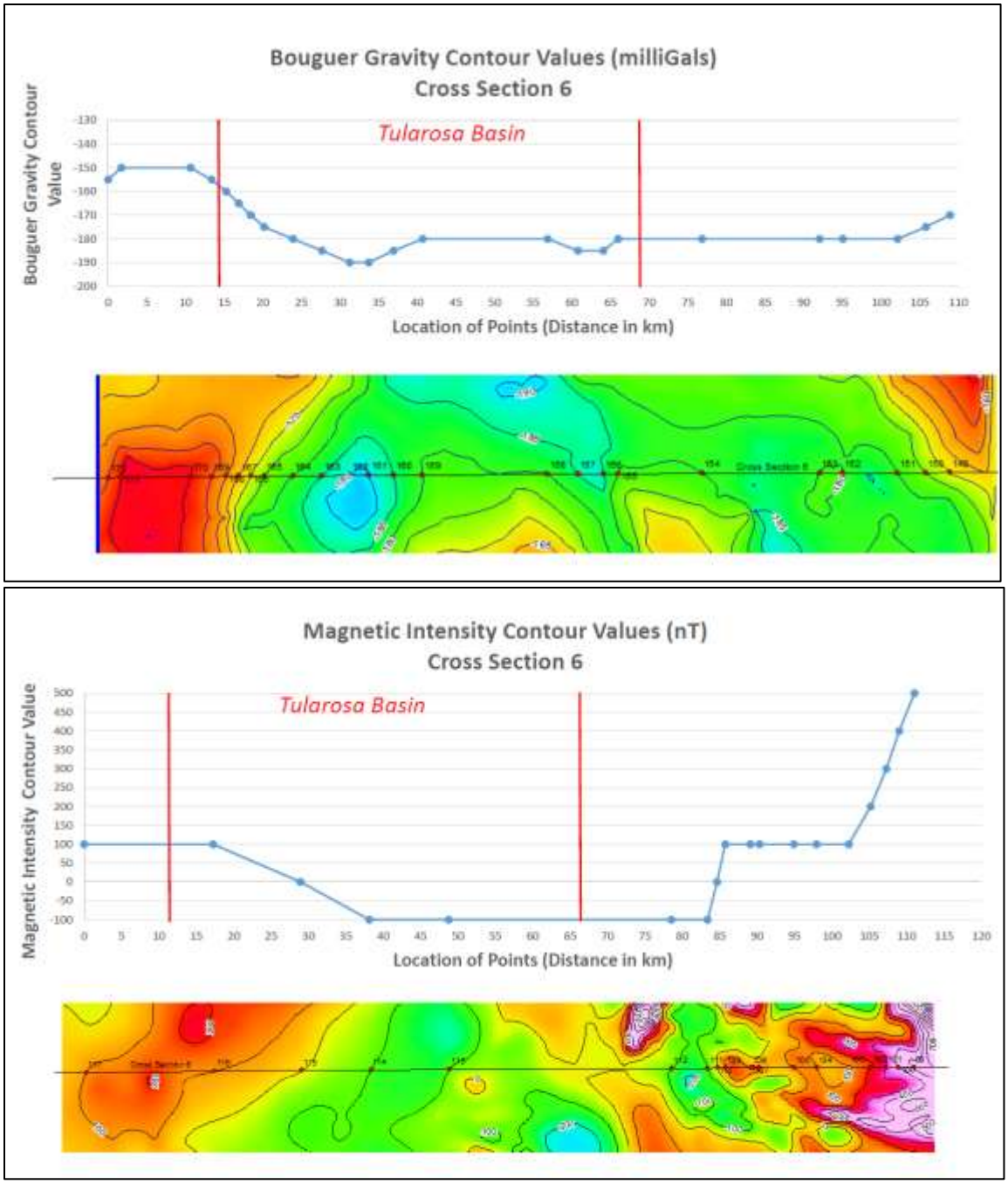

Figure 8. The gravity data profile (top) is relatively flat along the eastern basin margin with only a slight dip. This may be related to relatively young fault propagation of the Sacramento Range bounding faults in this area – a location where fault-tips are coalescing producing critical stress. A basement high is also apparent in the gravity profile. A well-developed east-dipping fault along the western basin margin is suggested by both data profiles.

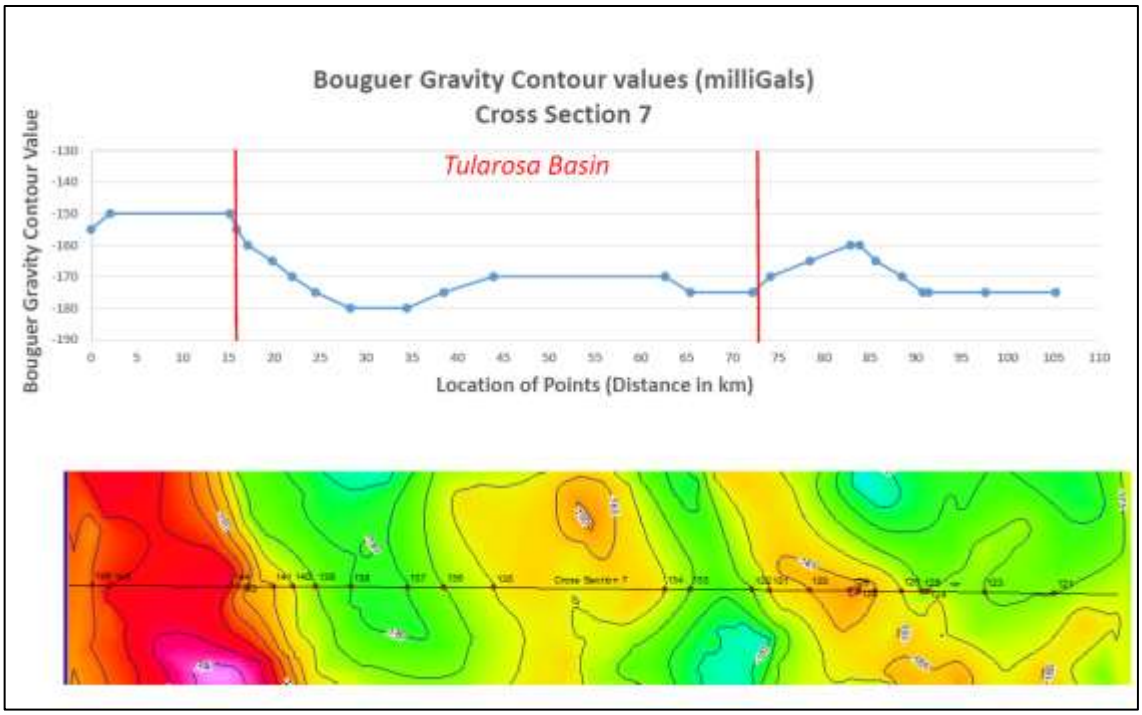

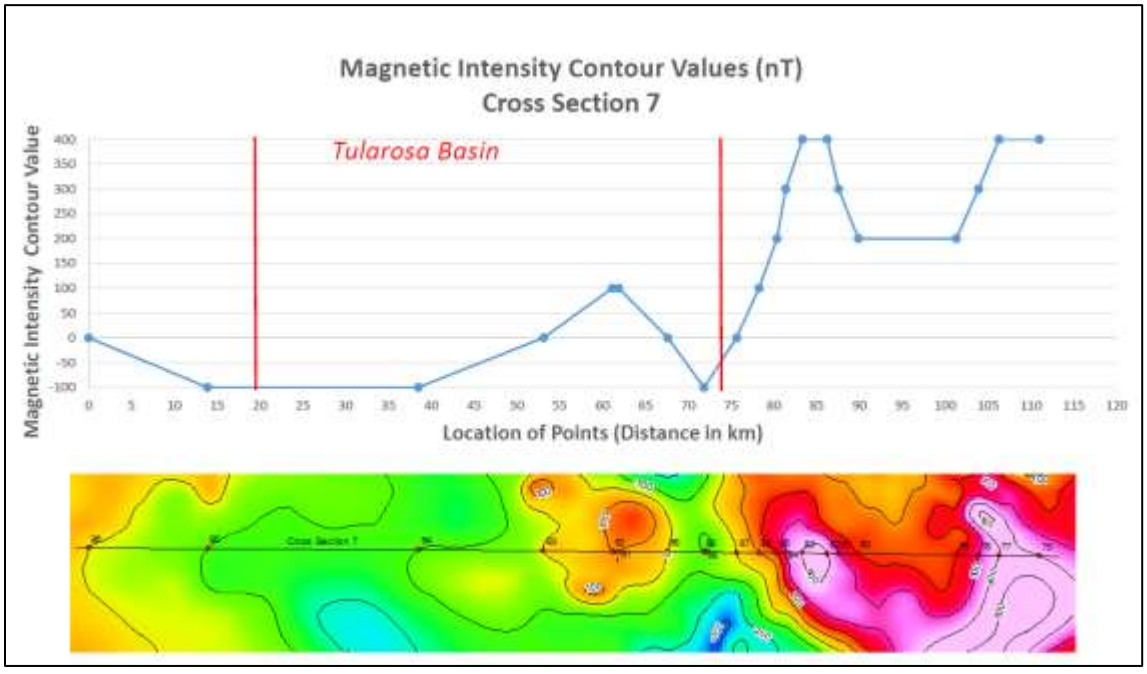

Figure 9. The gravity profile (top) again suggests normal faults bounding both the eastern and western margins of the basin. The basement high is more prominent than in Figure 8 suggesting a buried horst with faulting conjugate to the basin bounding faults. A magnetic high across part of the horst suggests that a portion of its lithology consist of volcanic, volcaniclastic, or intrusive rock. Both datasets suggest a basin flexure in this area, with fault-strikes changing from a predominantly NE direction to a NNW direction.

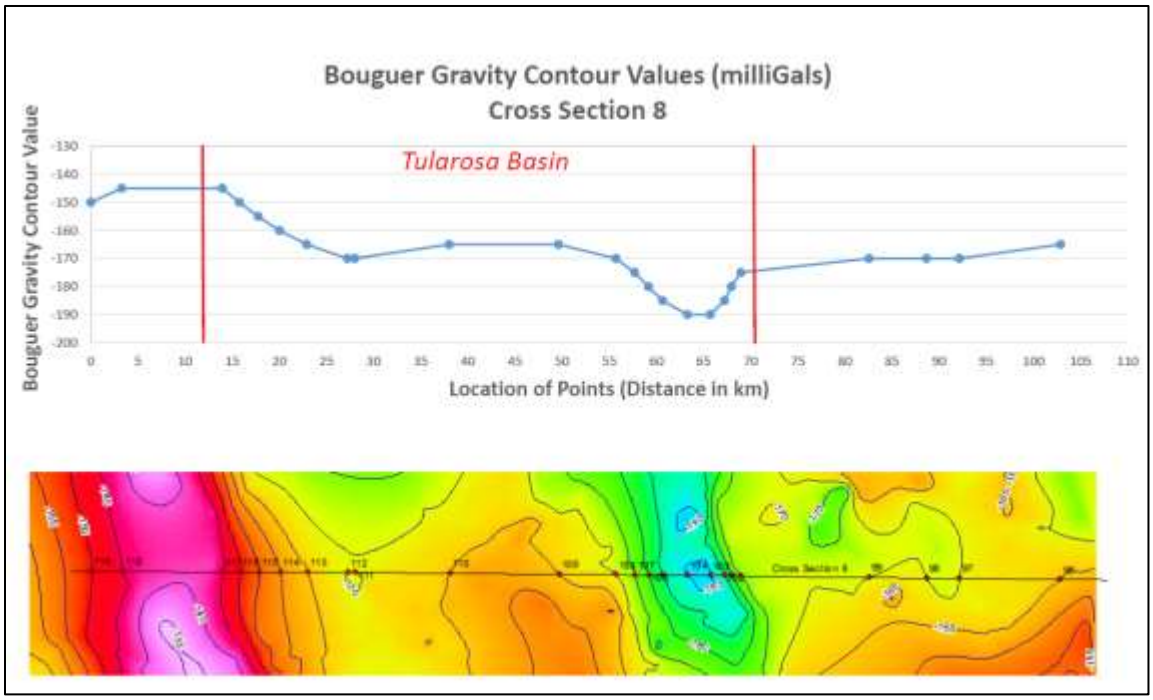

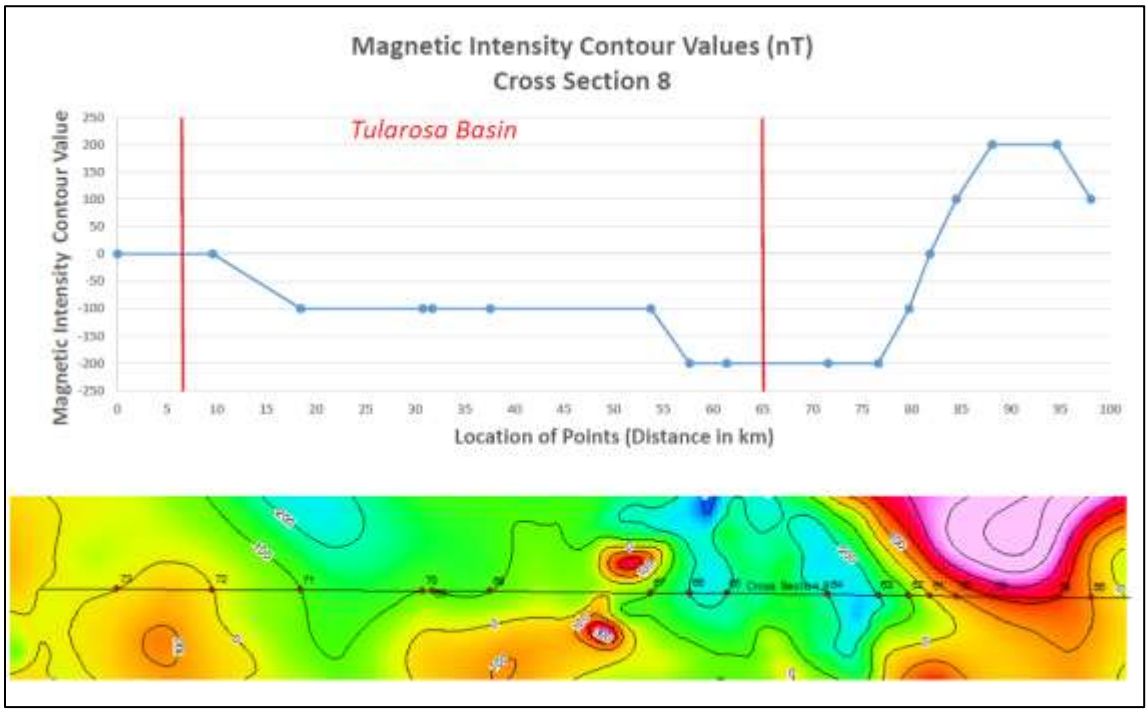

Figure 10. The gravity profile (top) continues to suggest a basement high, which may be an extension of the horst postulated in Figure 9. This is also suggested by the magnetic profile (bottom), although the western edge is truncated.

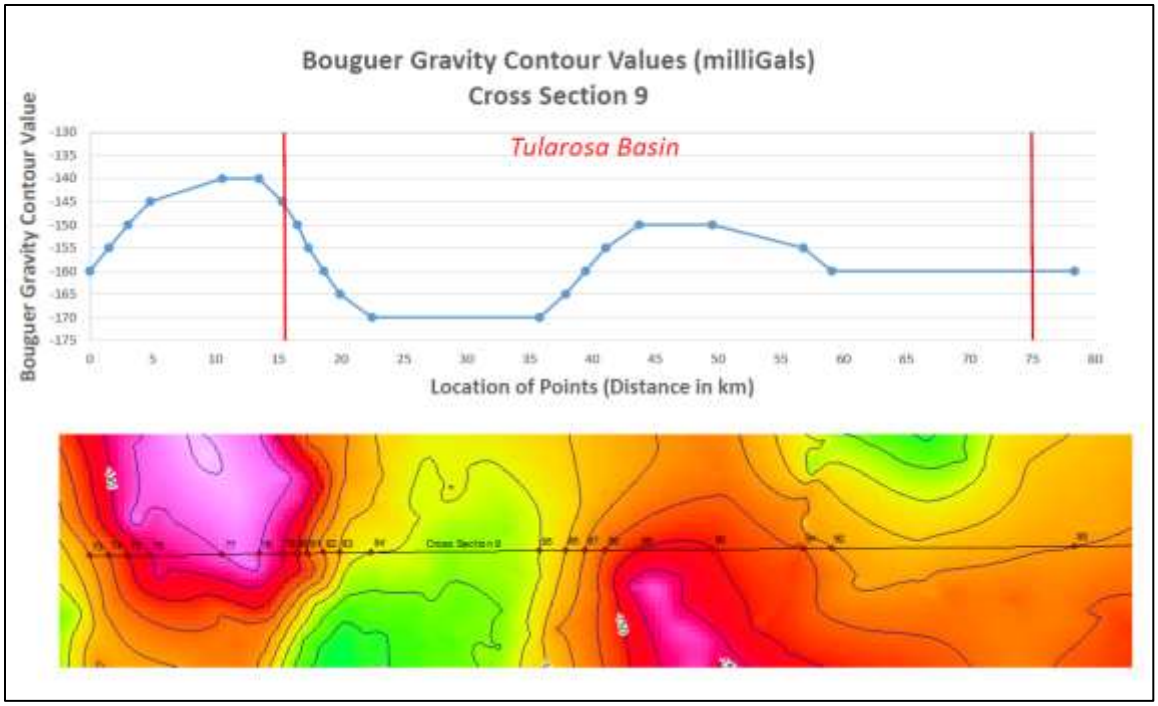

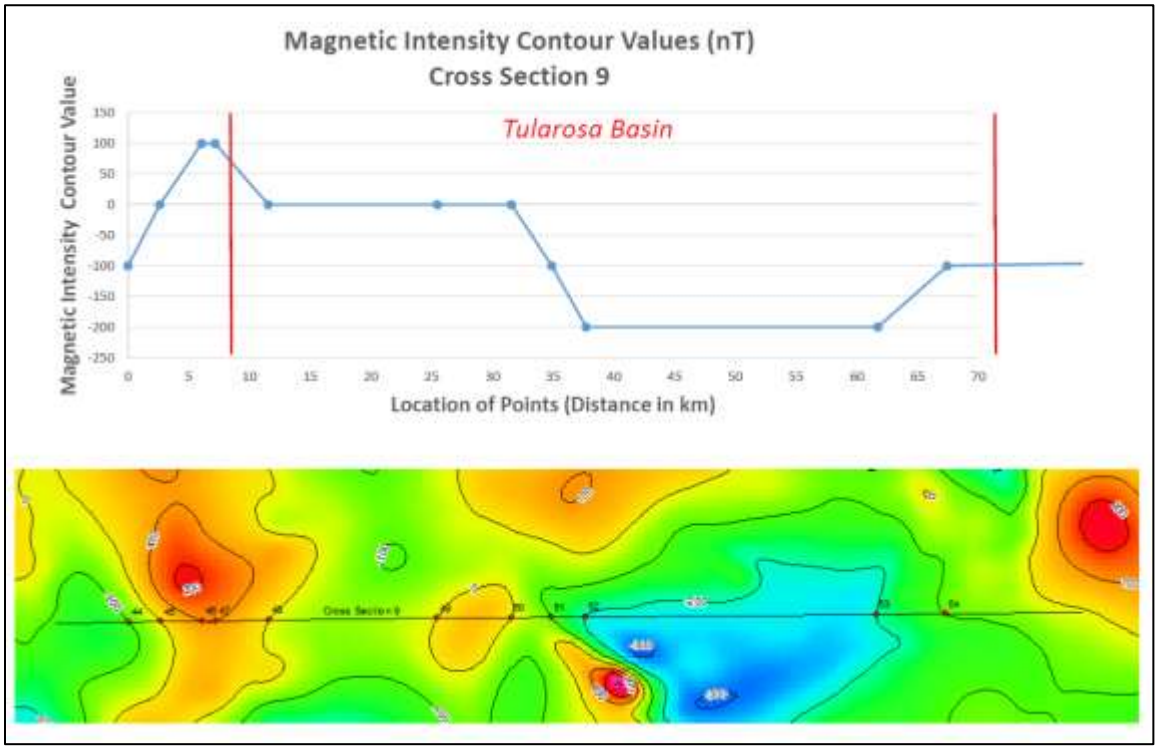

Figure 11. The gravity profile (top) again suggests well developed basin-bounding fault systems. The magnetic profile (bottom) suggests a transition from buried volcanic/intrusive rock to sedimentary rock to the east.

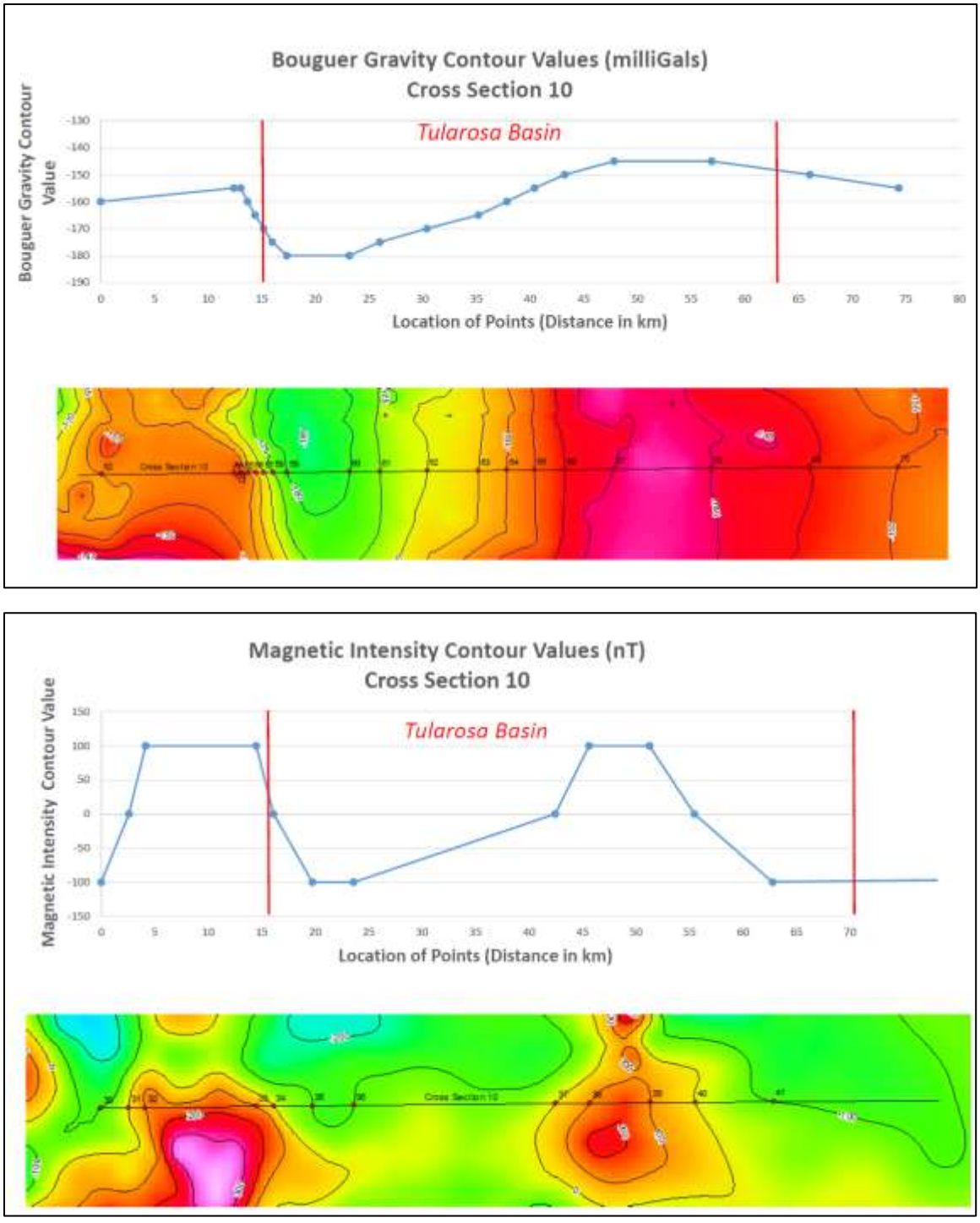

Figure 12. These profiles cross near the southern terminus of the Sacramento Range. The gravity profile has a steep gradient on the western basin margin, but the gradient on the eastern margin is significantly more gentle, suggesting less fault offset. The significant magnetic high on the eastern side of the bottom profile suggests an intrusion in the Sacramento Range and that seen to the west may result from Paleoproterozoic igneous rocks in the San Andreas Range.

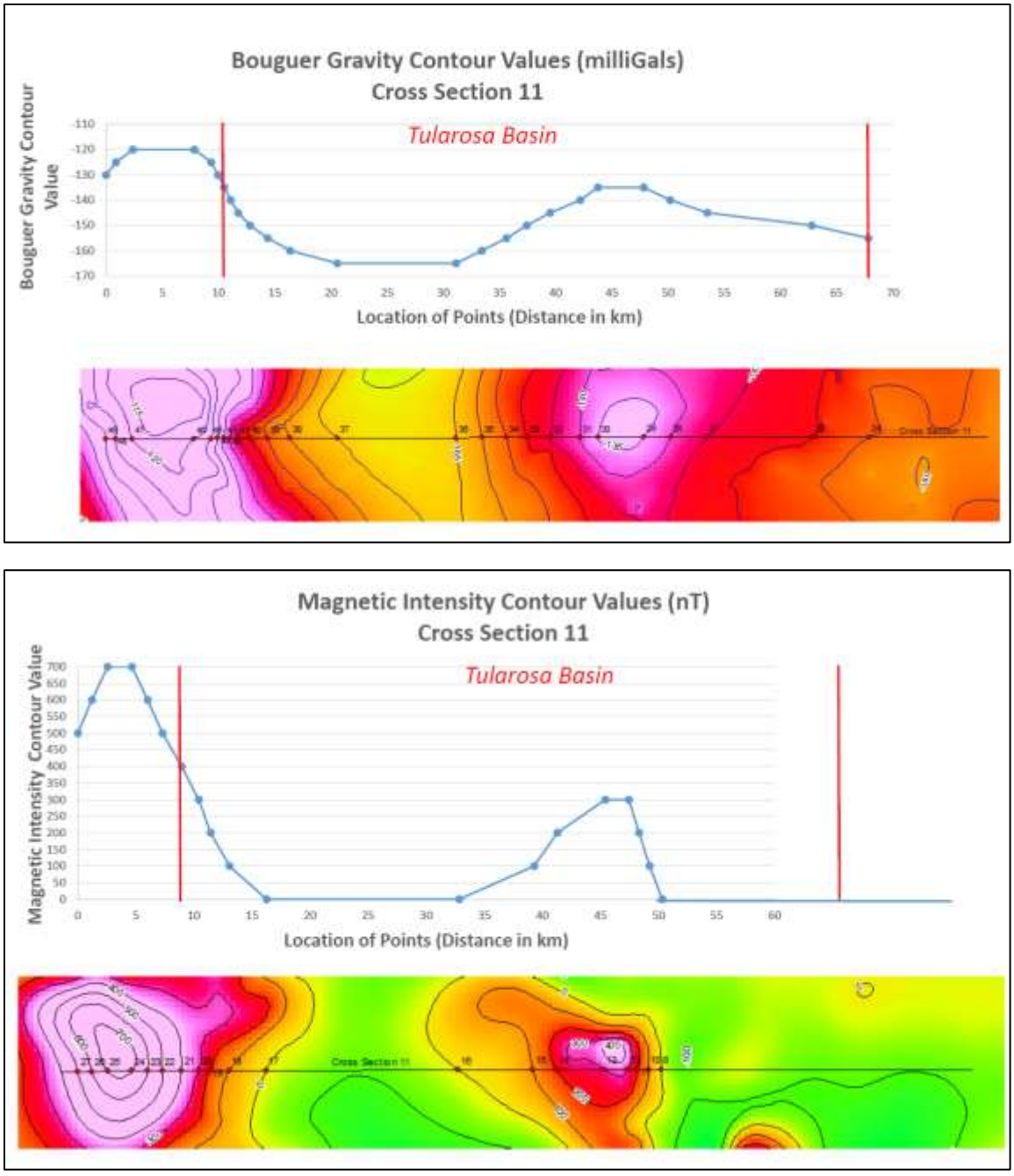

Figure 13. The profiles in this figure cross the basin between the San Andreas and Franklin Mountains. Both the gravity (top) and the Magnetic (bottom) data define basin-bounding normal faults.

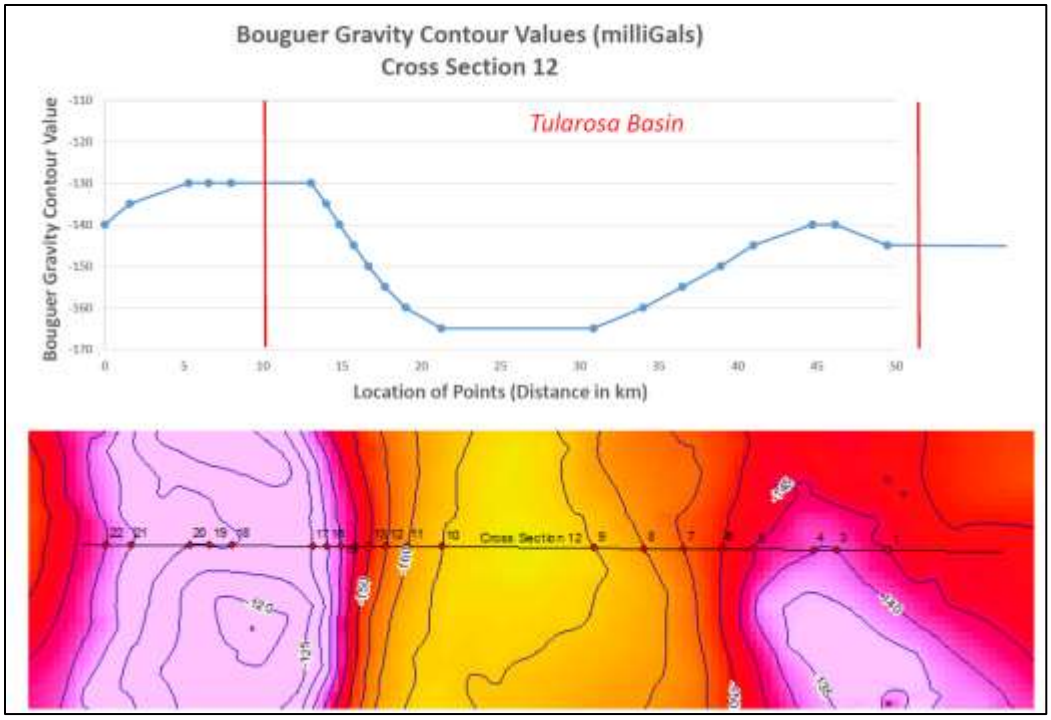

Figure 14. The profiles in this figure cross the basin between near the center of the Franklin Mountains. The gravity profile once again defines basin-bounding normal faults.

North to South Geophysical Profiles of Tularosa Basin

We also constructed north-south profiles of the Tularosa basin using Bouguer gravity anomaly and magnetic intensity counter values. Since these cross sections are free from the east-west margin topographic effects of the basin, they even better depict the heterogeneity in rock properties within and along the basin from north to south. Four such geophysical "highs" are identified to exist approximately at spatial intervals of (A) 50-90 km (A), 125-135 km (B), 170-190 km (C), and 220-240 km (D), as measured from the northern limit of the basin. In all of these localities, both Bouguer gravity and magnetic intensity show relatively higher values (compared to the surrounding areas in the basin) indicating the presence of higher density and more magnetic rocks. These heterogeneous localities seem to be "basement highs" of "more magnetic rocks" which may be mafic intrusions (dikes) and/or fault-bounded basement highs. Interestingly these features appear to strike in an east-west direction perpendicular to the general north-south trend of the basin. The heterogeneous nature of rocks within the basin and the basement underlying the basin has critical impact on the structural configuration, fracture permeability, heat flow of the Tularosa basin. Therefore, more detailed modeling of these geophysical data will be important in Phase II, especially given that there is also scarcity of well data from the basin.

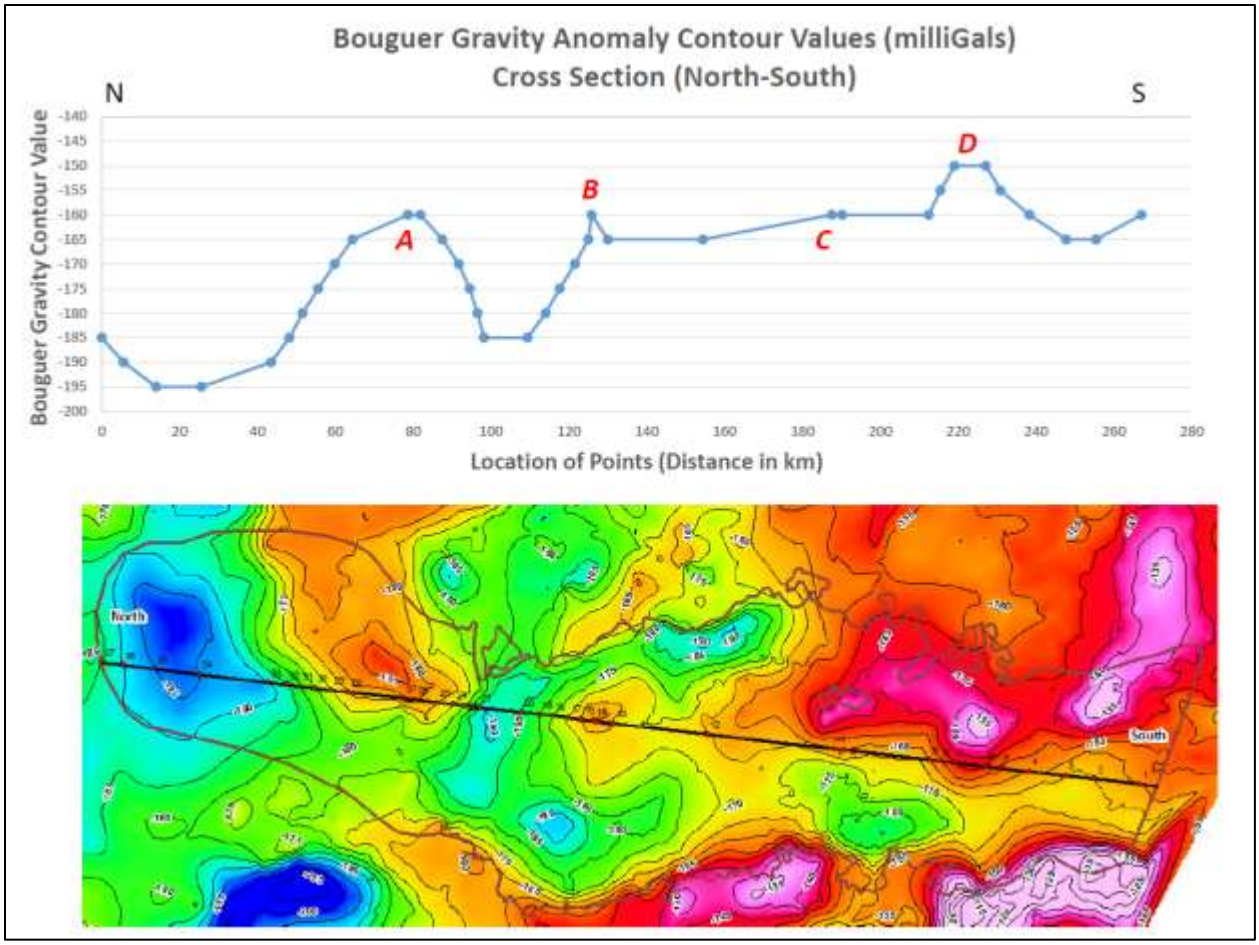

Figure 15. A north-south cross-section of Bouguer gravity anomaly (in milliGals) across the Tularosa basin

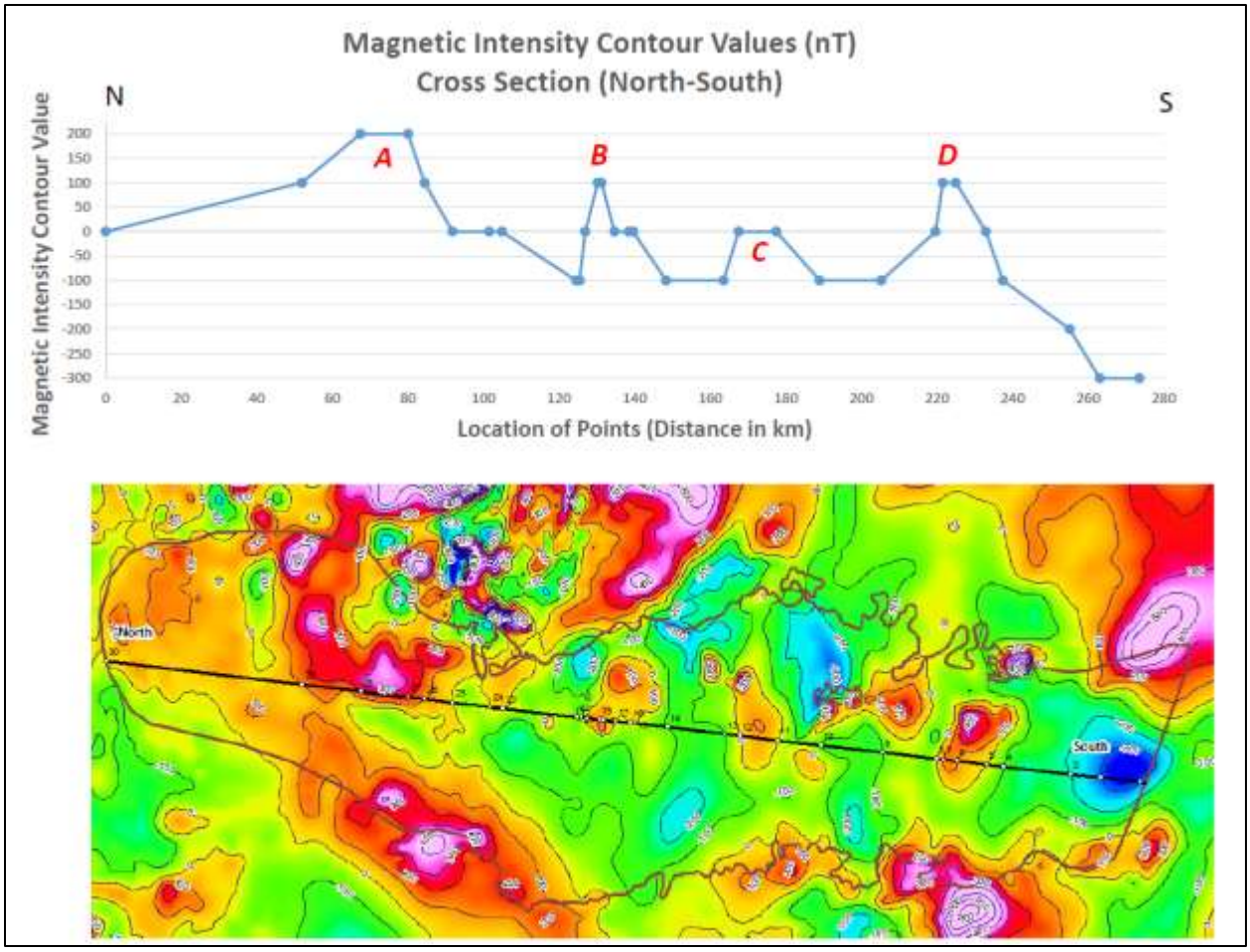

Figure 16. A north-south cross-section of magnetic intensity (in nanno-Tesla) across the Tularosa basin

BIBLIOGRAPHY

Bibliographic Database: Tularosa Basin and Rio Grande Rift, New Mexico

Adams, D.C. and Keller, G.R. (1994) Crustal Structure and Basin Geometry in South-Central New Mexico, *in* Keller G.R. and Cather, S.M., eds., *Basins of the Rio Grande Rift: Structure, Stratigraphy, and Tectonic Setting*, Geological Society of America Special Paper, No. 291, p. 241-256.

Albrecht, M. (2011) *Innovative Exploration Techniques for Geothermal Assessment at Jemez Pueblo, New Mexico*, U.S. Department of Energy, Division of Geothermal Energy, 16 p.

Aldrich, M.J. and Dethier, D.P. (1990) Stratigraphic and tectonic evolution of the northern Espanola basin Rio Grande
Rift, New Mexico, *Geological Society of America Bulletin*, Vol. 102, p. 1695-1705.

Aldrich, M.J., Chapin, C.E., and Laughlin, A.W. (1986) Stress History and Tectonic Development of the Rio Grande Rift, New Mexico, *Journal of Geophysical Research*, Vol. 91, No. B6, p. 6199-6211.

Aldrich, M.J., Jr. (1986) Tectonics of the Jemez Lineament in the Jemez Mountains and Rio Grande Rift, *Journal of Geophysical Research*, Vol. 91, No. B2, p. 1753-1762.

Ander, M.E. (1981) Geophysical Study of the Crust and Upper Mantle beneath the Central Rio Grande Rift and Adjacent Great Plains and Colorado Plateau, United States Department of Energy, University of California, 218 p.

Anderson, O.J. and Jones, G.E. (1994) Geologic Map of New Mexico, 1:500,000, New Mexico Bureau of Mines and Mineral Resources Open File Report, No. 408, 32 p.

Ankeny, L.A. and Braile, L.W. (1986) Upper Crustal Structure beneath the Jemez Mountains Volcanic Field, New Mexico, Determined by Three-Dimensional Simultaneous Inversion of Seismic Refraction and Earthquake Data, *Journal of Geophysical Research*, Vol. 91, No. B6, p. 6188-6198.

Aprea, C.M., Hildebrand, S., Fehler, M., et al. (2002) Three-dimensional Kirchhoff migration: Imaging of the Jemez volcanic field using teleseismic data, *Journal of Geophysical Research*, Vol. 107, No. B10, p. 15 p.

Armstrong, C., Dutrow, B.L., Henry, D.J., et al. (2013) Provenance of volcanic clasts from the Santa Fe Group, Culebra graben of the San Luis Basin, Colorado: A guide to tectonic evolution, *in* Hudson, M.R. and Grauch, V.J.S., *New Perspectives on Rio Grande Rift Basins: From Tectonics to Groundwater*, *The Geological Society of America Special Paper*, No. 494, p. 21-46.

Atkinson, P.G. and Gulati, M.S. (1979) Status Report on Geothermal Development in the Valles Caldera, New Mexico, Union Oil Co., p. 257-259.

Averill, M.G. and Miller, K.C. (2013) Upper crustal structure of the southern Rio Grande rift: A composite record of rift and pre-rift tectonics, *in* Hudson, M.R. and Grauch, V.J.S., eds., *New Perspectives on Rio Grande Rift Basins: From Tectonics to Groundwater*, *The Geological Society of America Special Paper*, No. 494, p. 463-474.

Bailey, R.A. and Ross, C.S. (1969) Stratigraphic Nomenclature of Volcanic Rocks in the Jemez Mountains, New

Mexico, *Contributions to Stratigraphy, New stratigraphic names and revisions in nomenclature of upper Tertiary and Quaternary volcanic rocks in the Jemez Mountains*, Geological Survey Bulletin 1274, 19 p.

Bailey, R.A., Smith, R.L., and Ross, C.S. (1961) Outline of the geology of the Jemez Mountains, New Mexico, New Mexico Geological Society, Twelfth Field Conference, p. 139-143.

Baldridge, W.S. (1978) Petrology and Petrogenesis of Plio-Pleistocene Basaltic Rocks from the Central Rio Grande Rift, New Mexico, and Their Relation to Rift Structure, *in* Riecker, R.E., eds., *Rio Grande Rift: Tectonics and Magmatism*, American Geophysical Union, p. 323-354.

Baldridge, W.S. and Olsen, K.H. (1989) The Rio Grande Rift, *American Scientist*, Vol. 77, No. 3, p. 240-247.

Baldridge, W.S., et al. (1984) Rio Grande Rift: Problems and Perspectives, *New Mexico Geological Society Guidebook, 35th Field Conference*, 13 p.

Baldridge, W.S., Olsen, K.H., and Callender, J.F. (2015) Multimodal Geothermal Development in the Tularosa Basin, NM, *Fortieth Workshop on Geothermal Reservoir Engineering*, Stanford University, 7 p.

Barker, D.S. (1978) Cenozoic Magmatism in the Trans-Pecos Province: Relation to the Rio Grande Rift, *in* Riecker, R.E., eds., *Rio Grande Rift: Tectonics and Magmatism*, American Geophysical Union, p. 382-392.

Barroll, M.W. and Reiter, M. (1990) Analysis of the Socorro Hydrogeothermal System: Central New Mexico, *Journal of Geophysical Research*, Vol. 95, No. B13, p. 21949-21963.

Barrow, R. and Keller, G.R. (1994) An Integrated Geophysical Study of the Estancia Basin, Central New Mexico, *in* Keller G.R. and Cather, S.M., eds., *Basins of the Rio Grande Rift: Structure, Stratigraphy, and Tectonic Setting*, *The Geological Society of America Special Paper*, No. 291, p. 171-186.

Barse, K.A., McDonald, M.R., and Crowell, A.M. (2012) Evaluation of the Geothermal Potential in the Rio Grande Rift: Truth or Consequences, New Mexico, GRC Transactions, Vol. 36, p. 1315-1320.

Barton, C.A. and Zoback, M.D. (1988) In-Situ Stress Orientation and Magnitude at the Fenton Geothermal Site, New Mexico, Determined from Wellbore Breakouts, *Geophysical Research Letters*, Vol. 15, No. 5, p. 467-470.

Beck, W.C. and Chapin, C.E. (1994) Structural and Tectonic Evolution of the Joyita Hills, Central New Mexico: Implications of Basement Control on Rio Grande Rift, *in* Keller G.R. and Cather, S.M., eds., *Basins of the Rio Grande Rift: Structure, Stratigraphy, and Tectonic Setting*, *The Geological Society of America Special Paper*, No. 291, p. 187-206.

Berglund, H.T., Sheehan, A.F., Murray, M.H., et al. (2012) Distributed deformation across the Rio Grande Rift, Great Plains, and Colorado Plateau, *Geology*, Vol. 40, No. 1, p. 23-26.

Birch, F.S. (1982) Gravity models of the Albuquerque basin, Rio Grande rift, New Mexico, *Geophysics*, Vol. 47, No. 8, p. 1185-1197.

Blanchard, W.G., Jr. and Davis, M.J. (1929) Permian Stratigraphy and Structure of Parts of Southeastern New Mexico
and South-western Texas, *AAPG Bulletin*, Vol. 13, p. 957-995.

Bowsher, A.L. (1991) Some effects of the Precambrian basement on the development of the Sacramento Mountains,
Geology of the Sierra Blanca, Sacramento, and Capitan Ranges, New Mexico, Annual NMGS Fall Field Conference Guidebooks, New Mexico Geological Society, p. 81-89.

Boyd, T., et al. (2011) The feasibility of Geothermal Potential in the Rio Grande Rift Area of New Mexico and Texas, *GHC Bulletin*, p. 10-16.

Bridwell, R.J. and Anderson, C.A. (1980) *Thermomechanical Models of the Rio Grande Rift, Los Alamos Scientific Laboratory*, U.S. Department of Energy, 24 p.

Brister, B.S. and Gries, R.R. (1994) Tertiary Stratigraphy and Tectonic Development of the Alamosa Basin (Northern San Luis Basin) Rio Grande Rift, South-Central Colorado, *in* Keller G.R. and Cather, S.M., eds., *Basins of the Rio Grande Rift: Structure, Stratigraphy, and Tectonic Setting*, *The Geological Society of America Special Paper*, No. 291, p. 39-58.

Broadhead, R.F. (2003) Petroleum Geology of the McGregor Range Otero County, New Mexico, *New Mexico Bureau of Geology and Mineral Resources, Search and Discovery Article*, No. 10052, 13 p.

Brocher, T.M. (1981) Shallow Velocity Structure of the Rio Grande Rift North of Socorro, New Mexico: A Reinterpretation, *Journal of Geophysical Research*, Vol. 86, No. B6, p. 4960-4970.

Brown, C.D. and Phillips, R.J. (1999) Flexural rift flank uplift at the Rio Grande rift, New Mexico, *Tectonics*, Vol. 18, No. 6, p. 1275-1291.

Brown, L.D., Krumhansl, P.A., Chapin, C.E., et al. (1978) Cocorp Seismic Reflection Studies of the Rio Grande Rift, *in* Riecker, R.E., eds., *Rio Grande Rift: Tectonics and Magmatism*, American Geophysical Union, p. 169-184.

Brown, L.D., Kaufman, S., and Oliver, J.E. (1983) Cocorp Seismic Traverse across the Rio Grande Rift, *Seismic Expression of Structural Styles: A Picture and Work Atlas, Studies in Geology 15*, Vol. 2, 6 p.

Brown, L.L. and Caffall, N.M. (1993) Paleomagnetism and tectonic interpretations of the Taos Plateau Volcanic Field, Rio Grande Rift, New Mexico, *Journal of Geophysical Research*, Vol. 98, No. B12, p. 22401-22413.

Broxton, D.E. and Vaniman, D.T. (2005) Geologic Framework of a Groundwater System on the Margin of a Rift Basin, Pajarito Plateau, North-Central New Mexico, Los Alamos National Laboratory, *Vadose Zone Journal*, Vol. 4, p. 522-550.

Caine, J.S. and Minor, S.A. (2009) Structural and geochemical characteristics of faulted sediments and inference on the role of water in deformation, Rio Grande Rift, New Mexico, *GSA Bulletin*, Vol 121, No. 9-10, p. 1325-1340.

Callender, J.F. (1978) Evaluation of geothermal potential of Rio Grande rift and Basin and Range province, New Mexico, U.S. Geological Survey, 263 p.

Cape, C.D., McGeary, S., and Thompson, G.A. (1983) Cenozoic normal faulting and the shallow structure of the Rio Grande rift near Socorro, New Mexico, *Geological Society of America Bulletin*, Vol. 94, p. 3-14.

Carciumaru, D. and Ortega, R. (2011) On the origin of low angle normal faulting in the Southern Rio Grande Rift, *Geofisica Internacional*, p. 177-190.

Carter, K.F. and Winter, C.I. (1995) Fractal nature and scaling of normal faults in the Espanola Basin, Rio Grande rift, New Mexico: implications for fault growth and brittle strain, *Journal of Structural Geology*, Vol. 17, No. 6, p. 863-873.

Cather, S.M., Karlstrom, K.E., Timmons, J.M., et al. (2006) Palinspastic reconstruction of Proterozoic basement related aeromagnetic features in north-central New Mexico: Implications for Mesoproterozoic to late Cenozoic tectonism, *Geosphere*, Geologic Society of America, Vol. 2, No. 6, p. 299-323.

Cather, S.M., Chamberlin, R.M., Chapin, C.E., et al. (1994) Stratigraphic Consequences of Episodic Extension in the Lemitar Mountains, Central Rio Grande Rift, *in* Keller G.R. and Cather, S.M., eds., *Basins of the Rio Grande Rift: Structure, Stratigraphy, and Tectonic Setting*, *The Geological Society of America Special Paper*, No. 291, p. 157-170.

Chaimov, T.A. (1988) A 3-D Seismic Modeling Study of the Ladron Horst near Socorro, New Mexico, *Geophysical Research Letters*, Vol. 15, No. 11, p. 1207-1210.

Chamberlin, R.M. (2001) Waning-Stage Eruptions of the Oligocene Socorro Caldera, Central New Mexico, *Volcanology in New Mexico, New Mexico Museum of Natural History and Science Bulletin*, p. 69-77.

Chamberlin, R.M. and McIntosh, W.C. (2007) Chronology and structural control of Late Cenozoic volcanism in the Loma Creston quadrangle, southern Jemez volcanic field, New Mexico, *Geology of the Jemez Region II, New Mexico Geological Society 58th Annual Fall Field Conference Guidebook*, p. 248-261.

Chamberlin, R.M., McIntosh, W.C., and Chapin, C.E. (2003) Oligocene calderas, mafic lavas and radiating mafic dikes of the Socorro-Magdalena magmatic system, Rio Grande rift, New Mexico: surface expression of a miniplume?, Bureau of Geology and Mineral Resources, New Mexico Tech, 5 p.

Chapin, C.E. (1978) Evolution of the Rio Grande Rift: A Summary, *in* Riecker, R.E., eds., *Rio Grande Rift: Tectonics and Magmatism*, American Geophysical Union, p. 1-6.

Chapin, C.E. and Cather, S.M. (1994) Tectonic Setting of the Axial Basins of the Northern and Central Rio Grande Rift, *in* Keller G.R. and Cather, S.M., eds., *Basins of the Rio Grande Rift: Structure, Stratigraphy, and Tectonic Setting, The Geological Society of America Special Paper*, No. 291, p. 5-26.

Clarkson, G. and Reiter, M. (1984) Analysis of Terrestrial Heat-Flow Profiles Across the Rio Grande Rift and Southern Rocky Mountains in Northern New Mexico, *New Mexico Geological Society Guidebook, 35th Field Conference*, p. 39-44.

Collins, E.W. and Raney, J.A. (1994) Tertiary and Quaternary Tectonics of the Hueco Bolson, Trans-Pecos Texas and Chihuahua, Mexico, *in* Keller G.R. and Cather, S.M., eds., *Basins of the Rio Grande Rift: Structure, Stratigraphy, and Tectonic Setting*, *The Geological Society of America Special Paper*, No. 291, p. 265-282.

Connell, S.D., Smith, G.A., Geissman, J.W., et al. (2013) Climatic controls on nonmarine depositional sequences in the Albuquerque Basin, Rio Grande rift, north-central New Mexico, *in* Hudson, M.R. and Grauch, V.J.S., eds., *New Perspectives on Rio Grande Rift Basins: From Tectonics to Groundwater*, *The Geological Society*

of America Special Paper, No. 494, p. 383-426.

Cook, F.A., McCullar, D.B., Decker, E.R., et al. (1978) Crustal Structure and Evolution of the Southern Rio Grande Rift, *in* Riecker, R.E., eds., *Rio Grande Rift: Tectonics and Magmatism*, American Geophysical Union, p. 195-208.

Cooper, J.R. (2006) Igneous Intrusions and Thermal Evolution in the Raton Basin, CO-NM: Contact Metamorphism and Coal-Bed Methane Generation, University of Missouri-Columbia Thesis, 249 p.

Copeland, P., Murphy, M.A., Dupre, W.R., et al. (2011) Oligocene Laramide deformation in southern New Mexico and its implications for Farallon plate geodynamics, *Geosphere*, Geological Society of America, Vol. 7, No. 5, p. 1209-1219.

Cordell, L. (1978) Regional geophysical setting of the Rio Grande rift, *Geological Society of America Bulletin*, Vol. 89, p. 1073-1090.

Cordell, L. (1982) Extension in the Rio Grande Rift, *Journal of Geophysical Research*, Vol. 87, No. B10, p. 8561-8569.

Cordell, L., Zorin, Y.A., and Keller, G.R. (1991) The Decompensative Gravity Anomaly and Deep Structure of the Region of the Rio Grande Rift, *Journal of Geophysical Research*, Vol. 96, No. B4, p. 6557-6568.

Cordell, L., Long, C.L., and Jones, D.W. (1985) Geophysical Expression of the Batholith beneath Questa Caldera, New Mexico, *Journal of Geophysical Research*, Vol. 90, No. B13, p. 11263-11269.

Crumpler, L.S. (2001) Volcanism in New Mexico: An Overview, *Volcanology in New Mexico, New Mexico Museum of Natural History and Science Bulletin*, p. 17-29.

Crumpler, L.S. and Aubele, J.C. (2001) Volcanoes of New Mexico: An Abbreviated Guide for Non-Specialists, *Volcanology in New Mexico, New Mexico Museum of Natural History and Science Bulletin*, p. 5-15.

Culbertson, J.K. (1967) Evidence of Secondary Circulation in an Alluvial Channel, *Geological Survey Research 1967, Chapter D, Geological Survey Professional Paper*, No. 575-D, p. D214-D216.

Daggett, P.H., Keller, G.R., Morgan, P., et al. (1986) Structure of the Southern Rio Grande Rift from Gravity Interpretation, *Journal of Geophysical Research*, Vol. 91, No. B6, p. 6157-6167.

Dahal, S., McDonald, M.R., Bubach, B., et al. (2012) Evaluation of Geothermal Potential of Lighting Dock KGRA, New Mexico, GRC Transactions, Vol. 36, p. 638-640.

D'Alfonso, D., Hardwick, C., Hollingshaus, B., et al. (2011) *Geothermal Potential of the Rio Grande Rift: A Critical Assessment*, University of Utah, 50 p.

Darton, N.H. (1920) *Geothermal Data of the United States*, Department of the Interior, United States Geological Survey, 97 p.

Davidson, M.E. (2000) *Seismic Modeling of the Valles Caldera, Jemez Mountains, New Mexico*, Purdue University Thesis, ProQuest, UMI Dissertation Publishing, 250 p.

Davis, T.L. and Stoughton, D. (1978) Interpretation of Seismic Reflection Data from the Northern San Luis Valley,

South-Central Colorado, *in* Riecker, R.E., eds., *Rio Grande Rift: Tectonics and Magmatism*, American Geophysical Union, p. 185-194.

De Voogd, B., Serpa, L., and Brown, L. (1988) Crustal extension and magmatic processes: COCORP profiles from Death Valley and the Rio Grande rift, *Geological Society of America Bulletin*, Vol. 100, p. 1550-1567.

Decker, E.R. and Smithson, S.B. (1975) Heat Flow and Gravity Interpretation Across the Rio Grande Rift in Southern New Mexico and West Texas, *Journal of Geophysical Research*, Vol. 80, No. 17, p. 2542-2552.

Dethier, D.P. and Martin, B.A. (1984) Geology and Structure along part of the Northeast Jemez Mountains, New Mexico, *Rio Grande Rift: Northern New Mexico, New Mexico Geological Society Guidebook, 35th Field Conference*, p. 145-150.

Dickerson, P.W. (2013) Tascotal Mes transfer zone-An element of the Border Corridor transform system, Rio Grande
rift of West Texas and adjacent Mexico, *in* Hudson, M.R. and Grauch, V.J.S., eds., *New Perspectives on Rio Grande Rift Basins: From Tectonics to Groundwater*, *The Geological Society of America Special Paper*, No. 494, p. 475-500.

Dickerson, P.W. and Muehlberger, W.R. (1994) Basins in the Big Bend Segment of the Rio Grande Rift, Trans-Pecos Texas, *in* Keller G.R. and Cather, S.M., eds., *Basins of the Rio Grande Rift: Structure, Stratigraphy, and Tectonic Setting*, *The Geological Society of America Special Paper*, No. 291, p. 283-297.

Doughty, P.T. (2003) Clay Smear seals and fault sealing potential of an exhumed growth fault, Rio Grande rift, New Mexico, *AAPG Bulletin*, Vol. 87, No. 3, p. 427-444.

Drenth, B.J., Grauch, V.J.S., and Rodriguez, B.D. (2013) Geophysical constraints on Rio Grande rift structure in the central San Luis Basin, Colorado and New Mexico, *in* Hudson, M.R. and Grauch, V.J.S., eds., *New Perspectives on Rio Grande Rift Basins: From Tectonics to Groundwater*, *The Geological Society of America Special Paper*, No. 494, p. 75-100.

Eardley, A.J. (1963) Relation of Uplifts to Thrusts in Rocky Mountains, Backbone of the Americas: Tectonic History from Pole to Pole, American Association of Petroleum Geologists, p. 209-219.

Easley, E., Garchar, L., Bennett, M. et al. (2011) Investigation of Geothermal Resource Potential in the Northern Rio Grande Rift, Colorado and New Mexico, *GRC Transactions*, Vol. 35, p. 761-768.

Easley, E., Garchar, L., Bennett, M. et al. (2011), A Geochemical and Isotopic Study of Two Geothermal Prospects in the Rio Grande Rift, Colorado and New Mexico, *The Mountain Geologist*, Vol. 48, No. 4, p. 95-106.

Eaton, G.P. (1978) A Plate-Tectonic Model for Late Cenozoic Crustal Spreading in the Western United States, *in* Riecker, R.E., eds., *Rio Grande Rift: Tectonics and Magmatism*, American Geophysical Union, p. 7-32.

Elston, W.E. (2001) The Ignimbrite Flareup in Southwestern New Mexico: What Have we Learned these Last 50 Years, *Volcanology in New Mexico, New Mexico Museum of Natural History and Science Bulletin*, p. 49
67.

Elston, W.E. and Bornhorst, T.J. (1978) The Rio Grande Rift in Context of Regional Post-40 M.Y. Volcanic and Tectonic Events, *in* Riecker, R.E., eds., *Rio Grande Rift: Tectonics and Magmatism*, American

Geophysical Union, p. 416-438.

Faust, C.R., Mercer, J.W., and Thomas, S.D. (1984) Quantitative Analysis of Existing Conditions and Production Strategies for the Baca Geothermal System, New Mexico, *Water Resources Research*, Vol. 20, No. 5, p. 601-618.

Ferguson, J.F., Baldridge, W.S., Braile, L.W., et al. (1995) Structure of the Espanola Basin, Rio Grande Rift, New Mexico, from SAGE seismic and gravity data, *New Mexico Geological Society fall Field Conference 1995*, Los Alamos National Laboratory, United States Department of Energy, 20 p.

Fialko, Y. and Simons, M. (2001) Evidence for on-going inflation of the Socorro magma body, New Mexico, From Interferometric Synthetic Aperture Radar imaging, *Geophysical Research Letters*, Vol. 28, No. 18, p. 3549-3552.

Finger, J.T. and Jacobson, R.D. (1997) *Fort Bliss Exploratory Slimholes: Drilling and Testing*, Sandia National Laboratories, United States Department of Energy, 181 p.

Fischer, H.B. (1967) Transverse Mixing in a Sand-Bed Channel, *Geological Survey Research 1967, Chapter D, Geological Survey Professional Paper*, No. 575-D, p. D267-D272.

Fleischmann, D.J. (2006) *Geothermal Resource Development Needs in New Mexico*, Geothermal Energy Association for the U.S. Department of Energy, 30 p.

Gao, W. (2006) *Upper Mantle Seismic Structure beneath the Central Rio Grande Rift and beneath Eastern Mexico and their Implications*, The University of Texas at Austin Dissertation, 218 p.

Gao, W., Grand, S.P., Baldridge, W.S., et al. (2004) Upper Mantle Convection Beneath the Central Rio Grande Rift, *Journal of Geophysical Research*, Vol. 109, No. B3, 50 p.

Gardner, J.N. and Goff, F. (1986) Stratigraphic relations and lithologic variations in the Jemez Volcanic Field, New Mexico, *Journal of Geophysical Research*, Vol. 91, No. B2, p. 1763-1778.

Gardner, J.N., Lavine, A., WoldeGabriel, G., et al. (1999) Structural Geology of the Northwestern Portion of Los Alamos National Laboratory, Rio Grande Rift, New Mexico: Implications for Seismic Surface Rupture Potential from TA-3 to TA-55, Los Alamos National Laboratory, United States Department of Energy, 112 p.

Gardner, J.N., Goff, F., Goff, S., et al. (1987) Core Lithology Valles Caldera #1, New Mexico, Los Alamos National Laboratory, United States Department of Energy, 273 p.

Goff, F. (2002) Geothermal Potential of the Valles Caldera, New Mexico, *GHC Bulletin*, p. 7-12.

Goff, F. and Gardner, J.N. (1994) Evolution of a Mineralized Geothermal System, Valles Caldera, New Mexico, *Economic Geology*, Vol. 89, p. 1803-1832.

Goff, F. and Gardner, J.N. (2004) Late Cenozoic Geochronology of Volcanism and Mineralization in the Jemez Mountains and Valles Caldera, North Central New Mexico, *The Geology of New Mexico, A Geologic History*, New Mexico Geological Society, p. 295-312.

Goff, F. and Shevenell, L. (1987) Travertine deposits of Soda Dam, New Mexico, and their implications for the age and evolution of the Valles caldera hydrothermal system, *Geological Society of America Bulletin*, Vol. 99, p. 292-302.

Goff, F., Shevenell, L., and Gardner, J.N. (1988) The Hydrothermal Outflow Plume of Valles Caldera, New Mexico, and a Comparison with Other Outflow Plumes, *Journal of Geophysical Research*, Vol. 93, No. B6, p. 6041-6058.

Goff, F., Gardner, J., Rosemary, V., et al. (1985) Geochemistry and Isotopes of Fluids from Sulphur Springs, Valles Caldera, New Mexico, *Journal of Volcanology and Geothermal Research*, Elsevier Science Publishers B.V., Vol 23, p. 273-297.

Goff, F., McCormick, T., Trujilo, P.E., Jr., et al. (1982) Geochemical Data for 95 Thermal and Nonthermal Waters of the Valles Caldera-Southern Jemez Mountains Region, New Mexico, Los Alamos National Laboratory, 51 p.

Golombek, M.P. (1983) Geology, structure, and tectonics of the Pajarito fault zone in the Espanola basin of the Rio Grande rift, New Mexico, *Geological Society of America Bulletin*, Vol. 94, p. 192-205.

Golombek, M.P. (1981) Geometry and rate of extension across the Pajarito fault zone, Espanola basin, Rio Grande rift, northern New Mexico, *Geology*, Vol. 9, p. 21-24.

Gornitz, V. (1982) Volcanism and the Tectonic Development of the Rio Grande Rift and Environs, New Mexico – Colorado, from Analysis of Petrochemical Data, *The Mountain Geologist*, Vol. 19, No. 2, p. 41-58.

Goteti, R., Mitra, G., Becene, A., et al. (2013) Three-dimensional finite-element modeling of fault interactions in rift scale normal fault systems: Implications for the late Cenozoic Rio Grande rift of north-central New Mexico, *in* Hudson, M.R. and Grauch, V.J.S., eds., *New Perspectives on Rio Grande Rift Basins: From Tectonics to Groundwater*, *The Geological Society of America Special Paper*, No. 494, p. 157-184.

Grant, P.R., Jr. (1982) Geothermal Potential in the Albuquerque Area, New Mexico, *New Mexico Geological Society Guidebook, 33rd Field Conference*, p 325-331.

Grauch, V.J.S. and Connell, S.D. (2013) New perspectives on the geometry of the Albuquerque Basin, Rio Grande rift, New Mexico: Insights from geophysical models of rift-fill thickness, *in* Hudson, M.R. and Grauch, V.J.S., eds., *New Perspectives on Rio Grande Rift Basins: From Tectonics to Groundwater*, *The Geological Society of America Special Paper*, No. 494, p. 427-462.

Grauch, V.J.S. and Hudson, M.R. (2007) Guides to understanding the aeromagnetic expression of faults in sedimentary basins: Lessons learned from the central Rio Grande rift, New Mexico, *Geosphere*, Geological Society of America, Vol. 3, No. 6, p. 596-623.

Grauch, V.J.S., Phillips, J.D., Koning, D.J., et al. (2009) Geophysical Interpretations of the Southern Espanola Basin, New Mexico, That Contribute to Understanding Its Hydrogeologic Framework, U.S. Department of the Interior, U.S. Geologic Survey, 87 p.

Gries, J.C. (1978) Problems of Delineation of the Rio Grande Rift into the Chihuahua Tectonic Belt of Northern Mexico, *in* Riecker, R.E., eds., *Rio Grande Rift: Tectonics and Magmatism*, American Geophysical Union, p. 107-114.

Grigsby, C.O. (1984) Geochemical Behavior of a Hot Dry Rock Geothermal Reservoir, Rio Grande Rift: Northern New Mexico, *New Mexico Geological Society Guidebook, 35th Field Conference*, p. 265-270.

Hagstrum, J.T. and Lipman, P.W. (1986) Paleomagnetism of the structurally deformed Latir volcanic field, northern New Mexico: Relations to formation of the Questa caldera and development of the Rio Grande rift, *Journal of Geophysical Research*, Vol. 91, No. B7, p. 7383-7402.

Hagstrum, J.T., Lipman, P.W., and Elston, D.P. (1982) Paleomagnetic evidence bearing on the structural development
on the Latir Volcanic Field near Questa, New Mexico, *Journal of Geophysical Research*, Vol. 87, No. B9, p. 7833-7842.

Hamblock, J.M., Adronicos, C.L., Miller, K.C., et al. (2007) A composite geologic and seismic profile beneath the southern Rio Grande rift, New Mexico, based on xenolith mineralogy, temperature, and pressure, *Tectonophysics*, Vol. 442, p. 14-48.

Harder, V., Morgan, P., and Swanberg, C.A. (1980) Geothermal Resources in the Rio Grande Rift: Origins and Potential, *Geothermal Resources Council, Transactions*, Vol. 4, p. 61-64.

Harlan, S.S. and Geissman, J.W. (2009) Paleomagnetism of Tertiary intrusive and volcaniclastic rocks of the Cerrillos Hills and surrounding region, Expanola Basin, New Mexico, U.S.A.: Assessment and implications of vertical-axis rotations associated with extension of the Rio Grande rift, *Lithosphere*, Vol. 1, No. 3, p. 155-173.

Harrison, R.W. (1994) Winston Graben: Stratigraphy, Structure, and Tectonic Setting, *in* Keller G.R. and Cather, S.M., eds., *Basins of the Rio Grande Rift: Structure, Stratigraphy, and Tectonic Setting*, *The Geological Society of America Special Paper*, No. 291, p. 227-240.

Harrison, T.M., Morgan, P., and Blackwell, D.D. (1986) Constraints on the age of heating at the Fenton Hill Site, Valles Caldera, New Mexico, *Journal of Geophysical Research*, Vol. 91, No. B2, p. 1899-1908.

Hawley, J. (1999) Overview of the Hydrogeology of the Northern Rio Grande Basin - Colorado, New Mexico, and Texas, WRRI Conference Proceedings, 24 p.

Hawley, J.W., Haase, C.S., and Lozinsky, R.P. (1994) An Underground View of the Albuquerque Basin, *The Water Future of Albuquerque and Middle Rio Grande Basin*, New Mexico Water Resources Research Institute, p. 37-55.

Heiken, G., Goff, F., Stix, J., et al. (1986) Intracaldera volcanic activity, Toledo Caldera and Embayment, Jemez Mountains, New Mexico, *Journal of Geophysical Research*, Vol. 91, No. B2, p. 1799-1815.

Heiken, G., Goff, F., Gardner, J.N., et al. (1990) The Valles/Toledo Caldera Complex, Jemez Volcanic Field, New Mexico, *Annual Rev. Earth Planetary Science*, Vol. 18, p. 27-53.

Hermance, J.F. (1979) Toward Assessing the Geothermal Potential of the Jemez Mountains Volcanic Complex: A Telluric-Magnetotelluric Survey, Los Alamos National Laboratory, United States Department of Energy, 86 p.

Hermance, J.F. and Pedersen, J. (1980) Deep structure of the Rio Grande Rift: A magnetotelluric interpretation, *Journal of Geophysical Research*, Vol. 85, No. B7, p. 3899-3912.

Herrick, C.L. (1900) The Geology of the White Sands of New Mexico, *The Journal of Geology*, Vol. 8, No. 2, p. 112-128.

Hills, J.M. (1970) Late Paleozoic Structural Directions in Southern Perpian Basin, West Texas and Southeastern New Mexico, *The American Association of Petroleum Geologists Bulletin*, Vol. 54, No. 10, p. 1809-1827.

Hoffer, J.M. (2001) Geology of Potrillo Maar, Southern New Mexico and Northern Chihuahua, Mexico, *Volcanology in New Mexico, New Mexico Museum of Natural History and Science Bulletin*, p. 137-140.

Hoffer, J.M. (2001) Geology of the West Potrillo Mountains, *Volcanology in New Mexico, New Mexico Museum of Natural History and Science Bulletin*, p. 141-145.

Holt, B. and Ghormley, E.L. (1976) Energy Conversion and Economics for Geothermal Power Generation at Heber, California, Valles Caldera, New Mexico, and Raft River, Idaho - Case Studies, *Geothermal Energy Conversion and Economics - Case Study*, Electric Power Research Institute, 114 p.

House, M.A., Kelley, S.A., and Roy, M. (2003) Refining the footwall cooling history of a rift flank uplift, Rio Grande rift, New Mexico, *Tectonics*, Vol. 22, No. 5, 18 p.

Huang, L. and Albrecht, M. (2011) Seismic and Magneto-Telluric Imaging for Geothermal Exploration at Jemez Pueblo in New Mexico, *Thirty-Sixth Workshop on Geothermal Reservoir Engineering, Stanford University,* Los Alamos National Laboratory, Los Alamos Geothermal Technology Center, 6 p.

Hudson, M.R., Grauch, V.J.S., and Minor, S.A. (2008) Rock magnetic characterization of faulted sediments with associated magnetic anomalies in the Albuquerque Basin, Rio Grande rift, New Mexico, *GSA Bulletin*, Vol. 120, No. 5/6, p. 641-658.

Huff, G.F. (2004) Simulation of Ground-Water Flow in the Basin-Fill Aquifer of the Tularosa Basin, South-Central New Mexico, Predevelopment through 2040, *USGS Scientific Investigations Report*, No. 2004-5197, 108 p.

Ingersoll, R.V., Cavazza, W., Baldridge, W.S., et al. (1990) Cenozoic sedimentation and paleotectonics of north central New Mexico: Implications for initiation and evolution of the Rio Grande rift, *Geological Society of America Bulletin*, Vol. 102, p. 1280-1296.

Jiracek, G.R. (1974) Geophysical Studies in the Jemez Mountains Region New Mexico, *New Mexico Geological Society Guidebook, 25th Field Conference*, p. 137-144.

Jiracek, G.R., Ander, M.E., and Holcombe, H.T. (1978) Magnetotelluric Soundings of Crustal Conductive Zones in Major Continental Rifts, *in* Riecker, R.E., eds., *Rio Grande Rift: Tectonics and Magmatism*, American Geophysical Union, p. 209-222.

Johnson, C.M. (1991) Large-scale crustal formation and lithosphere modification beneath Middle to Late Cenozoic calderas and volcanic fields, western North America, *Journal of Geophysical Research*, Vol. 96, No. B8, p. 13485-13507.

Johnson, C.M. and Thompson, R.A. (1991) Isotopic composition of Oligocene mafic volcanic rocks in the Northern Rio Grande Rift: Evidence for contributions of ancient intraplate and subduction magmatism to evolution of

lithosphere, *Journal of Geophysical Research*, Vol. 96, No. B8, p. 13593-13608.

Johnson, P.S., Koning, D.J., and Partey, F.K. (2013) Shallow groundwater geochemistry in the Espanola Basin, Rio Grande rift, New Mexico: Evidence for structural control of a deep thermal source, *in* Hudson, M.R. and Grauch, V.J.S., eds., *New Perspectives on Rio Grande Rift Basins: From Tectonics to Groundwater*, The Geological Society of America Special Paper, No. 494, p. 261-302.

Jones, D., Chu, S., Barghouty, L., et al. (2013) Magnetotelluric Investigation of Structures Related to a Geothermal Anomaly in the Buckman Well field in the Rio Grande Rift, New Mexico, American Geophysical Union, Vol. 2013, 1 p.

Jurdy, D.M. and Brocher, T.M. (1980) Shallow velocity model of the Rio Grande rift near Socorro, New Mexico, *Geology*, Vol. 8, p. 185-189.

Kaufman, G. (2013) Innovative Exploration Techniques for Geothermal Assessment at Jemez Pueblo, New Mexico, U.S. Department of Energy, Division of Geothermal Energy, 18 p.

Keller, G.R. and Baldridge, W.S. (1999) The Rio Grande rift: A geological and geophysical overview, *Rocky Mountain Geology*, Vol. 34, No. 1, p. 121-130.

Keller, G.R., Braile, L.W., and Schlue, J.W. (1978) Regional Crustal Structure of the Rio Grande Rift from Surface Wave Dispersion Measurements, *in* Riecker, R.E., eds., *Rio Grande Rift: Tectonics and Magmatism*, American Geophysical Union, p. 115-126.

Kelley, S.A. and Duncan, I.J. (1986) Late Cretaceous to middle Tertiary tectonic history of the northern Rio Grande Rift, New Mexico, *Journal of Geophysical Research*, Vol. 91, No. B6, p. 6246-6262.

Kelley, S.A., Kempter, K.A., McIntosh, et al. (2013) Syndepositional deformation and provenance of Oligocene to Lower Miocene sedimentary rocks along the western margin of the Rio Grande rift, Jemez Mountains, New Mexico, *in* Hudson, M.R. and Grauch, V.J.S., eds., *New Perspectives on Rio Grande Rift Basins: From Tectonics to Groundwater*, *The Geological Society of America Special Paper*, No. 494, p. 101-124.

Kelley, S.A., McIntosh, W.C., Goff, F., et al. (2013) Spatial and temporal trends in pre-caldera Jemez Mountains volcanic and fault activity, *Geosphere*, Geological Society of America, Vol. 9, No. 3, p. 614-646.

Kelley, S.A., Osburn, G.R., and Kempter, K.A. (2007) Geology of Canon de San Diego, southwestern Jemez Mountains, north-central New Mexico, *Geology of the Jemez Region II, New Mexico Geological Society 58th Annual Fall Field Conference Guidebook*, p. 169-138.

Kelley, V.C. (1978) Tectonics, Middle Rio Grande Rift, New Mexico, *in* Riecker, R.E., eds., *Rio Grande Rift: Tectonics and Magmatism*, American Geophysical Union, p. 57-70.

Kellogg, K.S. (1999) Neogene basins of the northern Rio Grande rift: partitioning and asymmetry inherited from Laramide and older uplifts, *Tectonophysics*, Vol. 305, p. 141-152.

Kil, Y. and Wendlandt, R.F. (2006) Depleted and enriched mantle processes under the Rio Grande rift: spinel peridotite xenoliths, *Contributions to Mineralogy and Petrology*, p. 135-151.

Kil, Y. and Wendlandt, R.F. (2004) Pressure and temperature evolution of upper mantle under the Rio Grande Rift,

Contributions to Mineralogy and Petrology, p. 265-280.

King, D. and Metcalfe, E. (2013) Rift Zones as a Case Study for Advancing Geothermal Occurrence Models, AAAS Science and Technology Policy Fellow, 11 p.

Klenner, R., McDonald, M.R., Dahal, S., et al. (2011) Evaluation of the Geothermal Potential in the Rio Grande Rift: San Luis Basin, Colorado and New Mexico, *The Mountain Geologist*, Vol. 48, No. 4, p. 107-119.

Kluth, C.F. and Schaftenaar, C.H. (1994) Depth and Geometry of the Northern Rio Grande Rift in the San Luis Basin, South-Central Colorado, *in* Keller G.R. and Cather, S.M., eds., *Basins of the Rio Grande Rift: Structure, Stratigraphy, and Tectonic Setting*, *The Geological Society of America Special Paper*, No. 291, p. 27-38.

Koning, D.J., Grauch, V.J.S., Connell, S.D., et al. (2013) Structure and tectonic evolution of the eastern Espanola Basin, Rio Grande rift, north central New Mexico, *in* Hudson, M.R. and Grauch, V.J.S., eds., *New Perspectives on Rio Grande Rift Basins: From Tectonics to Groundwater*, *The Geological Society of America Special Paper*, No. 494, p. 185-220.

Landman, R.L. and Flowers, R.M. (2013) (U-Th)/He thermochronologic constraints on the evolution of the northern Rio Grande Rift, Gore Range, Colorado, and implications for rift propagation models, *Geosphere*, Vol. 9, No. 1, p. 170-187.

Larsen, S., Reilinger, R., and Brown, L. (1986) Evidence of Ongoing Crustal Deformation Related to Magmatic Activity near Socorro, New Mexico, *Journal of Geophysical Research*, Vol. 91, No. B6, p. 6283-6292.

Lawton, T.F. and McMillan, N.J. (1999) Arc abandonment as a cause for passive continental rifting: Comparison of the Jurassic Mexican Borderland rift and the Cenozoic Rio Grande rift, *Geology*, Vol. 27, No. 9, p. 779-782.

Lewis, C.J. and Baldridge, W.S. (1994) Crustal Extension in the Rio Grande Rift, New Mexico: Half Grabens, Accommodation Zones, and Shoulder Uplifts in the Ladron Peak-Sierra Lucero Area, *in* Keller G.R. and Cather, S.M., eds., *Basins of the Rio Grande Rift: Structure, Stratigraphy, and Tectonic Setting*, *The Geological Society of America Special Paper*, No. 291, p. 135-156.

Lewis, C.J., Gardner, J.N., Schultz-Fellenz, E.S., et al. (2009) Fault interaction and along-strike variation in throw in the Pajarito fault system, Rio Grande rift, New Mexico, *Geosphere*, Vol. 9, No. 3, p. 252-269.

Lipman, P.W. and McIntosh, W.C. (2008) Eruptive and noneruptive calderas, northeastern San Juan Mountains, Colorado: Where did the ignimbrites come from?, *GSA Bulletin*, Vol. 120, No. 7/8, p. 771-795.

Lipman, P.W. and Mehnert, H.H. (1978) The Taos Plateau Volcanic Field, Northern Rio Grande Rift, New Mexico, *in* Riecker, R.E., eds., *Rio Grande Rift: Tectonics and Magmatism*, American Geophysical Union, p. 289-312.

Lipman, P.W., Mehnert, H.H., and Naeser, C.W. (1986) Evolution of the Latir Volcanic Field, Northern New Mexico, and Its Relation to the Rio Grande Rift, as Indicated by Potassium-Argon and Fission Track Dating, *Journal of Geophysical Research*, Vol. 91, No. B6, p. 6329-6345.

Lipman, P.W., Logatchev, N.A., Zorin, Y.A., et al. (1989) Intracontinental rift comparisons: Baikal and Rio Grande Rift Systems, *Eos*, Vol. 70, No. 19, p. 578-579.

Lisenbee, A.L. (2013) Multistage Laramide deformation in the area of the southern Santa Fe embayment (Rio Grande
rift) north-central New Mexico, *in* Hudson, M.R. and Grauch, V.J.S., eds., *New Perspectives on Rio Grande Rift Basins: From Tectonics to Groundwater*, *The Geological Society of America Special Paper*, No. 494, p. 239-260.

Lozinsky, R.P. (1994) Cenozoic Stratigraphy, Sandstone Petrology, and Depositional History of the Albuquerque Basin, Central New Mexico, *in* Keller G.R. and Cather, S.M., eds., *Basins of the Rio Grande Rift: Structure, Stratigraphy, and Tectonic Setting*, *The Geological Society of America Special Paper*, No. 291, p. 73-82.

Lucas, S.G. (2001) The Age of Mammals and the Age of Volcanoes in New Mexico: An Outline of the Cenozoic\ Geology and Paleontology of the State, *Volcanology in New Mexico, New Mexico Museum of Natural History and Science Bulletin*, p. 30-48.

Machette, M.N. (1986) History of Quaternary Offset and Paleoseismicity along the La Jencia Fault, Central Rio Grande Rift, New Mexico, *Bulletin of the Seismological Society of America*, Vol. 76, No. 1, p. 259-272.

Machette, M.N., Thompson, R.A., Marchetti, D.W., et al. (2013) Evolution of ancient Lake Alamosa and integration of the Rio Grande during the Pliocene and Pleistocene, *in* Hudson, M.R. and Grauch, V.J.S., eds., *New Perspectives on Rio Grande Rift Basins: From Tectonics to Groundwater*, *The Geological Society of America Special Paper*, No. 494, p. 1-20.

Mack, G.H. and Leeder, M.R. (1999) Climatic and Tectonic Controls on Alluvial-Fan and Axial-Fluvial Sedimentation in the Plio-Pleistocene Palomas Half Graben, Southern Rio Grande Rift, *Journal of Sedimentary Research*, Vol. 69, No. 3, p. 635-652.

Mack, G.H. and Seager, W.R. (1990) Tectonic control on facies distribution of the Camp Rice and Palomas Formations (Pliocene-Pleistocene) in southern Rio Grande rift, *Geological Society of America Bulletin*, Vol. 102, p. 45-53.

Mack, G.H. and Seager, W.R. (1995) Transfer zones in the southern Rio Grande rift, *Journal of the Geological Society*, London, Vol. 152, p. 551-560.

Mack, G.H., Jones, M.C., Tabor, N.J., et al. (2012) Mixed Geothermal and Shallow Meteoric Origin of Opal and Calcite Beds in Pliocene Lower Pleistocene Axial-Fluvial Strata, Southern Rio Grande Rift, Rincon Hills, New Mexico, U.S.A., *Journal of Sedimentary Research*, Vol. 82, No. 8, p. 616-631.

Mack, G.H., Cole, D.R., and Trevino, L. (2000) The distribution and discrimination of shallow, authigenic carbonate in the Pliocene Pleistocene Palomas Basin, southern Rio Grande rift, *GSA Bulletin*, Vol. 112, No. 5, p. 643-656.

Mack, G.H., Leeder, M., Perez-Arlucea, M., et al. (2011) Tectonic and climatic controls on Holocene channel migration, incision and terrace formation by the Rio Grande in the Palomas half graben, southern Rio Grande Rift, USA, Department of Geological Sciences, *Sedimentology*, Vol. 58, p. 1065-1086.
Mack, G.H., James, W.C., and Salyards, S.L., (1994) Late Pliocene and Early Pleistocene Sedimentation as Influenced by Intrabasinal Faulting, Southern Rio Grande Rift, *in* Keller G.R. and Cather, S.M., eds., *Basins of the Rio Grande Rift: Structure, Stratigraphy, and Tectonic Setting*, *The Geological Society of America Special Paper*, No. 291, p. 257-264.

Mack, G.H., Seager, W.R., and Leeder, M.R. (2003) Synclinal-horst basins: examples from the southern Rio Grande rift and southern transition zone of southwestern New Mexico, USA, *Basin Research*, Vol. 15, p. 365-377.

Mailloux, B.J., Person, M., Kelley, S., et al. (1999) Tectonic controls on the hydrogeology of the Rio Grande Rift, New Mexico, *Water Resources Research*, Vol. 35, No. 9, p. 2641-2659.

Maldonado, F., Miggins, D.P., Budahn, J.R., et al. (2013) Deformational and erosional history for the Abiquiu and contiguous area, north central New Mexico: Implications for formation of the Abiquiu embayment and a discussion of new geochronological and geochemical analysis, *in* Hudson, M.R. and Grauch, V.J.S., eds., *New Perspectives on Rio Grande Rift Basins: From Tectonics to Groundwater*, *The Geological Society of America Special Paper*, No. 494, p. 125-156.

Manley, K. (1978) Stratigraphy and Structure of the Espanola Basin, Rio Grande Rift, New Mexico, *in* Riecker, R.E., eds., *Rio Grande Rift: Tectonics and Magmatism*, American Geophysical Union, p. 71-86.

Manley, K. (1984) Brief summary of the Tertiary geologic history of the Rio Grande rift in northern New Mexico, *New Mexico Geologic Society, 35th Annual Fall Field Conference Guidebook*, p. 63-66.

Mattick, R.E. (1967) A Seismic and Gravity Profile across the Hueco Bolson, Texas, Geological Survey Research 1967, Chapter D, *Geological Survey Professional Paper*, No. 575-D, p. D85-D91.

May, S.J. and Russell, L.R. (1994) Thickness of the Syn-Rift Santa Fe Group in the Albuquerque Basin and Its Relation to Structural Style, *in* Keller G.R. and Cather, S.M., eds., *Basins of the Rio Grande Rift: Structure, Stratigraphy, and Tectonic Setting, The Geological Society of America Special Paper*, No. 291, p. 113-124.

May, S.J., Kelley, S.A., and Russell, L.R. (1994) Footwall Unloading and Rift Shoulder Uplifts in the Albuquerque Basin: Their Relation to Syn-Rift Fanglomerates and Apatite Fission-Track Ages, *in* Keller G.R. and Cather, S.M., eds., *Basins of the Rio Grande Rift: Structure, Stratigraphy, and Tectonic Setting*, *The Geological Society of America Special Paper*, No. 291, p. 125-134.

McCalpin, J.P. (2005) Late Quaternary activity of the Pajarito fault, Rio Grande rift of northern New Mexico, USA, *Tectonophysics*, Vol. 408, p. 213-236.

McMillan, N.J., Dickin, A.P., and Haag, D. (2000) Evolution of magma source regions in the Rio Grande rift, southern New Mexico, *GSA Bulletin*, Vol. 112, No. 10, p. 1582-1593.

Meinzer, O.E. and Hare, R.F. (1915) Geology and Water Resources of Tularosa Basin, New Mexico, Department of the Interior, *United States Geological Survey Water-Supply Paper*, No. 343., 317 p.

Meyer, J. and Foland, K.A. (1991) Magmatic-tectonic interaction during early Rio Grande rift extension at Questa, New Mexico, *Geological Society of America Bulletin*, Vol. 103, p. 993-1006.

Meyer, J. and Foland, K.A. (1991) A geophysical model of the Espanola Basin, Rio Grande Rift, New Mexico, *Geological Society of America Bulletin*, Vol. 103, p. 993-1006.

MicroGeophysics Corporation (1977) *Crustal Seismic - Refraction Investigations of the Geothermal Potential in the Central Rocky Mountains*, United States Geological Survey, 14 p.

Minor, S.A., Hudson, M.R., Caine, J.S., et al. (2013) Oblique transfer of extensional strain between basins of the

middle Rio Grande rift, New Mexico: Fault kinematic and paleostress constraints, *in* Hudson, M.R. and Grauch, V.J.S., eds., *New Perspectives on Rio Grande Rift Basins: From Tectonics to Groundwater*, *The Geological Society of America Special Paper*, No. 494, p. 345-382.

Morgan, P. and Witcher, J.C. (2011) Geothermal Resources along the Southern Rocky Mountains and the Rio Grande Rift, *The Mountain Geologist*, Vol. 48, No. 4, p. 81-93.

Morgan, P., Harder, V., Swanberg, C.A., et al. (1981) A groundwater convection model for Rio Grande rift geothermal
resources, *Geothermal Resource Council*, Vol. 5, p. 228-231.

Morgan, P., Seager, W.R., and Golombek, M.P. (1986) Cenozoic Thermal, Mechanical and Tectonic Evolution of the Rio Grande Rift, *Journal of Geophysical Research*, Vol. 91, No. B6, p. 6263-6276.

Morton, E.A. and Bilek, S.L. (2014) Limited Dynamic Earthquake Triggering in the Socorro Magma Body Region, Rio Grande Rift, New Mexico, *Bulletin of the Seismological Society of America*, Vol. 104, No. 5,
p. 2182-2193.

Moucha, R., Forte, A.M., Rowley, D.B., et al. (2008) Mantle convection and the recent evolution of the Colorado Plateau and the Rio Grande Rift valley, *Geology*, Geological Society of America, Vol. 36, No. 6, p. 439-442.

Mozley, P.S. and Davis, J.M. (2005) Internal structure and mode of growth of elongate calcite concretions: Evidence for small-scale, microbial induced, chemical heterogeneity in groundwater, *GSA Bulletin*, Vol.
117, No. 11/12, p. 1400-1312.

Muehlberger, W.R., Belcher, R.C., and Goetz, L.K. (1978) Quaternary faulting in Trans-Pecos Texas, *Geology*, Vol. 6, p. 337-340.

Murphy, H.D., Tester, J.W., Grigsby, C.O., et al. (1981) Energy Extraction from Fractured Geothermal Reservoirs in Low-Permeability Crystalline Rock, *Journal of Geophysical Research*, Vol. 86, No. B8, p. 7145-7158.

Nielson, D.L. and Hulen, J.B. (1984) Internal Geology and Evolution of the Redondo Dome, Valles Caldera, New Mexico, *Journal of Geophysical Research*, Vol. 89, No. B10, p. 8695-8711.

Nishimura, T., Fehler, M., Baldridge, W.S., et al. (1996) Heterogeneous structure around the Jemez volcanic field, New Mexico, USA, as inferred from the envelope inversion of active-experiment seismic data, *Geophysical Journal*, Vol. 131, p. 667-681.

O'Donnell, T.M., Miller, K.C., and Witcher, J.C. (2001) A seismic and gravity study of the McGregor geothermal system, southern New Mexico, *Geophysics*, Vol. 66 No. 4, p. 1002-1014.

Olsen, K.H., Braile, L.W., Stewart, J.N., et al. (1986) Jemez Mountains volcanic field, New Mexico: Time term interpretation of the CARDEX seismic experiment and comparison with Bouguer gravity, *Journal of Geophysical Research*, Vol. 91, No. B6, p. 6175-6187.

Olsen, K.H., Keller, G.R., and Stewart, J.N. (1978) Crustal Structure Along the Rio Grande Rift from Seismic Refraction Profiles, *in* Riecker, R.E., eds., *Rio Grande Rift: Tectonics and Magmatism*, American Geophysical Union, p. 127-144.

Orr, B.R. and Myers, R.G. (1986) Water Resources in Basin-Fill Deposits in the Tularosa Basin, New Mexico, U.S. Geological Survey Water-Resources Investigations Report, No. 85-94

Parker, E.C., Davis, P.M., Evans, J.R., et al. (1984) Upwarp of anomalous asthenosphere beneath the Rio Grande rift,
Nature, Vol. 312, p. 354-356.

Pearse, J. and Fialko, Y. (2010) Mechanics of active magmatic intraplating in the Rio Grande Rift near Socorro, New Mexico, *Journal of Geophysical Research*, Vol. 115, 16 p.

Pearson, C. and Goff, F. (1981) Schlumberger Resistivity Study of the Jemez Springs Region of Northwestern New Mexico, *Geothermal Resource Council*, Vol. 5, p. 119-122.

Pepin, J., Person, M., Phillips, F., et al. (2015) Deep fluid circulation within crystalline basement rocks and the role of hydrologic windows in the formation of the Truth or Consequences, New Mexico low-temperature geothermal system, *Geofluids*, Vol. 15, p. 139-160.

Perez-Arlucea, M., Mack, G., and Leeder, M. (2000) Reconstructing the ancestral (Plio-Pleistocene) Rio Grande in its active tectonic setting, southern Rio Grande rift, New Mexico, USA, *Sedimentology*, Vol. 47, p. 701-720.

Perry, F.V., Baldridge, W.S., and DePaolo, D.J. (1988) Chemical and isotopic evidence for lithospheric thinning beneath the Rio Grande rift, *Nature*, Vol. 332, p. 432-434.

Peters, T.J., Menzies, M., Thirlwall, M., et al. (2007) Zuni-Bandera volcanism, Rio Grande, USA - Melt Formation in garnet- and spinel-facies mantle straddling the asthenosphere-lithosphere boundary, *Lithos*, Vol. 102, p. 295-315.

Peterson, C. and Roy, M. (2005) Gravity and Flexure Models of the San Luis, Albuquerque, and Tularosa Basin in the Rio Grande rift, New Mexico, and Southern Colorado, *56th Field Conference Guidebook, Geology of the Chama Basin*, New Mexico Geological Society, p. 105-114.

Phillips, F.M., Goff, F., Vuataz, F., et al. (1984) 36CL as a Tracer in Geothermal Systems: Example from Valles Caldera, New Mexico, *Geophysical Research Letters*, Vol. 11, No. 12, p. 1227-1230.

Porreca, C., Selverstone, J., and Samuels, K. (2006) Pyroxenite xenoliths from the Rio Puerco volcanic field, New Mexico: Melt metasomatism at the margin of the Rio Grande rift, *Geosphere*, Vol. 2, No. 7, p. 333-351.

Raatz, W.D. (2005) *Devonian Shelf to Basin Facies Distributions and Source Rock Potential, South-central and Southwestern New Mexico*, New Mexico Bureau of Geology and Mineral Resources Open File Report, No. 484, 38 p.

Ramberg, I.B. and Smithson, S.B. (1975) Gridded fault patterns in a late Cenozoic and a Paleozoic continental rift, *Geology*, Vol. 3, p. 201-205.

Ramberg, I.B., Cook, F.A., and Smithson, S.B. (1978) Structure of the Rio Grande rift in southern New Mexico and West Texas based on gravity interpretation, *Geological Society of America Bulletin*, Vol. 89, p. 107-123.

Rawling, G.C. and Goodwin, L.B. (2006) Structural record of the mechanical evolution of mixed zones in faulted poorly lithified sediments, Rio Grande rift, New Mexico, USA, *Journal of Structural Geology*, Vol. 28, p. 1623-1639.

Rawling, G.C. and Goodwin, L.B. (2006) Structural of the mechanical evolution of mixed zones in faulted poorly lithified sediments, Rio Grande rift, New Mexico, USA, *Journal of Structural Geology*, Vol 28, p. 1623-1639.

Reilinger, R.E., Brown, L.D., and Oliver, J.E. (1978) Recent Vertical Crustal Movements from Leveling Observations in the Vicinity of the Rio Grande Rift, *in* Riecker, R.E., eds., *Rio Grande Rift: Tectonics and Magmatism*, American Geophysical Union, p. 223-236.

Reiter, M. (2005) Subsurface temperatures and crustal strength changes within the seismogenic layer at Arroyo del coyote in the Socorro seismic area, central Rio Grande Rift, New Mexico, *GSA Bulletin*, Vol. 117, No. 3/4, p. 307-318.

Reiter, M., Chamberlin, R.M., and Love, D.W. (2010) New data reflect on the thermal antiquity of the Socorro magma body locale, Rio Grande Rift, New Mexico, *Lithosphere*, Vol. 2, No. 6, p. 447-453.

Reiter, M., Edwards, C.L., Hartman, H., et al. (1975) Terrestrial Heat Flow along the Rio Grande Rift, New Mexico and Southern Colorado, *Geological Society of America Bulletin*, Vol. 86, p. 811-818.

Reiter, M., Eggleston, R.E., Broadwell, B.R., et al. (1986) Estimates of Terrestrial Heat Flow From Deep Petroleum Tests Along the Rio Grande Rift in Central and Southern New Mexico, *Journal of Geophysical Research*, Vol. 91, No. B6, p. 6225-6245.

Reiter, M., Shearer, C., and Edwards, C.L. (1978) Geothermal anomalies along the Rio Grande rift in New Mexico, *Geology*, Vol. 6, No. 2, p. 85-88.

Reiter, M., Mansure, A.J., and Shearer, C. (1978) Geothermal Characteristics of the Rio Grande Rift with the Southern Rocky Mountain Complex, *in* Riecker, R.E., eds., *Rio Grande Rift: Tectonics and Magmatism*, American Geophysical Union, p. 253-268.

Ricketts, J.W., Karlstrom, K.E., Priewisch, A., et al. (2014) Quaternary extension in the Rio Grande rift at elevated strain rates recorded in travertine deposits, central New Mexico, *Lithosphere*, Vol. 6, p. 3-16.

Ricketts, J.W., Karlstrom, K.E., and Kelley, S.A. (2015) Embryonic core complexes in narrow continental rifts: The importance of low-angle normal faults in the Rio Grande rift of central New Mexico, *Geosphere*, Geologic Society of America, Vol. 11, No. 2, p. 425-444.

Riley, P.R., Goodwin, L.B., and Lewis, C.J. (2010) Controls on fault damage zone width, structure, and symmetry in the Bandelier Tuff, New Mexico, *Journal of Structural Geology*, Vol 32, p. 766-780.

Rinehart, E.J., Sanford, A.R., and Ward, R.M. (1978) Geographic Extent and Shape of an Extensive Magma Body at Midcrustal Depths in the Rio Grande Rift near Socorro, New Mexico, *in* Riecker, R.E., eds., *Rio Grande Rift: Tectonics and Magmatism*, American Geophysical Union, p. 237-253.

Rodriguez, B.D. and Sawyer, D.A. (2013) Geophysical constraints on Rio Grande rift structure and stratigraphy from magnetotelluric models and borehole resistivity logs, northern New Mexico, *in* Hudson, M.R. and

Grauch, V.J.S., eds., *New Perspectives on Rio Grande Rift Basins: From Tectonics to Groundwater*, *The Geological Society of America Special Paper*, No. 494, p. 323-344.

Rowe, M.C. and Lassiter, J.C. (2009) Chlorine enrichment in central Rio Grande Rift basalt melt inclusions: Evidence for subduction modification of the lithospheric mantle, *Geology*, Geological Society of America, Vol. 37, No. 5, p. 439-442.

Rowe, M.C., Lassiter, J.C., and Goff, K. (2015) Basalt volatile fluctuations during continental rifting: An example from the Rio Grande Rift, USA, *Geochemistry, Geophysics, Geosystems*, American Geophysical Union, p. 1254-1273.

Roy, M., MacCarthy, J.K., and Selverstone, J. (2005) Upper mantle structure beneath the eastern Colorado Plateau and Rio Grande rift revealed by Bouguer gravity, seismic velocities, and xenolith data, *An Electronic Journal of the Earth Sciences*, AGU, Geochemical Society, Vol. 6, No. 10, 19 p.

Ruhe, R.V. (1962) Age of the Rio Grande Valley in Southern New Mexico, *The Journal of Geology*, Vol. 70, No. 2, p. 151-167.

Ruhl, C., Bilek, S.L., and Stankova-Pursley, J. (2010) Relocation and characterization of the August 2009 microearthquake swarm above the Socorro magma body in the central Rio Grande Rift, *Geophysical Research Letters*, American Geophysical Union, Vol. 37, No. 23, 4 p.

Ruleman, C.A., Thompson, R.A., Shroba, R.R., et al. (2013) Late Miocene-Pleistocene evolution of a Rio Grande rift subbasin, Sunshine Valley Costilla Plain, San Luis Basin, New Mexico and Colorado, *in* Hudson, M.R. and Grauch, V.J.S., eds., *New Perspectives on Rio Grande Rift Basins: From Tectonics to Groundwater*, *The Geological Society of America Special Paper*, No. 494, p. 47-74.

Russell, L.R. and Snelson, S. (1994) Structure and Tectonics of the Albuquerque Basin Segment of the Rio Grande Rift: Insights from Reflection Seismic Data, *in* Keller G.R. and Cather, S.M., eds., *Basins of the Rio Grande Rift: Structure, Stratigraphy, and Tectonic Setting*, *The Geological Society of America Special Paper*, No. 291, p. 83-112.

Russell, L.R. and Snelson, S. (1994) Structural Style and Tectonic Evolution of the Albuquerque Basin Segment of the Rio Grande Rift, New Mexico, U.S.A., *Interior Rift Basin*, *American Association of Petroleum Geologists Memoir 59*, p. 205-258.

Ryder, R.T. (1983) *Petroleum Potential of Wilderness Lands, New Mexico*, United States Department of the Interior, Geological Survey, 38 p.

Salyards, S.L., Ni, J.F., and Aldrich, J., Jr. (1994) Variation in Paleomagnetic Rotations and Kinematics of the North Central Rio Grande Rift, New Mexico, *in* Keller G.R. and Cather, S.M., eds., *Basins of the Rio Grande Rift: Structure, Stratigraphy, and Tectonic Setting*, The Geological Society of America Special Paper, No. 291, p. 59-72.

Sanford, A. (1983) Magma Bodies in the Rio Grande Rift in Central New Mexico, *New Mexico Geological Society Guidebook, 34th Field Conference*, p. 123-125.

Sanford, A.R., Budding, A.J., Hoffman, J.P., et al. (1972) *Seismicity of the Rio Grande Rift in New Mexico*, New Mexico State Bureau of Mines and Mineral Resources, 23 p.

Sanford, A.R., Olsen, K.H., and Jaksha, L.H. (1978) Seismicity of the Rio Grande Rift, *in* Riecker, R.E., eds., *Rio Grande Rift: Tectonics and Magmatism*, American Geophysical Union, p. 145-168.

Sass, J.H. and Morgan, P. (1988) Conductive heat flux in VC-1 and the thermal regime of Valles Caldera, Jemez Mountains, New Mexico, *Journal of Geophysical Research*, Vol. 93, No. B6, p. 6027-6039.

Savage, J.C., Lisowski, M., and Prescott, W.H. (1980) Geodetic Measurement of Horizontal Deformation across the Rio Grande Rift Near Socorro, New Mexico, *Journal of Geophysical Research*, Vol. 85, No. B12, p. 7215-7220.

Schlue, J.W. and Aster, R.C. (1996) A lower crustal extension to a midcrustal magma body in the Rio Grande Rift, New Mexico, *Journal of Geophysical Research*, Vol. 101, No. B11, p. 25283-25291.

Schlue, J.W. and Hostettler, K.K. (1987) Evidence from Rayleigh Wave Data for Magma in an Upper Crustal Dike in the Albuquerque-Belen Basin of the Rio Grande Rift, New Mexico, *Journal of Geophysical Research*, Vol. 92, No. B9, p. 9281-9292.

Schneider, R.V. and Keller, G.R. (1994) Crustal Structure of the Western Margin of the Rio Grande Rift and Mogollon-Datil Volcanic Field, Southwestern New Mexico and Southeastern Arizona, *in* Keller G.R. and Cather, S.M., eds., *Basins of the Rio Grande Rift: Structure, Stratigraphy, and Tectonic Setting*, *The Geological Society of America Special Paper*, No. 291, p. 207-226.

Seager, W.R. and McCurry, M. (1988) The Cogenetic Organ Cauldron and Batholith, South Central New Mexico: Evolution of a Large-Volume Ash Flow Cauldron and Its Source Magma Chamber, *Journal of Geophysical Research*, Vol. 93, No. B5, p. 4421-4433.

Seager, W.R. and Morgan, P. (1978) Rio Grande Rift in Southern New Mexico, West Texas, and Northern Chihuahua,
in Riecker, R.E., eds., *Rio Grande Rift: Tectonics and Magmatism*, American Geophysical Union, p. 87-106.

Self, S., Goff, F., Gardner, J.N., et al. (1986) Explosive Rhyolitic volcanism in the Jemez Mountains: Vent locations, caldera development and relation to regional structure, *Journal of Geophysical Research*, Vol. 91, No. B2, p. 1779-1798.

Semken, S.C. (2001) The Navajo Volcanic Field, Volcanology in New Mexico, *New Mexico Museum of Natural History and Science Bulletin*, p. 79-83.

Shafike, N.G. and Flanigan, K.G. (1999) Hydrologic modeling of the Estancia Basin, New Mexico, *Albuquerque Geology, Annual NMGS Fall Field Conference Guidebooks*, New Mexico Geological Society, p. 81-89.

Sheetz, K.E. and Schlue, J.W. (1992) Inferences for the Socorro magma body from teleseismic receiver functions, *Geophysical Research Letters*, Vol. 19, No. 18, p. 1867-1870.

Shevenell, L., Goff, F., Vuataz, F., et al. (1987) Hydrogeochemical Data for Thermal and Nonthermal Waters and Gases of the Valles Caldera- Southern Jemez Mountains Region, New Mexico, Los Alamos National Laboratory, United States Department of Energy, 51 p.

Sinno, Y.A., Daggett, P.H., Keller, G.R., et al. (1986) Crustal Structure of the Southern Rio Grande Rift Determined

From Seismic Refraction Profiling, *Journal of Geophysical Research*, Vol. 91, No. B6, p. 6143-6156.

Slack, P.D., Davis, P.M., Baldridge, W.S., et al. (1996) The upper mantle structure of the central Rio Grande rift region from teleseismic P and S wave travel time delays and attenuation, *Journal of Geophysical Research*, Vol. 101, No. B7, p. 16003-16023.

Slate, J.L., et al. (2013) Upper Neogene tephrochronologic correlations of the Espanola Basin and Jemez Mountains volcanic field, northern Rio Grande rift, north-central New Mexico, *in* Hudson, M.R. and Grauch, V.J.S., eds., *New Perspectives on Rio Grande Rift Basins: From Tectonics to Groundwater*, *The Geological Society of America Special Paper*, No. 494, p. 303-322.

Smith, D.L. and Jones, R.L. (1978) Thermal Anomaly in Northern Mexico: An Extension of the Rio Grande Rift?, *in* Riecker, R.E., eds., *Rio Grande Rift: Tectonics and Magmatism*, American Geophysical Union, p. 269-278.

Smith, G.A. (2001) Development of a Pyroclastic Apron Adjacent to Rhyolite Domes in a Subsiding Basin: Upper Miocene Peralta Tuff, Jemez Mountains, New Mexico, *Volcanology in New Mexico, New Mexico Museum of Natural History and Science Bulletin*, p. 85-96.

Smith, G.A., McIntosh, W., and Kuhle, A.J. (2001) Sedimentologic and geomorphic evidence for seesaw subsidence of the Santo Domingo accommodation-zone basin, Rio Grande rift, New Mexico, *GSA Bulletin*, Vol. 113, No. 5, p. 561-574.

Smith, G.A., Moore, J.D., and McIntosh, W.C. (2002) Assessing Roles of Volcanism and Basin Subsudence in Causing Oligocene-Lower Miocene Sedimentation in the Northern Rio Grande Rift, New Mexico, U.S.A., J*ournal of Sedimentary Research*, Vol. 72, No. 6, p. 836-848.

Smith, L.N., Lucas, S.G., and Elston, W.E. (1985) Paleogene Stratigraphy, Sedimentation and Volcanism of New Mexico, *Cenozoic Paleogeography of the West-Central United States, The Rocky Mountain Section SEPM (Society for Sedimentary Geology)*, p. 293-315.

Smith, R.R. (1978) Early Rift Magmatism at Spanish Peaks, Colorado, *in* Riecker, R.E., eds., *Rio Grande Rift: Tectonics and Magmatism*, American Geophysical Union, p. 313-322.

Sosa, A., Thompson, L., Velasco, A.A., et al. (2014) 3-D structure of the Rio Grande Rift from 1-D constrained joint inversion of receiver functions and surface wave dispersion, *Earth and Planetary Science Letters*, Vol. 402, p. 127-137.

Spence, W. (1990) A Tomographic Glimpse of the Upper Mantle Source of Magmas of the Jemez Lineament, New Mexico, *Journal of Geophysical Research*, Vol. 95, No. B7, p. 10829-10849.

Spohn, T. and Schubert, G. (1982) Convective thinning of the lithosphere: A mechanism for the initiation of continental rifting, *Journal of Geophysical Research*, Vol. 87, No. B6, p. 4669-4681.

Steck, L.K., Thurber, C.H., Fehler, M.C., et al. (1998) Crust and upper mantle P wave velocity structure beneath Valles Caldera, New Mexico: Results from the Jemez teleseismic tomography experiment, *Journal of Geophysical Research*, Vol. 103, No. B10, p. 24301-24320.

Stix, J., Pearson, C., Vuataz, F., et al. (1982) Geology, Resistivity, and Hydrogeochemistry of the Ojo Caliente Hot

Springs Area, Northern New Mexico, *Geothermal Resources Council, Transactions*, Vol. 6, p. 55-58.

Sussman, A.J., Lewis, C.J., Masin, S.N., et al. (2011) Paleomagnetism of the Quaternary Bandelier Tuff; implications for the tectonic evolution of the Espanola Basin, Rio Grande Rift, *Lithosphere*, Vol. 3, No. 5, p. 328-345.

Swanberg, C.A. (1978) Chemistry of Thermal and Nonthermal Groundwaters in the Rio Grande Rift and Adjacent Tectonic Provinces, *in* Riecker, R.E., eds., *Rio Grande Rift: Tectonics and Magmatism*, American Geophysical Union, p. 279-288.

Swanberg, C.A. and Morgan, P. (1980) The Silica Heat Flow Interpretation Technique: Assumptions and Applications, *Journal of Geophysical Research*, Vol. 85, No. B12, p. 7206-7214.

Tandon, K., Brown, L., and Hearn, T. (1999) Deep structure of the northern Rio Grande rift beneath the San Luis basin (Colorado) from a seismic reflection survey: implications for rift evolution, *Tectonophysics*, Vol. 302, p. 41-56.

Tappa, M.J., Coleman, D.S., Mills, R.D., et al. (2011) The plutonic record of a silicic ignimbrite from the Latir volcanic field, New Mexico, *Geochemistry, Geophysics, Geosystems*, American Geophysical Union, 16 p.

Tomczyk, T. and Morgan, P. (1987) Evaluation of the thermal regime of the Valles Caldera, New Mexico, U.S.A., by downward continuation of temperature data, *Tectonophysics*, Elsevier Science Publishers B.V., Vol. 134, p. 339-345.

Towle, J.N. (1980) New evidence for magmatic intrusion beneath the Rio Grande rift, New Mexico, *Geological Society of America Bulletin*, Vol. 91, p. 626-630.

Townsend, D.A. and Sonder, L.J. (2001) Rheologic controls of buoyancy-driven extension of the Rio Grande rift, *Journal of Geophysical Research*, Vol. 106, No. B8, p. 16515-16523.

Trainer, F.W. (1974) Ground water in the southwestern part of the Jemez Mountains volcanic region, New Mexico, *New Mexico Geological Society 25th Annual Fall Field Conference Guidebook*, p. 337-345.

Trainer, F.W. and Lyford, F.P. (1979) Geothermal Hydrology in the Rio Grande Rift, North-Central New Mexico, *New Mexico Geological Society Guidebook, 30th Field Conference*, p. 299-306.

Trainer, F.W., Rogers, R.J., and Sorey, M.L. (2000) Geothermal Hydrology of Valles Caldera and the Southwestern Jemez Mountains, *New Mexico, U.S. Geological Survey, Water-Resources Investigations Report 00-4067*, 115 p.

Turbeville, B.N. and Self, S. (1988) San Diego Canyon Ignimbrites: Pre-Bandelier Tuff Explosive Rhyolitic Volcanism in the Jemez Mountains, New Mexico, *Journal of Geophysical Research*, Vol. 93, No. B6, p. 6148-6156.

Tweto, O. (1978) The Rio Grande Rift System in Colorado, *in* Riecker, R.E., eds., *Rio Grande Rift: Tectonics and Magmatism*, American Geophysical Union, p. 33-56.

van Wijk, J., van Hunen, J., and Goes, S. (2008) Small-scale convection during continental rifting: Evidence from the Rio Grande rift, *Geology*, The Geological Society of America, Vol. 36, No. 7, p. 575-578.

Vernon, J.H. and Riecker, R.E. (1989) Significant Cenozoic faulting, east margin of the Espanola Basin, Rio Grande rift, New Mexico, *Geology*, Vol. 17, p. 230-233.

Vuataz, F.D. and Goff, F. (1986) Isotope geochemistry of thermal and nonthermal waters in the Valles Caldera, Jemez Mountains, Northern New Mexico, *Journal of Geophysical Research*, Vol. 91, No. B2, p. 1835-1853.

Vuataz, F.D., Goff, F., Fouillac, C., et al. (1988) A strontium isotope study of the VC-1 core hole and associated hydrothermal fluids and rocks from Valles Caldera, Jemez Mountains, New Mexico, *Journal of Geophysical Research*, Vol. 93, No. B6, p. 6059-6067.

Ward, R.M., Schlue, J.W., and Sanford, A.R. (1981) Three-dimensional velocity anomalies in the upper crust near Socorro, New Mexico, *Geophysical Research Letters*, Vol. 8, No. 6, p. 553-556.

Warren, R.G., Kudo, A.M., and Keil, K. (1978) Geochemistry of Lithic and Single-Crystal Inclusions in Basalt and a Characterization of the Upper Mantle-Lower Crust in the Engle Basin, Rio Grande Rift, New Mexico, *in* Riecker, R.E., eds., *Rio Grande Rift: Tectonics and Magmatism*, American Geophysical Union, p. 393-415.

Weir, J.E., Jr. (1965) Geology and Availability of Ground Water in the Northern Part of the White Sands Missile Range and Vicinity New Mexico, United States Department of the Interior, Geological Survey, 82 p.

Wendlandt, R.F., Baldridge, W.S., and Neumann, E.R. (1991) Modification of Lower Crust by Continental Rift Magmatism, *Geophysical Research Letters*, Vol. 18, No. 9, p. 1759-1762.

White, A.F., Delany, J.M., Truesdell, A., et al. (1984) Fluid Chemistry of the Baca Geothermal Field, Valles Caldera, New Mexico, *New Mexico Geological Society Guidebook, 35th Field Conference, Rio Grande Rift: Northern New Mexico*, p. 257-263.

Williams, A.J., Crossey, L.J., Karlstrom, K.E., et al. (2013) Hydrogeochemistry of the Middle Rio Grande aquifer system - Fluid mixing and salinization of the Rio Grande due to fault inputs, *Chemical Geology*, Vol. 351, p. 281-298.

Williams, R.T. and Rodriguez, B.D. (2002) Magnetotelluric Data in the Middle Rio Grande Basin, Albuquerque Volcanoes, New Mexico, U.S. Department of the Interior, U.S. Geologic Survey, 90 p.

Williams, R.T., Goodwin, L.B., Mozley, P.S., et al. (2015) Tectonic controls on fault zone flow pathways in the Rio Grande rift, New Mexico, USA, *Geology*, Geologic Society of America, Vol. 43, No. 8, p. 723-726.

Wilson, D., Aster, R., West, M., et al. (2005) Lithospheric structure of the Rio Grande rift, *Nature*, Vol. 433, p. 851-855.

Wilson, D., Aster, R., Ni, J., et al. (2005) Imaging the seismic structure of the crust and upper mantle beneath the Great Plains, Rio Grande Rift, and Colorado Plateau using receiver functions, *Journal of Geophysical Research*, Vol. 110, 14 p.

Witcher, J.C. (1995) Geothermal Resource Data Base, New Mexico, Southwest Technology Development Institute, 32 p.

Witcher, J.C. (2002) *Field Studies of Geothermal Reservoirs Rio Grande Rift, New Mexico*, United States Department of Energy, 10 p.

Witcher, J.C. (2001) Deep Production Well for Geothermal Direct-Use Heating of a Large CommercialGreenhouse, Radium Springs, Rio Grande Rift, New Mexico, United States Department of Energy, 29 p.

Witcher, J.C. (2002) Geothermal Energy in New Mexico, *GHC Bulletin*, p. 2-10.

Withjack, M.O. and Schlische, R.W. (2002) Rift-Basin Structure and Its Influence on Sedimentary Systems, *Sedimentation in Continental Rifts, Society for Sedimentary Geology Special Publication*, No. 73, p. 57-81.

WoldeGabriel, G., Koning, D.J., Broxton, D., et al. (2013) Chronology of volcanism, tectonics, and sedimentation near the western boundary fault of the Espanola Basin, Rio Grande rift, New Mexico, *in* Hudson, M.R. and Grauch, V.J.S., eds., *New Perspectives on Rio Grande Rift Basins: From Tectonics to Groundwater*, *The Geological Society of America Special Paper*, No. 494, p. 221-238.

Woldegabriel, G., Warren, R.G., Broxtoni, D.E., et al. (2001) Episodic Volcanism, Petrology, and Lithostratigraphy of the Pajarito Plateau and Adjacent Areas of the Espanola Basin and the Jemez Mountains, *Volcanology in New Mexico, New Mexico Museum of Natural History and Science Bulletin*, p. 97-129.

Wolff, J.A., Rowe, M.C., Teasdale, R., et al. (2005) Petrogenesis of Pre-caldera Mafic Lavas, Jemez Mountains Volcanic Field (New Mexico, USA) *Journal of Petrology*, Vol. 46, No. 2, p. 407-439.

Woodward, L.A. (1977) Rate of crustal extension across the Rio Grande Rift near Albuquerque, New Mexico, *Geology*, Vol. 5, p. 269-272.

Woodward, L.A. and Duchene, H.R. (1975) Geometry of Sierrita fault and its bearing on tectonic development of the Rio Grande rift, New Mexico, *Geology*, Vol. 3, p. 114-116.

Zimbelman, J.R. and Johnston, A.K. (2001) Improved Topography of the Carrizozo Lava Flow: Implications for Emplacement Conditions, *Volcanology in New Mexico, New Mexico Museum of Natural History and Science Bulletin*, p. 131-136.

Zimmerman, C. and Kudo, A.M. (1978) Geochemistry of Andesites and Related Rocks, Rio Grande Rift, New Mexico, *in* Riecker, R.E., eds., *Rio Grande Rift: Tectonics and Magmatism*, American Geophysical Union, p. 355-381.

Appendix B
PFA Associated Data

Table 2. WoE Training Sites

Name	Power Plant	State
Baltazor Hot Springs	No	Nevada
Bog Hot Springs	No	Nevada
Howard Hot Springs	No	Nevada
East Pinto Hot Springs	No	Nevada
Soldier Meadow Hot Springs	No	Nevada
Double Hot Springs	No	Nevada
Trego Hot Springs	No	Nevada
Gerlach Hot Springs	No	Nevada
San Emidio Hot Springs	Yes	Nevada
Bradys Hot Spring	Yes	Nevada
Patua Hot Springs	No	Nevada
Walleys Hot Springs	No	Nevada
McLeod Ranch Hot Springs	No	Nevada
Smith Creek Hot Springs	No	Nevada
Tungsten Mountain	No	Nevada
Dixie Meadows Hot Springs	No	Nevada
Hot Springs Ranch	No	Nevada
Jersey Valley Hot Springs	Yes	Nevada
Sou Hot Springs	No	Nevada
Leach Hot Springs	No	Nevada
Kyle Hot Springs	No	Nevada
Bass Hot Spring	No	Nevada
Buffalo Valley Hot Springs	No	Nevada
Golconda Hot Springs	No	Nevada
Carlin Hot Springs	No	Nevada
Beowawe/PP	Yes	Nevada
Cresent Valley Hot Springs	No	Nevada
Dann Hot Springs	No	Nevada
Bruffeys Hot Springs	No	Nevada
Upper Hot Creek Ranch springs	No	Nevada
Bartholomae Hot Springs	No	Nevada
Walti Hot SPrings	No	Nevada
Cherry Creek Hot Springs	No	Nevada
Hot Creek Springs	No	Nevada
Three Mile Spring	No	Nevada
Hot Sulpur Springs/Tuscorora	Yes	Nevada
Mineral Hot Springs	No	Nevada
Joseph Hot Springs	No	Utah
Red Hill Hot Springs	No	Utah

Cove Fort PP	Yes	Utah
Meadow Hatton Hot Springs	No	Utah
Roosevelt Hot Springs	Yes	Utah
Abraham Hot Springs	No	Utah
McGinness Hills	Yes	Nevada
Hondo Hot Springs	No	New Mexico
Gila Hot Springs	No	New Mexico
Souse Springs	No	New Mexico
T or C Warm Spring	No	New Mexico
Ponce de Leon Hot Spring	No	New Mexico
Jemez Pueblo Indian Hot Spring	No	New Mexico

Appendix C
Methodology Flow Charts

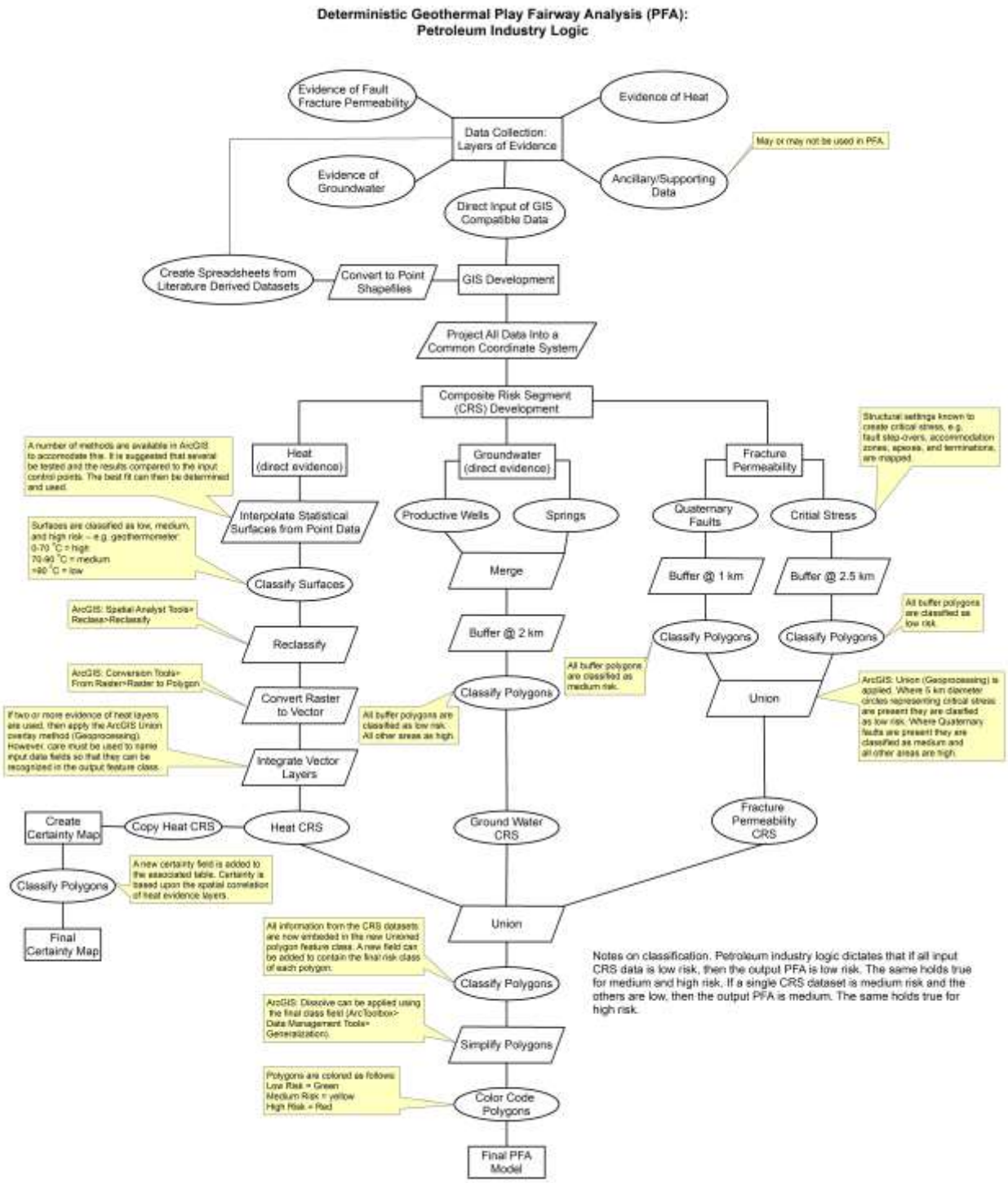
Deterministic Geothermal Play Fairway Analysis (PFA):
Petroleum Industry Logic
Evidence of Fault Fracture Permeability
Evidence of Heat
Data Collection: Layers of Evidence
Evidence of Groundwater
Ancillary/Supporting Data
May or may not be used in PFA
Direct Input of GIS Compatible Data
Create Spreadsheets from Literature Derived Datasets
Convert to Point Shapefiles
GIS Development
Project All Data Into a Common Coordinate System
Composite Risk Segment (CRS) Development
Heat (direct evidence)
Groundwater (direct evidence)
Fracture Permeability
Structural settings known to create critical stress, e.g. fault step-overs, accommodation zones, apexes, and terminations, are mapped.
A number of methods are available in ArcGIS to accomodate this. It is suggested that several be tested and the results compared to the input control points. The best fit can then be determined and used.
Interpolate Statistical Surfaces from Point Data
Productive Wells
Springs
Quaternary Faults
Critial Stress
Surfaces are classified as low, medium, and high risk -- e.g. geothermometer:
0-70 °C = high
70-90 °C = medium
>90 °C = low
Classify Surfaces
Merge
Buffer @ 1 km
Buffer @ 2.5 km
ArcGIS: Spatial Analyst Tools> Reclass>Reclassify
Reclassify
Buffer @ 2 km
All buffer polygons are classified as low risk.
Classify Polygons
Classify Polygons
Classify Polygons
ArcGIS: Conversion Tools> From Raster>Raster to Polygon
All buffer polygons are classified as medium risk.
Convert Raster to Vector
Classify Polygons
Union
ArcGIS: Union (Geoprocessing) is applied. Where 5 km diameter circles representing critical stress are present they are classified as low risk. Where Quaternary faults are present they are classified as medium and all other areas are high.
If two or more evidence of heat layers are used, then apply the ArcGIS Union overlay method (Geoprocessing). However, care must be used to name input data fields so that they can be recognized in the output feature class.
All buffer polygons are classified as low risk. All other areas as high.
Integrate Vector Layers
Create Certainty Map
Copy Heat CRS
Heat CRS
Ground Water CRS
Fracture Permeability CRS
A new certainty field is added to the associated table. Certainty is based upon the spatial correlation of heat evidence layers.
Classify Polygons
Final Certainty Map
Union
All information from the CRS datasets are now embedded in the new Unioned polygon feature class. A new field can be added to contain the final risk class of each polygon.
Classify Polygons
Notes on classification. Petroleum industry logic dictates that if all input CRS data is low risk, then the output PFA is low risk. The same holds true for medium and high risk. If a single CRS dataset is medium risk and the others are low, then the output PFA is medium. The same holds true for high risk.
ArcGIS: Dissolve can be applied using the final class field (ArcToolbox> Data Management Tools> Generalization).
Simplify Polygons
Polygons are colored as follows:
Low Risk = Green
Medium Risk = yellow
High Risk = Red
Color Code Polygons
Final PFA Model

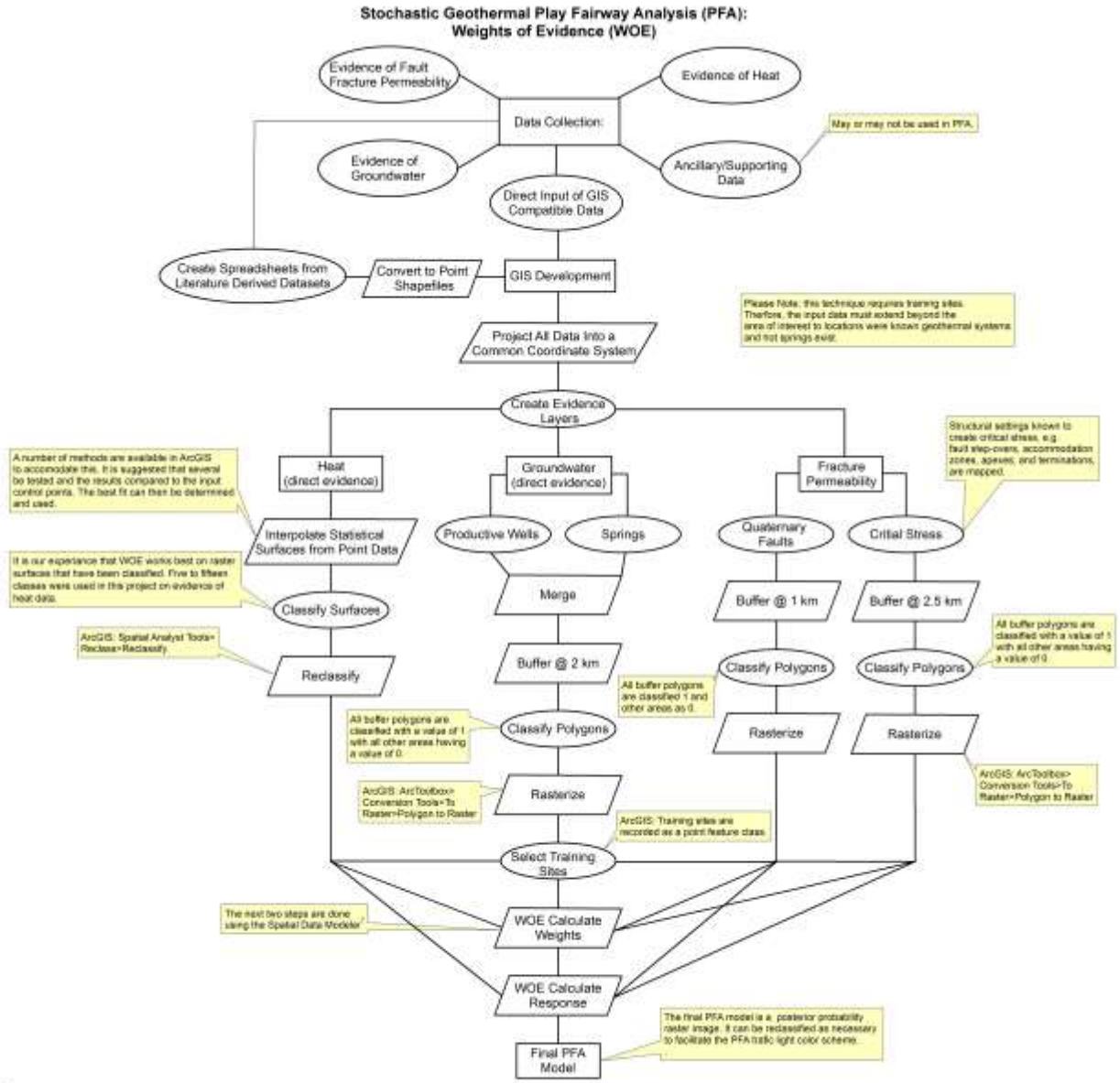

[1]Sawatzky, D.L., Raines, G.L. , Bonham-Carter, G.F., and Looney, C.G., 2009, Spatial Data Modeller (SDM): ArcMAP 9.3 geoprocessing tools for spatial data modelling using weights of evidence, logistic regression, fuzzy logic and neural networks. http://arcscripts.esri.com/details.asp?dbid=15341.

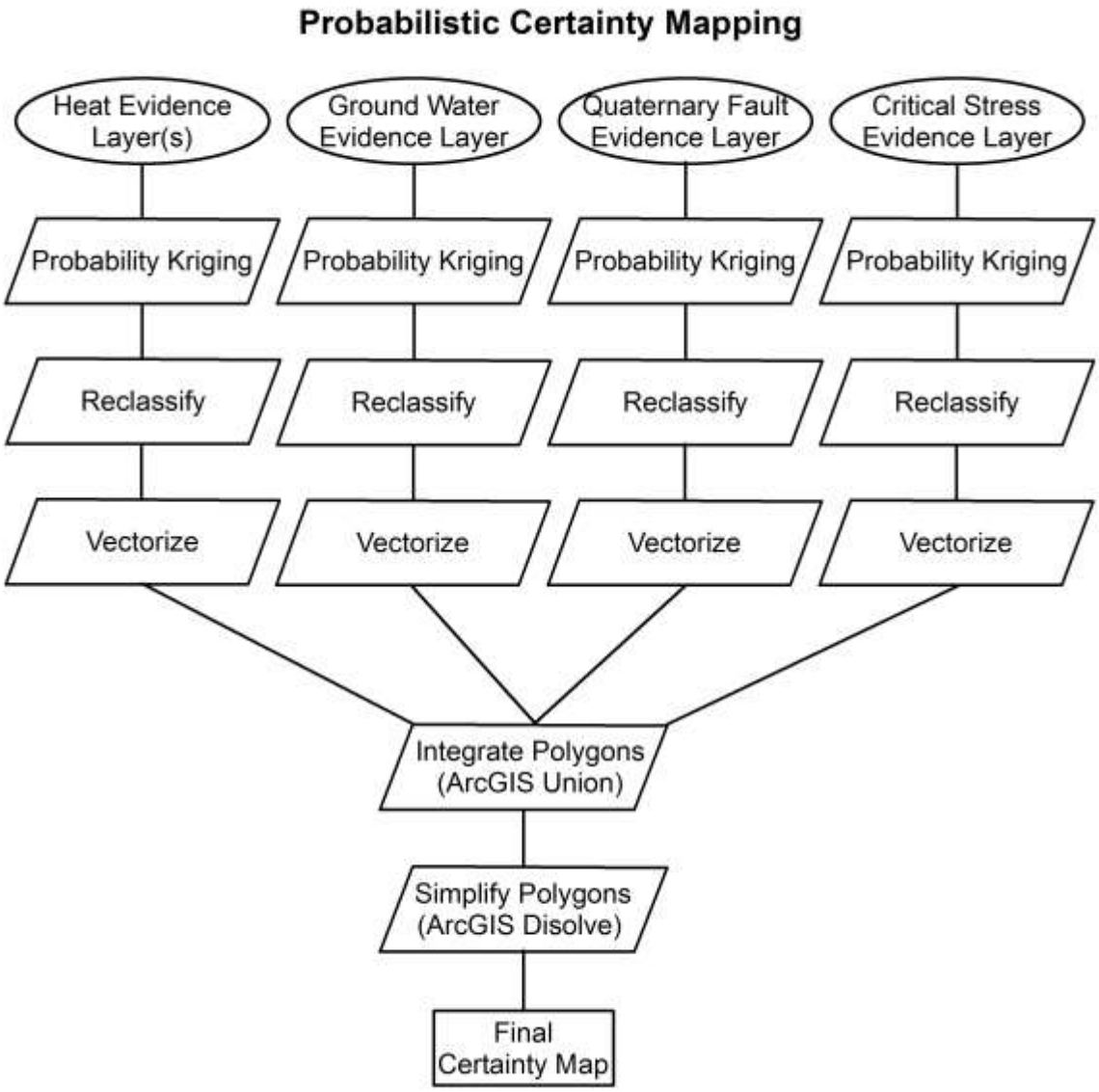
Probabilistic Certainty Mapping
Heat Evidence Layer(s)
Ground Water Evidence Layer
Quaternary Fault Evidence Layer
Critical Stress Evidence Layer
Probability Kriging
Probability Kriging
Probability Kriging
Probability Kriging
Reclassify
Reclassify
Reclassify
Reclassify
Vectorize
Vectorize
Vectorize
Vectorize
Integrate Polygons (ArcGIS Union)
Simplify Polygons (ArcGIS Disolve)
Final Certainty Map